Taylor & Francis
Taylor & Francis Group

ORIGINAL RESEARCH

Dynamic alterations of bone marrow cytokine landscape of myelodysplastic syndromes patients treated with 5-azacytidine

Alena Moudra[a], Sona Hubackova[a,b], Veronika Machalova[a], Marketa Vancurova[a], Jiri Bartek[a,c,d], Milan Reinis[e,f], Zdenek Hodny[a], and Anna Jonasova[g]

[a]Department of Genome Integrity, Institute of Molecular Genetics, v.v.i., Academy of Sciences of the Czech Republic, Prague, Czech Republic; [b]Laboratory of Molecular Therapy, Institute of Biotechnology, v.v.i., Academy of Sciences of the Czech Republic, BIOCEV, Vestec, Czech Republic; [c]Danish Cancer Society Research Center, Copenhagen, Denmark; [d]Department of Medical Biochemistry and Biophysics, Science For Life Laboratory, Division of Translational Medicine and Chemical Biology, Karolinska Institute, Solna, Sweden; [e]Department of Transgenic Models of Diseases, Institute of Molecular Genetics, v.v.i., Academy of Sciences of the Czech Republic, Prague, Czech Republic; [f]Immunology Unit, Czech Center for Phenogenomics, Institute of Molecular Genetics, v.v.i., Academy of Sciences of the Czech Republic, Prague, Czech Republic; [g]1st Department of Medicine, First Faculty of Medicine, Charles University in Prague and General University Hospital, Prague, Czech Republic

ABSTRACT

Myelodysplastic syndromes (MDS) represent a heterogeneous group of clonal stem cell disorders characterized by ineffective hematopoiesis frequently progressing into acute myeloid leukemia (AML), with emerging evidence implicating aberrant bone marrow (BM) microenvironment and inflammation-related changes. 5-azacytidine (5-AC) represents standard MDS treatment. Besides inhibiting DNA/RNA methylation, 5-AC has been shown to induce DNA damage and apoptosis in vitro. To provide insights into in vivo effects, we assessed the proinflammatory cytokines alterations during MDS progression, cytokine changes after 5-AC, and contribution of inflammatory comorbidities to the cytokine changes in MDS patients. We found that IL8, IP10/CXCL10, MCP1/CCL2 and IL27 were significantly elevated and IL12p70 decreased in BM of MDS low-risk, high-risk and AML patients compared to healthy donors. Repeated sampling of the high-risk MDS patients undergoing 5-AC therapy revealed that the levels of IL8, IL27 and MCP1 in BM plasma were progressively increasing in agreement with in vitro experiments using several cancer cell lines. Moreover, the presence of inflammatory diseases correlated with higher levels of IL8 and MCP1 in low-risk but not in high-risk MDS. Overall, all forms of MDS feature a deregulated proinflammatory cytokine landscape in the BM and such alterations are further augmented by therapy of MDS patients with 5-AC.

Abbreviations: 5-AC, 5-azacytidine; AML, acute myeloid leukemia; BM, bone marrow; BM-MNC, bone marrow mononucleated cells; CMML, chronic myelomonocytic leukemia; CR, complete remission; DDR, DNA damage response; FAB, French, American, British classification; IPSS, International Prognostic Scoring System; IWG, International Working Group; HSC, hematopoietic stem cell; MB, myeloblasts; MDS, myelodysplastic syndrome; MDS 5q, myelodysplastic syndrome associated with isolated del(5q); MDS/MPN-u, myelodysplastic syndrome/myeloproliferative neoplasm unclassified; MRSA, methicilin resistant Staphylococus aureus infection; OS, overall survival; PB, peripheral blood; PD, progressive disease; PR, partial remission; RA, refractory anemia; RAEB, refractory anemia with excess blasts; RAEB-T, refractory anemia with excess blasts in transformation; RARS, refractory anemia with ringed sideroblasts; RCMD, refractory anemia with multilineage dysplasia; RN, refractory neutropenia; SA-β-Gal, senescence-associated β-galactosidase; SCF, stem cell factor; SD with HI, stable disease with hematologic improvement; SD without HI, stable disease without hematologic improvement

Introduction

Myelodysplastic syndromes (MDS) represent a heterogeneous group of clonal stem cell disorders characterized by ineffective hematopoiesis, peripheral cytopenia, morphological dysplasia and the risk of transformation to acute myeloid leukemia (AML). The pathogenesis of MDS is highly complex. Besides cytogenetic, molecular and genetic abnormalities in hematopoietic stem cells (HSC), extrinsic factors such as interaction with immune system and bone marrow (BM) microenvironment alterations are involved not only in the BM failure, but also in clonal expansion of

the aberrant HSC and impaired cellular differentiation.[1-4] There is growing evidence implicating inflammation-related changes, inhibitory cytokines and increased intramedullary apoptosis as contributors to ineffective hematopoiesis, specifically in the early stages of MDS.[5-7] Moreover, several recent studies implicate aberrant BM microenvironment and inflammation-related changes in progression of the MDS.[5,8] MDS has also higher rate of incidence and earlier onset among patients with autoimmune diseases.[4,9-11]

MDS treatment was rather ineffective until recent introduction of two new therapeutic approaches: immunomodulation

therapy with lenalidomide and hypomethylating therapy with nucleotide analogs 5-azacytidine (5-AC) and 5-aza-2′-deoxycytidine (decitabine).

Both hypomethylating agents are currently considered as a standard treatment for high-risk MDS (i.e., intermediate 2 and high-risk, according to the International Prognostic Scoring System [IPSS]).[12] 5-AC significantly prolongs overall survival (OS) of patients with high-risk MDS, leads to improvements in cytopenias, reduces leukemic progression and improves quality of life.[13-16] 5-AC induces 50%–60% responses in those patients, including 10%–20% complete remissions according to International Working Group (IWG) 2006 criteria.[13,14]

The mechanism of action of 5-AC is not yet fully understood. Beside the DNA demethylation, 5-AC induces DNA damage and apoptosis, and it probably exerts also immunomodulatory effects.[17,18]

As 5-AC therapy induces not only transient but also long-term changes of the cell populations in BM niche, it is of growing importance to measure and analyze these changes during the treatment. Despite the urgent need to elucidate the cytokine landscapes, however, a comprehensive analysis focusing on changes of proinflammatory cytokines in BM niche over the course of MDS is still lacking. Inspired by such pressing and clinically relevant unmet need, here we evaluated the levels of main proinflammatory cytokines in BM plasma during progression of MDS and assessed the impact of 5-AC treatment, both in clinical specimens and cultured model cancer cell lines.

Results

Therapeutic doses of 5-azacytidine induce expression of proinflammatory cytokines in vitro

Genotoxic effects of nucleotide analogs promote DNA damage response (DDR)[19] that is associated with modified expression of several cytokines.[20] Therefore, we first examined whether 5-AC used in the clinic to treat high-risk MDS patients is capable of modulating cytokine expression similarly to some other nucleotide analogs. For this purpose, we exposed HeLa cells and the immortalized BM HS-5 cells to doses of 5-AC within the range of 5-AC concentrations reached in clinical use (see Materials and Methods for details) and measured mRNA levels of 84 cytokines included in the Human Common Cytokines PCR Array at day 7 of the daily administration of 5-AC. In HeLa cells treated with 2 μM 5-AC for 7 d, 27 cytokines were at least 2-fold upregulated and three cytokines downregulated. Among the analyzed cytokines, mRNA levels of IL6, IL8, IL24, IL11, OSM and IL20 were upregulated the most (see Table S1a). Similarly, HS-5 cells exposed to 0.5 μM 5-AC resulted in the elevation of mRNA levels of 37 cytokines and 1 downregulation (Table S1b), where transcripts of OSM, IL20 and IL24 were again the most 5-AC-induced cytokines (transcripts of IL6 and IL11 were also upregulated). In summary, prolonged administration of 5-AC altered the level of several cytokine transcripts in two different cancer cell models, in a partly cell-type-dependent manner.

Apart from profiling the cytokine mRNAs, protein levels of 11 proinflammatory cytokines (IFNγ, IL1α, IL1β, IL6, IL8, IL10, IL12p70, IL27, IP10, TNFα, and MCP1) were also estimated in culture medium after the treatment with 5-AC. Fig. 1A shows that the levels of IL1α, IL6, IL8 and MCP1 were significantly elevated in supernatants of HS-5 cells treated with 0.5 μM 5-AC for 7 d. Cytokines altered at the protein level in other cell types including several AML cell lines (BM-MNC, HL-60, OCI-M2, SKM-1, HeLa, MCF7) are summarized in Fig. 1B–G.

Together, our data show that 5-AC can modify the expression of several cytokines in human cells cultured in vitro and that the spectrum of affected cytokine species is cell-type-dependent. Several proinflammatory cytokines including IL1α, IL6, IL8 and MCP1 were induced in vitro by the addition of 5-AC.
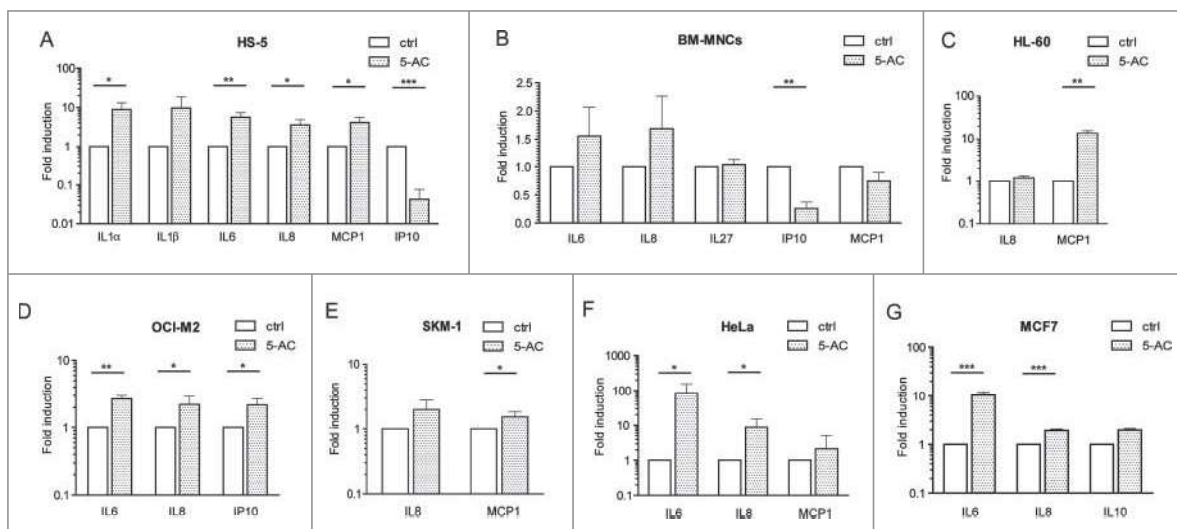
Figure 1. In vitro changes in proinflammatory cytokines after treatment with 5-AC. Changes in proinflammatory cytokines secreted by HS-5 cells after treatment with 0.5 μM 5-AC for 7 d (A), in freshly isolated BM-MNCs from five healthy donors treated with 4 μM 5-AC for 3 d (B), in HL-60 cells treated with 1 μM 5-AC for 7 d (C), in OCI-M2 cells treated with 1 μM 5-AC for 7 d (D), in SKM-1 cells treated with 0.5 μM 5-AC for 7 d (E), in HeLa cells treated with 2 μM 5-AC for 7 d (F), and in MCF7 cells treated with 2 μM 5-AC for 7 d (G). The changes in cytokine secretion are given only for the cytokines with measured values above the lower limit of detection. The data represent the mean of at least two independent experiments +/− SD for all cell types, all treated in at least triplicates. The resulting measurements were analyzed by paired t-test. p values < 0.05 were considered as statistically significant. Following proinflammatory cytokine changes reached the statistical significance: for HS-5 cell line (A) IL1α ($p = 0.017$), IL6 ($p = 0.003$), IL8 ($p = 0.031$), MCP1 ($p = 0.025$), IP10 ($p < 0.001$); for HL-60 cells (C) MCP1 ($p = 0.005$); for OCI-M2 cells (D) IL6 ($p = 0.002$), IL8 ($p = 0.042$), IP10 ($p = 0.023$); for SKM-1 cells (E) MCP1 ($p = 0.042$); for HeLa cells (F) IL6 ($p = 0.031$) and IL8 ($p = 0.031$); and for MCF7 cells (G) IL6 ($p = 0.001$) and IL8 ($p < 0.001$). In case of freshly isolated BM-MNCs, only the downregulation of IP10 after 5-AC administration reached the statistical significance ($p = 0.002$).

Several proinflammatory cytokines are elevated in bone marrow of MDS patients

Before considering the effect of 5-AC therapy on cytokine milieu in BM of MDS patients, levels of 11 cytokines were estimated in BM plasma of large cohort of 188 MDS (both high- and low-risk) patients and compared with BM plasma levels in healthy donors. Based on robust linear mixed effects model analysis, IL8, IP10, MCP1 and IL27 were significantly elevated in BM of high-risk and low-risk MDS compared to healthy donors (Fig. 2A–D). The levels of IFNγ, IL1α, IL1β, IL6, IL10, and TNFα were not significantly altered in analyzed MDS samples (for details, see Fig. S1) As for IL12p70, its level in MDS was significantly lower ($p = 0.02$; Fig. S1).

Altogether, our data showed that interleukins IL8 and IL27 and chemokines IP10 and MCP1 were elevated in BM of all groups of MDS patients.

IL8, IL27 and MCP1 are further elevated in bone marrow plasma of MDS patients during 5-azacytidine therapy

To investigate the effect of 5-AC therapy on the level of proin-flammatory cytokines in BM of MDS patients, BM plasma samples of MDS patients (mostly high-risk—see Table 2 for details) were collected before the initiation of therapy, after the end of the 4th and 8th cycle (mostly at day 7 after the last dose of 5-AC) and levels of the 11 cytokines were measured as above. The statistical comparison of six groups (healthy donors, low-risk MDS, AML, 5-AC-treated before therapy, after four cycles of 5-AC and after eight cycles of 5-AC) using Kruskal–Wallis ANOVA revealed that the levels of IL8, IP10 and MCP1 were significantly altered in low-risk MDS, 5-AC-treated before therapy and in AML patients in comparison to healthy controls (Fig. 3A–D) underscoring the values obtained in a large non-structured cohort of patients. The increase in IL27 in this cohort did not reach the statistical significance ($p = 0.070$). Strikingly, when examined by robust linear mixed effects model analysis, the levels of IL8, IL27 and MCP1 in the 5-AC-treated group significantly increased during 5-AC therapy when compared to initial values before therapy (Fig. 3A–D). As for IP10, changes observed during the course of therapy were not significant.

To summarize, our data showed that interleukins IL8 and IL27 and chemokine MCP1 increased in BM of MDS patients during the therapy with 5-AC.
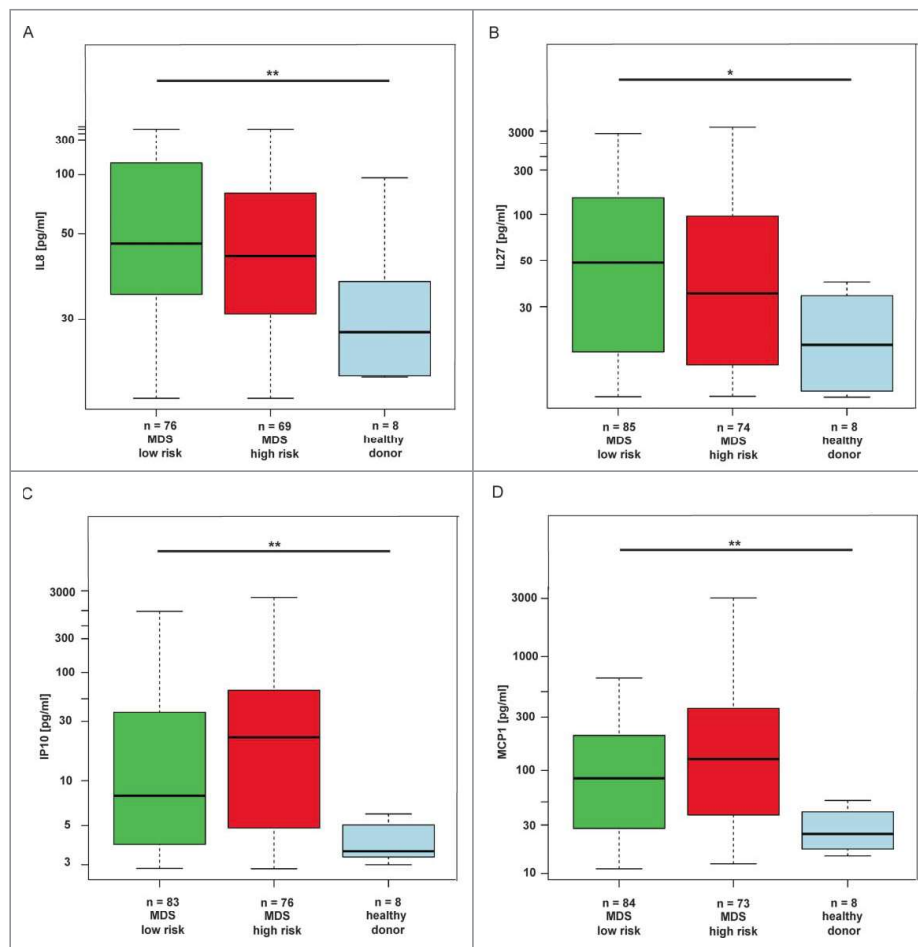
Figure 2. Changes in cytokines in low-risk MDS, high-risk MDS and AML compared to healthy donors. The box plot graphs demonstrate the upper and lower quartiles, and the median is represented by a short black line within the box for each group. The p value signifies the difference for the given cytokine measurements between all three groups. The data set was analyzed by robust linear mixed effects model at the 95% confidence interval. p values < 0.05 were considered as statistically significant. Each significantly upregulated cytokine is depicted in a separate graph, i.e., for (A) IL8 ($p = 0.01$), for (B) IL27 ($p = 0.04$), for (C) IP10 ($p = 0.01$) and for (D) MCP1 ($p < 0.01$).

Table 1. Clinical characteristics of 188 patients with samples of BM plasma analyzed for cytokine content with 11-plex.

MDS low risk group	
number of patients	94
number of samples	125
number of patients with multiple BM aspirations	31
patient age at BM aspiration (years), median (range)	72 (46-86)
males/females	54 / 71
Sample distribution according to WHO 2008	
MDS 5q	23
RCMD	56
RARS	1
MDS RA	1
MDS RN	3
RAEB I	31
CMML I	7
MDS/MPN-u	3
IPSS risk group	
low	58
intermediate I	67
intermediate II	0
high	0
red cells transfusion requiring, n (%)	84 (67.2%)
co-morbidities	
diabetes mellitus	33
other inflammatory diseases	34
psoriasis	3
asthma	3
chronic gastritis	1
rheumatoid arthritis	12
ongoing treatment of bladder carcinoma	2
lupus	2
MRSA	1
gout	3
renal insufficiency	10
metabolic syndrome	1
MDS high risk group and AML	
number of patients	94
number of samples	140
number of patients with multiple BM aspirations	46
patient age at BM aspiration (years), median (range)	72.5 (55-86)
males/females	68 / 72
Sample distribution according to WHO 2008	
RCMD	3
RARS	1
RAEB I	12
RAEB II	79
CMML I	5
CMML II	6
AML < 30% MB*	28
AML > 30% MB	4
IPSS risk group	
low	0
intermediate I	0
intermediate II	67
high	35
not applicable	38
red cells transfusion requiring, n (%)	77 (55%)
co-morbidities	
diabetes mellitus	28
other inflammatory diseases	18
hepatitis C	1
rheumatoid arthritis	5
Sweet syndrome	1
renal insufficiency	14

Table 2. Patient characteristics.

| 5-AC-treated patients with multiple BM aspirations	
number of patients	**38**
age, median (range)	70 (45-85)
male/female	19/19
WHO 2008	
AML/MDS < 30% MB*	5
RAEB I	9
RAEB II	18
RCMD	2
CMML I	1
CMML II	2
MDS/MPN-u	1
IPSS risk group	
low	0
intermediate I	9
intermediate II	20
high	4
response to 5-AC therapy	
number of samples at each time point	
before therapy	35
After 4 cycles	36
After 8 cycles	18
Response as evaluated after 4th cycle	
number of responders	**20**
SD with HI	2
PR	9
CR	2
Cri	7
number of non-responders	**16**
SD without HI	12
PD	4
MDS low risk group	
number of patients	**35**
age at diagnosis, median (range)	**68 (46-83)**
male/female	**9 / 26**
WHO 2008	
MDS 5q	10
RCMD	21
MDS RN	3
MDS/MPN-u	1
IPSS risk group	
low	35
intermediate I	0
intemediate II	0
high	0
AML sub-group	
number of patients	**24**
age at diagnosis, median (range)	73.5 (57-86)
male/female	16/8
WHO 2008	
AML/MDS < 30% MB*	12
AML > 30% MB	12
IPSS risk group	
high	12
not applicable	12
Healthy donors	
number of donors	8
age at BM aspiration, median (range)	39 (29-54)
male/female	5 / 3

Correlation of cytokine values with the responsiveness to 5-azacytidine therapy

Next, we tried to discriminate whether the increase of IL8, IL27 and MCP1 correlated with the outcome of the 5-AC therapy and hence whether they can be utilized as therapy response factors. For this purpose, the patients receiving 5-AC therapy were analyzed according to criteria of their response (see Materials and Methods for details). When comparing the IL8 levels among responders (n = 20) and non-responders (n = 18; see the colored dots in Fig. 3A), we found that responders have lower median levels of IL8 than non-responders after 4th and 8th cycle of 5-AC therapy; however, this difference did not reach the
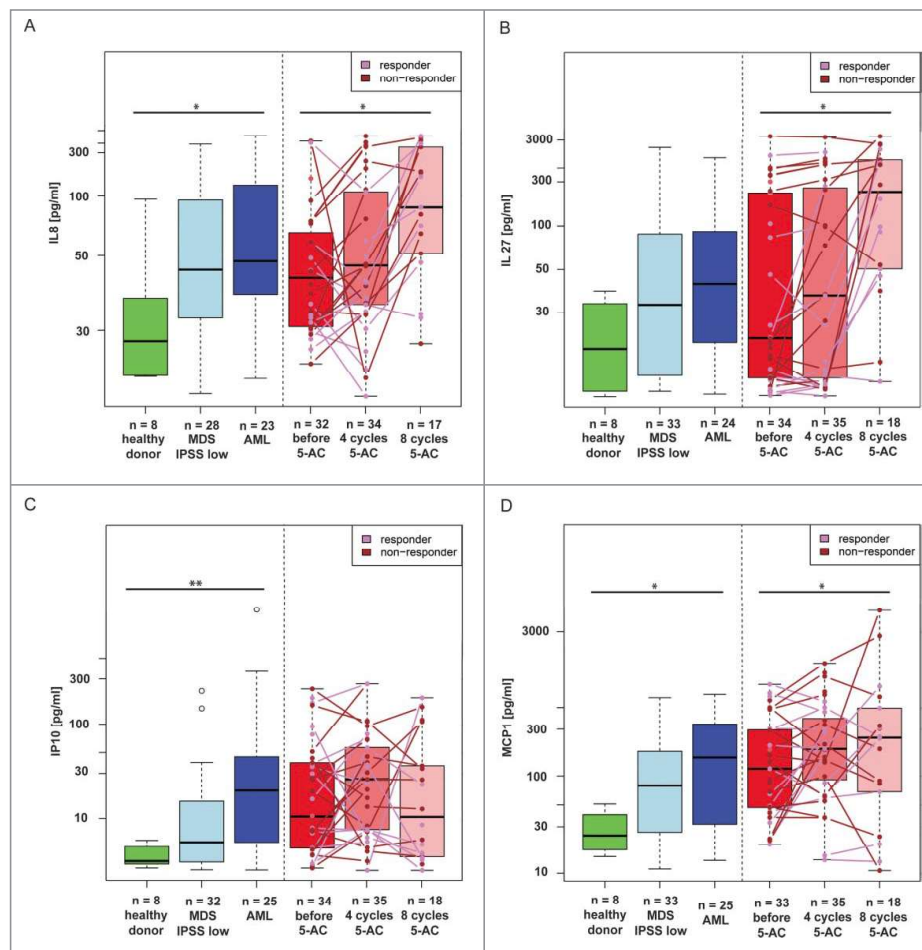
Figure 3. Changes in IL8, MCP1, IP10 and IL27 in BM of MDS patients during therapy with 5-AC. The box plot graphs demonstrate the upper and lower quartiles, and the median is represented by a short black line within the box for each group. The empty circles represent measurements for individual patients whose measured values were numerically distant from the other measurements (outliers; outside 1.5 times the interquartile range above the upper quartile and below the lower quartile). The changes of cytokine values among the individual 5-AC-treated patient (n = 38) are depicted as colored dots of either pink for responders (n = 20) or dark red for non-responders connected by the lines of the same color. Kruskal–Wallis ANOVA compared the changes among the cytokine values of healthy donors, AML patients and low-risk MDS (IPSS low) with the following results: IL8, $p = 0.041$ (A); IL27, $p = 0.07$ (B); IP10, $p = 0.002$ (C) and MCP1, $p = 0.018$ (D). The robust linear mixed effects model analysis compared changes in cytokine values in repeated samples of 38 5-AC-treated patients and showed the increase during 5-AC therapy when compared to initial values before therapy for IL8, $p = 0.01$ (A); IL27, $p < 0.01$(B); MCP1, $p < 0.01$ (D); but not for IP10, $p = 1.00$ (C).

statistical significance ($p = 0.06$). A similar scenario was observed for IL27 (Fig. 3B), where the levels of IL27 in responders showed again a lower median value compared to non-responders, but this change was not significant ($p = 0.22$). MCP1 levels did not show any correlation with the response to therapy ($p = 0.69$).

Among the 11 studied cytokines, the levels of IL8 and IL27 showed a trend of positive correlation with the response to 5-AC therapy in MDS patients; however, a larger cohort of 5-AC-treated MDS patients has to be analyzed in order to reach definitive conclusions.

Inflammatory comorbidities contribute to elevated levels of IL8 and MCP1 in low-risk MDS patients

Next, we asked whether the increased levels of IL8, IL27, IP10 and MCP1 found in our cohort of MDS patients are a characteristic feature of MDS *per se* or are due to other associated diseases, namely those with inflammatory component.[4,9,10] We compared the groups of patients with inflammatory diseases (see Materials and Methods) against those without diagnosed inflammation. Among low-risk MDS patients, significantly higher levels of

MCP1 and IL8 were found in patients with ongoing inflammation compared to those without inflammation, indicating that inflammatory comorbidities contribute further to enhanced levels of these two cytokines. On the other hand, among the high-risk MDS patients indication of such correlation, though statistically non-significant, was found only for IL8 ($p = 0.07$; Fig. 4A–B). Furthermore, levels of IP10 and IL27 did not show any correlation with inflammatory comorbidities among either low- or high-risk MDS patients (Fig. 4C–D).

To conclude, inflammatory comorbidities contribute to elevation of IL8 and MCP1 in low-risk MDS patients, while in high-risk patients such contribution was not statistically significant. Among high-risk MDS patients, only IL8 correlated with associated inflammatory diseases, whereas MCP1 levels were not affected by the associated inflammation.

The levels of cytokines in blood plasma do not strictly correlate with the levels in bone marrow plasma

In order to discriminate whether the source of IL8, IL27, IP10 and MCP1 is intramedullary or extramedullary, we have
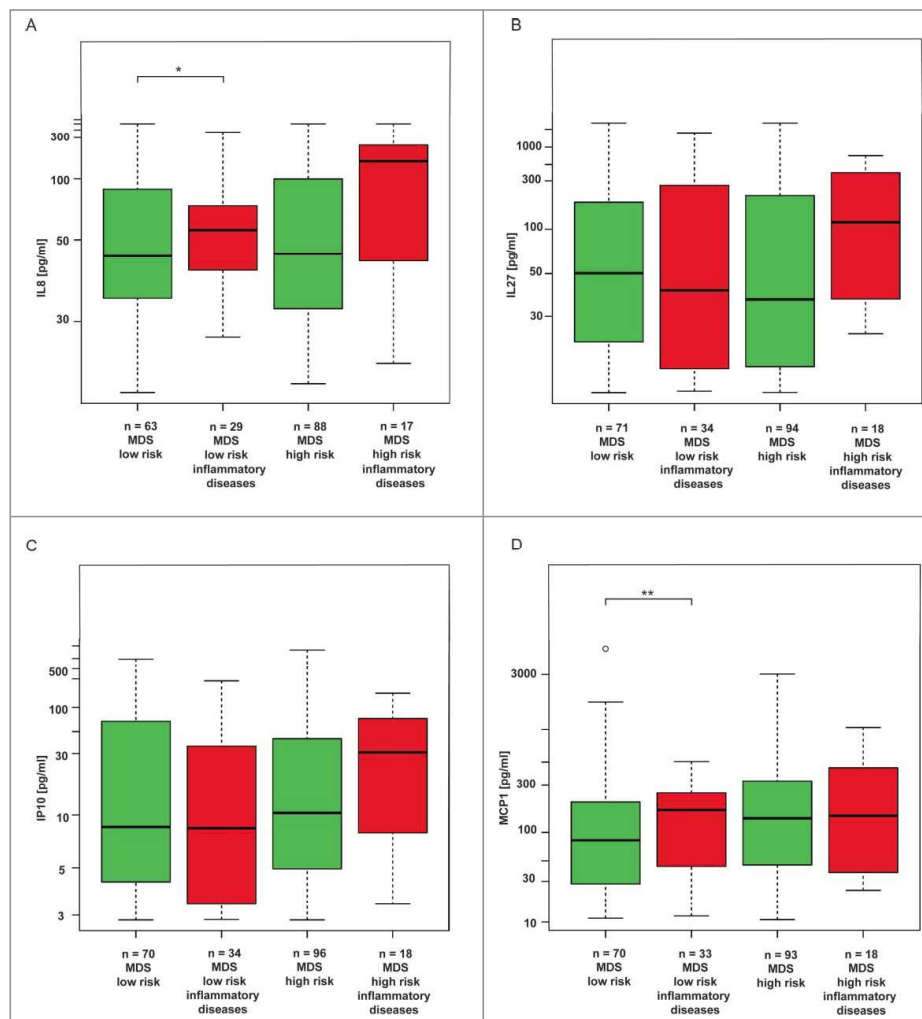
Figure 4. Analysis of the effect of inflammatory comorbidities on the cytokine values in low-risk MDS and high-risk MDS and AML. The box plot graphs demonstrate the upper and lower quartiles, and the median is represented by a short black line within the box for each group. The empty circle represents outlier measurement. The data set was analyzed by robust linear mixed effects model at the 95% confidence interval. p values < 0.05 were considered as statistically significant and were calculated for the measured differences among inflamed and non-inflamed MDS patients in their respective risk group, i.e. (A) IL8 for low-risk MDS $p = 0.05$; for high-risk MDS $p = 0.07$; (B) IL27 for low-risk MDS $p = 0.25$; for high-risk MDS $p = 0.48$; (C) IP10 for low-risk MDS $p = 0.37$; for high-risk MDS $p = 0.30$, and (D) MCP1 for low-risk MDS $p < 0.01$; for high-risk MDS $p = 0.61$.

collected peripheral blood (PB) sample from several patients (n = 22) shortly before the BM aspiration and compared the levels of proinflammatory cytokines in both fluids. The cytokine values of IL8 and MCP1 in PB plasma and BM plasma did not correlate well with each other (Fig. S2). For IL27 and IP10, the values appeared to be higher in BM than in PB and thus it is reasonable to assume that the BM was the source tissue. In contrast, for IL8, we observed the opposite tendency, indicating that estimation of cytokines from the PB plasma could be insufficient to obtain an accurate projection about the levels of these four cytokines in the BM milieu.

Discussion

The aberrant cytokine milieu in BM has been considered as one of the hallmarks of MDS. However, due to its more convenient accessibility, the vast majority of studies analyzed cytokine changes in PB.[21-23] In this study, we estimated the levels of key proinflammatory cytokines in BM plasma of patients suffering from MDS/AML. We found that IL8, IP10/CXCL10, MCP1/CCL2 and IL27 were significantly elevated and IL12p70

decreased in low-risk, high-risk and AML patients compared to healthy donors. Moreover, by repeated sampling of the high-risk MDS individuals undergoing 5-AC therapy, we found that the levels of IL8, IL27 and MCP1 in BM plasma were progressively and significantly increasing in agreement with our *in vitro* experiments, where the levels of IL8 and MCP1 and other proinflammatory cytokines were induced in several cells lines in response to short-term exposure to 5-AC.

It is generally accepted that the therapeutic anticancer effects of 5-AC and decitabine are attributable to alterations of epigenetic regulatory mechanisms affecting proliferation of malignant cells.[24-26] Moreover, it was shown that decitabine can cause replication stress-associated DDR.[27] As a result, DDR-induced block of cell cycle progression by activation of cell cycle checkpoints could act as a parallel mechanism of antiproliferative effects of decitabine and 5-AC. Indeed, in our *in vitro* experiments with cell lines exposed to therapeutic doses of 5-AC following the clinical regime of 5-AC administration in seven consecutive daily doses, we observed that 5-AC caused DNA damage already during 24 h after the first dose, which was associated with induction of p21$^{\text{waf1/cip1}}$, cell cycle block

and the development of senescence-like phenotype (data not shown). This is in concert with the previous study of Fandy et al. who showed that 5-AC induces DNA damage in PB mononuclear cells of MDS patients.[28] Therefore, both alteration of epigenetic control of gene expression and development of cellular senescence can affect the expression of cytokines, as was indeed confirmed by change of levels of several cytokine transcripts in the cell lines exposed to 5-AC *in vitro*. Thus, similar to other nucleotide analogs,[20] 5-AC affects cytokine expression. Although the precise spectra of 5-AC-altered cytokines were cell type-specific, induction of IL6, IL8 and MCP1 were commonly shared, consistent with previous studies using different senescence inductors.[29-31]

Given the cell type specificity in cytokine response to 5-AC and taking into account the complex signal communication among cells that compose tissues of the organism, presumably the final outcome of 5-AC-induced cytokine response at the systemic level would reflect such intricate interactions. Therefore, we focused on analyses of major proinflammatory cytokines in the BM environment, a tissue niche most intimately associated with MDS. Our analysis of the cohort of 188 MDS/AML patients showed that four cytokines IL8, IP10, MCP1 and IL27 were elevated and IL12p70 decreased in BM of both low-risk and high-risk MDS patients, as well as in AML patients indicating that the inflammatory mediators contribute to the pathogenesis of MDS.

IL8 is a cytokine, whose elevated protein levels have been already described in PB of MDS/AML patients.[32] IL8 plays a role in proinflammatory reactions, specifically in the activation and trafficking of neutrophils (reviewed in ref. 33). Its elevated levels are also characteristic for the primary myelofibrosis.[34,35] It has been proposed that CD34+ blasts are the major producers of IL8 in BM of MDS patients,[32] because the initially elevated levels of IL8 in BM serum of MDS or AML patients subsequently decrease with the complete remission and disappearance of CD34+ blasts. Later, Schinke et al. detected the elevated IL8 transcripts in AML/MDS BM samples.[36] Moreover, they found that IL8 supports growth and survival of leukemic cell lines and that the short-hairpin RNA-mediated downregulation of IL8 receptor CXCR2 resulted in increased survival of mice xenografted with lymphoma U-937 cells.[36] IL8 is elevated in blood also during other inflammatory diseases such as cystic fibrosis, rheumatoid arthritis, systemic lupus erythematosus, psoriasis, etc.[33] IL8 is also the factor being almost invariably induced in normal and cancer cells undergoing various types of cellular senescence including oncogene-,[29,30] stress/ionizing irradiation-,[31] bacterial toxin-,[37] drug-induced,[20] and replicative senescence.[38] Notably, IL8 itself can induce senescence *in vitro*.[29]

The mechanism of IL27 induction in MDS patients is unclear. IL27 is a member of IL12 family of cytokines with a pleiotropic role in proinflammatory and anti-inflammatory immune responses and acquired immunity. IL27 is produced by antigen-presenting cells and is regulating the development of Th cells (reviewed in ref. 39). Furthermore, IL27 is involved in differentiation of HSC.[40] Notably, besides other proinflammatory cytokines,[41] IL27 is capable of triggering both IP10 and MCP1[42] suggesting its upstream role in the induction of IP10 and MCP1. IL27 was not induced by 5-AC in several cell types *in vitro* (this study) or other senescence-inducing stimuli, such as ionizing radiation (data not shown). To our knowledge,

there is no report (or indication in available transcriptome profiles of senescent cells) that IL27 is induced during the development of senescence and produced by the senescent cells. This finding is unexpected, given that being a STAT1/STAT3 activator, IL27 might be expected to induce cellular senescence in a way similar to IFNγ[43,44] or IL6.[30]

Like IL8, IP10 and MCP1 are components of the senescence-associated secretome.[20,45] IP10/CXCL10 is also a protein of pleiotropic functions, involved in processes of chemoattraction, cell adhesion, and suggested to support proliferation of cancer cells.[46]

It was reported that senescent cells are present in BM of MDS patients, as suggested from elevated senescence-associated β-galactosidase (SA-β-Gal) staining and induction of the cyclin-dependent kinase inhibitor p16INK4a in BM.[47] Moreover, Xiao et al. showed recently that the number of CD34+ cells positive for SA-β-Gal increased in lower-risk MDS patients and these CD34+ cells were positive for other traits of senescence, such as elevated reactive oxygen species, DNA damage and p21wafl/cip1.[48] Besides, several other studies reported the presence of DNA damage, persistent activation of DDR and NFκB signaling in BM of MDS patients.[49-53] In addition, it should be noted that prolonged DDR caused by various factors including activated oncogenes is a driver of (proinflammatory) cytokine elevation (for further details, see e.g. refs. 31, 54) implicated in the development of leukemia.[55]

It is well known that several cytokine species are responsible for collateral DNA damage (bystander effect) induced by various settings such as radiotherapy (reviewed in ref. 56). Bystander effect is also thought to play an important role in the development of cancer and chronic diseases (reviewed in ref. 57). Cellular senescence as a precancerous state[58,59] contributes to the bystander DNA damage[60] by secretion of several cytokines that can trigger DDR in the neighboring cells.[38,44] Strikingly, MCP1/CCL2 elevated in MDS patients, as shown here, is a factor considered to cause systemic DNA damage.[57,61-63] Its source in MDS patients may be both activated macrophages[64] and senescent cells themselves. 5-AC-induced elevation of MCP1 (and IL8) observed *in vitro* and increasing levels of MCP1 (and IL8) in patients on 5-AC therapy is in line with the ability of 5-AC to induce DNA damage[28] and cellular senescence. Hence, the crosstalk among cytokine signaling, together with the ability of some cytokine pathways to induce DNA damage, can form an interlocked self-sustained network[65] that may contribute to the genomic instability in BM responsible both for the development of MDS and its progression to AML. However, further studies are needed to support this hypothesis. Like MCP1, the levels of IL8 and IL27 were even higher in BM plasma in patients undergoing 5-AC therapy.

We also considered the contribution of the inflammatory comorbidities frequently associated with MDS to the elevated levels of IL8, IP10, MCP1 and IL27. Our data showed that inflammatory diseases represent a significant factor supporting the elevation of IL8 both in low-risk and high-risk patients and MCP1 in low-risk patients, but not of IL27 and IP10.

IL12, an early proinflammatory cytokine linking innate and adaptive immunity, represents one of the most important cytokines in antitumor immunity (reviewed in ref. 66). This cytokine is produced mainly by antigen-presenting cells, such as dendritic cells, macrophages, monocytes or B cells upon their activation

via Toll/like receptor signaling. Here, we report downregulation of IL12 in BM plasma of both low-risk and high-risk MDS as well as in AML patients. Since IL12 is a principle cytokine produced by functional antigen-presenting cells, the observed decrease in its production suggests an impaired capacity to prime effective immune responses among MDS patients. Indeed, Wang et al. described that mesenchymal stem cells derived from high-risk MDS patients impaired functions of dendritic cells, including IL12 secretion.[67] On the other hand, levels of IFNγ, Th$_1$ cytokine, which is a crucial mediator of the IL12-primed immune responses, were not significantly changed among the MDS patients, as compared to healthy individuals. So the clinical significance of the IL12 downregulation is unclear, especially considering the effects of another IL12-family member, IL27 that also plays a role in the Th$_1$-response activation.

Due to the diverse pathophysiological functions of the IL8, IL27 and MCP1, we attempted to evaluate, whether their increase during the 5-AC therapy can serve as a prognostic factor of the therapeutic response. Although we observed indication that responders tend to harbor lower levels of IL8 during the course of therapy compared to non-responders, the relatively small sample size did not allow for a definitive conclusion.

Further work is needed to resolve the primary cause of DDR/senescence and impact of senescence and its proinflammatory component on progression of MDS to acute leukemia. Loss-of-function of the key DDR kinase ATM is frequently observed in lymphoproliferative diseases and the consecutive increase of tumor suppressor p19ARF[68] (due to loss of the ATM-regulated turnover of ARF protein in such tumors) can promote senescence as a secondary oncogenesis barrier. Indeed, some reports indicate that the loss of p19ARF has a negative impact on survival of AML patients (see e.g., reference 69) indicating that the p19ARF pathway may provide an oncogenesis barrier also in AML.

To conclude, all forms of MDS are associated with increased levels of several proinflammatory cytokines in the BM, a feature that is further augmented by therapy with 5-AC.

Materials and methods

Patients

In total, 265 BM samples from 188 patients diagnosed with MDS, AML or chronic myelomonocytic leukemia (CMML) were collected between 2009 and 2015. There were 125 samples from 94 patients with low-risk MDS (IPSS intermediate I or low) and 140 samples from 94 patients with high-risk MDS (IPSS high or intermediate II). Characteristics of patients are presented in Table 1. For controls, we used BM aspirates from eight healthy adult donors. Samples were obtained from patients diagnosed and treated at the Department of Haematology, 1st Faculty of Medicine, Charles University and General University Hospital. Written informed consent was provided in accordance with the Helsinki Declaration.

5-azacytidine-treated MDS cohort

As for BM analysis of 5-AC-treated patients, we collected repeated samples from 38 MDS patients (IPSS int I, int II or IPSS high). Characteristics of 5-AC-treated patients are in

Table 2. 5-AC was administered subcutaneously for 7 d (regime 5-2-2) at a dose of 75 mg/m^2/d. BM aspirates and PB were collected before 5-AC therapy and at day 7 after the completion of the 4th and 8th cycle, at which time the response to treatment was assessed according to IWG criteria.[70]

Bone marrow and peripheral blood plasma collection

BM aspirates were obtained from the posterior iliac crest and collected into EDTA-coated vacutainers (BD 367844, Becton Dickinson) and PB was collected into vacutainers with Lithium heparin (BD 368824, Becton Dickinson) shortly prior to the BM aspiration. The patients were not subjected to any type of transfusion therapy 24 h prior to the BM aspiration. PB plasma and BM plasma were separated from cells shortly after the aspiration by centrifugation at 300 × g for 3 min, resulting in the separation of plasma, which was transferred into microcentrifuge tube and centrifuged again at 3300 × g for 3 min. Resulting supernatants of both BM and PB plasma were snap frozen on dry ice and stored at –80°C until the time of analysis.

Inflammatory cytokine measurement in bone marrow and blood plasma

Inflammatory cytokine content in BM plasma and/or PB plasma were measured using Human Inflammation 11-Plex (IFNγ, IL1α, IL1β, IL6, IL8, IL10, IL12p70, IL27, IP10, MCP1, TNFα; YSL Bioprocess Development Co.). The samples were measured on LSRII flow cytometer (BD Biosciences). The BM aspiration and handling of the healthy donor samples was identical to the patient samples. By doing so, we have reduced the vacutainer coating-related changes in cytokine profiles.[71] For the purposes of data analysis, the measurements above the upper detection limits of the assay were set to the value of detection limit and samples with no detected beads for a given cytokine were regarded as missing measurements.

Human Common Cytokines PCR Array (PAHS-021, Qiagen) was done as published previously.[20]

Cell culture

Human cervical carcinoma cell line HeLa was cultured in Dulbecco's modified Eagle's medium (D-MEM) supplemented with 10% fetal bovine serum (FBS, Gibco, Thermo Fisher Scientific) and 100 U/mL penicillin/100 μg/mL streptomycin (Pen/Strep, Sigma-Aldrich). HPV-16 E6/E7-transformed human mesenchymal stem cell line HS-5 was cultured in Roswell Park Memorial Institute medium (RPMI-1640) supplemented with 10% FBS, 1% non-essential amino acids (NEAA; Sigma-Aldrich) and Pen/Strep (100 U/mL/100 μg/mL). Breast adenocarcinoma cell line MCF7 was cultured in D-MEM, 10% FBS and Pen/Strep (100 U/mL/100 μg/mL). Human promyelocytic leukemia cell line HL-60 was cultured in RPMI-1640, 10% heat-inactivated FBS, Pen/Strep (100 U/mL/100 μg/mL) and 1% NEAA. Human AML cell line OCI-M2 was cultured in Iscove's Modified Dulbecco's Medium supplemented with 20% heat-inactivated FBS, 1% NEAA and Pen/Strep (100 U/mL/100 μg/mL). Human AML cell line SKM-1 was cultured in RPMI-1640 supplemented with 20% heat-inactivated FBS, 1% NEAA and Pen/Strep (100 U/mL/100 μg/mL). Cells were kept at 37°C under 5% CO$_2$ atmosphere and 95% humidity.

Bone marrow cultivation

Fresh BM aspirates from healthy donors (see above for BM aspiration procedure) was subjected to erythrocyte lysis via addition of pre-warmed NH_4Cl lysis solution (156 mM NH_4Cl, 17 mM NaCl, 126.6 μM EDTA) in 1: 50 ratio. The tube was inverted several times and incubated at 37°C for 10 min. The cells were then pelleted by centrifugation at 400 × g for 10 min at 4°C and subsequently washed with 1 × PBS. The BM mononucleated cells (BM-MNC) were then cultured at density of 0.5–1.2 × 10^6/mL culture medium for 4 d in RPMI-1640 supplemented with 15% FBS with low endotoxin content, 1% NEAA, Pen/Strep (100 U/mL/100 μg/mL) and 20 μg/mL stem cell factor (SCF; Sigma-Aldrich).

5-azacytidine administration

5-AC was dissolved in distilled water and kept at −80°C in 10 mM aliquots. Daily dose of 5-AC was administered to cell cultures for seven (human cell lines) or three (in vitro BM experiments) consecutive days and cells were harvested 24 h after the last treatment. The concentration of 5-AC was selected according to response of the individual cell type (HeLa, HS-5, MCF7, HL-60, OCI-M2, SKM-1) for the best ratio between the cell cycle block and apoptosis (not shown). The selected dose of 5-AC was in the lower end of the concentration range measured in BM after the administration of 5-AC[72]: 2 μM for HeLa and MCF7, 0.5 μM for HS-5 and SKM-1, 1 μM for HL-60 and OCI-M2 and 4 μM for BM-MNCs, respectively.

Determination of inflammatory cytokines in cultivation media

The culture medium was collected 24 h after the change of fresh medium (and treatment with 5-AC when needed) and the number of cells per dish was counted. The concentration of secreted cytokines was measured using Human Inflammation 11-plex (YSL Bioprocess Development Co.) on flow cytometer LSRII (BD Biosciences) according to manufacturer's protocol. The cytokine levels were then calculated as pg/mL/10^5 cells.

Statistics

In vitro cytokine profiles

The obtained cytokine values in cultivation media for each cell line were compared to untreated sample via paired t-test. Analyses were conducted using the GraphPad Prism version 5.00 for Windows, GraphPad Software, San Diego California USA, www.graphpad.com.

5-azacytidine-treated patient cohort

For the purpose of data analysis, 5-AC-treated patients were divided into two groups depending on their response to therapy: responders (hematological improvement only, partial remission, complete remission, and complete remission with incomplete BM recovery) and non-responders (stable disease without HI, progressive disease) and the analyses of changes in cytokine levels were performed. The levels of cytokines in BM plasma of 5-AC-treated patients were compared to the cytokine levels in three other groups. First, eight healthy controls were used to measure the normal cytokine levels in the BM. Second,

the BM plasma from 35 treatment-naive MDS patients with IPSS low was used to set the baseline values of the MDS cytokine profile. To assess the BM cytokine levels at the disease final stage, BM aspirates from 24 AML patients on best supportive care therapy that were not treated with hypomethylating agents at least 2 months prior to the BM aspiration and their prior BM aspirations were not included in 5-AC-treated cohort, were used. Obtained cytokine values were transformed using Box-Cox procedure and repeated measurements of 5-AC-treated patients were analyzed using robust linear model with mixed effects. Comparisons of 5-AC-treated patients, MDS low risk, AML patients and healthy controls were subjected to a Kruskal–Wallis ANOVA. p values < 0.05 were considered as statistically significant.

Patient cohort with respect to comorbidities

The enlarged cohort of BM samples included a total number of 125 BM aspirates from 94 low-risk MDS patients and 140 BM aspirates from 94 high-risk patients whose proinflammatory diseases and transfusion dependency were detected at the time of BM aspiration and their diagnostic subgroup and IPSS risk was re-evaluated according to the clinical results at the given time point. For this analysis, other factors such as the ongoing therapy with 5-AC, lenalidomide, hydroxyurea (Litalir) or arabinoside were not taken into account. Inflammatory comorbidities identified at the time of BM aspiration as the potential sources of proinflammatory cytokines are listed in Table 1.

Since we were unable to find differences in any of the measured cytokines between the high-risk (IPSS int II and high) MDS and patients at the AML stage, when not controlling for other proinflammatory parameters, we have conducted further analysis by treating the values from high-risk MDS and AML as one group.

Obtained cytokine values were transformed using Box-Cox procedure, and analyzed using robust linear model with mixed effects. The p values <0.05 were considered as statistically significant. Analyses were conducted using the R statistical package, version 3.1.2, R Core Team (2014).

Disclosure of potential conflicts of interest

No potential conflicts of interest were disclosed.

Author contributions

References

1. Cogle CR, Saki N, Khodadi E, Li J, Shahjahani M, Azizidoost S. Bone marrow niche in the myelodysplastic syndromes. Leuk Res 2015; 39:1020-7; PMID:26276090; http://dx.doi.org/10.1016/j.leukres.2015.06.017

2. Abe-Suzuki S, Kurata M, Abe S, Onishi I, Kirimura S, Nashimoto M, Murayama T, Hidaka M, Kitagawa M. CXCL12+ stromal cells as bone marrow niche for CD34+ hematopoietic cells and their association with disease progression in myelodysplastic syndromes. Lab Invest 2014; 94:1212-23; PMID:25199050; http://dx.doi.org/10.1038/labinvest.2014.110

3. Balderman SR, Li AJ, Hoffman CM, Frisch BJ, Goodman AN, LaMere MW, Georger MA, Evans AG, Liesveld JL, Becker MW, et al. Targeting of the bone marrow microenvironment improves outcome in a murine model of myelodysplastic syndrome. Blood. 2016 Feb 4; 127 (5):616-25; PMID:26637787; http://dx.doi.org/10.1182/blood-2015-06-653113

4. Kristinsson SY, Bjorkholm M, Hultcrantz M, Derolf AR, Landgren O, Goldin LR. Chronic immune stimulation might act as a trigger for the development of acute myeloid leukemia or myelodysplastic syndromes. J Clin Oncol 2011; 29:2897-903; PMID:21690473; http://dx.doi.org/10.1200/JCO.2011.34.8540

5. Ganan-Gomez I, Wei Y, Starczynowski DT, Colla S, Yang H, Cabrero-Calvo M, Bohannan ZS, Verma A, Steidl U, Garcia-Manero G. Deregulation of innate immune and inflammatory signaling in myelodysplastic syndromes. Leukemia 2015; 29:1458-69; PMID:25761935; http://dx.doi.org/10.1038/leu.2015.69

6. Kurotaki H, Tsushima Y, Nagai K, Yagihashi S. Apoptosis, bcl-2 expression and p53 accumulation in myelodysplastic syndrome, myelodysplastic-syndrome-derived acute myelogenous leukemia and de novo acute myelogenous leukemia. Acta Haematol 2000; 102:115-23; PMID:10692673; http://dx.doi.org/10.1159/000040984

7. Albitar M, Manshouri T, Shen Y, Liu D, Beran M, Kantarjian HM, Rogers A, Jilani I, Lin CW, Pierce S. Myelodysplastic syndrome is not merely "preleukemia". Blood 2002; 100:791-8; PMID:12130488; http://dx.doi.org/10.1182/blood.V100.3.791

8. Mangan JK, Luger SM. A paraneoplastic syndrome characterized by extremity swelling with associated inflammatory infiltrate heralds aggressive transformation of myelodysplastic syndromes/myeloproliferative neoplasms to acute myeloid leukemia: a case series. Case Rep Hematol 2012; 2012:582950; PMID:22928125; http://dx.doi.org/10.1155/2012/582950

9. Anderson LA, Pfeiffer RM, Landgren O, Gadalla S, Berndt SI, Engels EA. Risks of myeloid malignancies in patients with autoimmune conditions. Br J Cancer 2009; 100:822-8; PMID:19259097; http://dx.doi.org/10.1038/sj.bjc.6604935

10. Ramadan SM, Fouad TM, Summa V, Hasan S, Lo-Coco F. Acute myeloid leukemia developing in patients with autoimmune diseases. Haematologica 2012; 97:805-17; PMID:22180424; http://dx.doi.org/10.3324/haematol.2011.056283

11. Al Ustwani O, Ford LA, Sait SJ, Block AM, Barcos M, Vigil CE, Griffiths EA, Thompson JE, Wang ES, Ambrus J Jr et al. Myelodysplastic syndromes and autoimmune diseases–case series and review of literature. Leuk Res 2013; 37:894-9; PMID:23692654; http://dx.doi.org/10.1016/j.leukres.2013.04.007

12. Greenberg P, Cox C, LeBeau MM, Fenaux P, Morel P, Sanz G, Sanz M, Vallespi T, Hamblin T, Oscier D et al. International scoring system for evaluating prognosis in myelodysplastic syndromes. Blood 1997; 89:2079-88; PMID:9058730

13. Silverman LR, Demakos EP, Peterson BL, Kornblith AB, Holland JC, Odchimar-Reissig R, Stone RM, Nelson D, Powell BL, DeCastro CM et al. Randomized controlled trial of azacitidine in patients with the myelodysplastic syndrome: a study of the cancer and leukemia group B. J Clin Oncol 2002; 20:2429-40; PMID:12011120; http://dx.doi.org/10.1200/JCO.2002.04.117

14. Fenaux P, Mufti GJ, Hellstrom-Lindberg E, Santini V, Finelli C, Giagounidis A, Schoch R, Gattermann N, Sanz G, List A et al. Efficacy of azacitidine compared with that of conventional care regimens in the treatment of higher-risk myelodysplastic syndromes: a randomised, open-label, phase III study. Lancet Oncol 2009; 10:223-32; PMID:19230772; http://dx.doi.org/10.1016/S1470-2045(09)70003-8

15. Xie M, Jiang Q, Xie Y. Comparison between decitabine and azacitidine for the treatment of myelodysplastic syndrome: a meta-analysis with 1,392 participants. Clin Lymphoma Myeloma Leuk 2015; 15:22-8; PMID:25042977; http://dx.doi.org/10.1016/j.clml.2014.04.010

16. Kornblith AB, Herndon JE, 2nd, Silverman LR, Demakos EP, Odchimar-Reissig R, Holland JF, Powell BL, DeCastro C, Ellerton J, Larson RA et al. Impact of azacytidine on the quality of life of patients with myelodysplastic syndrome treated in a randomized phase III trial: a Cancer and Leukemia Group B study. J Clin Oncol 2002; 20:2441-52; PMID:12011121; http://dx.doi.org/10.1200/JCO.2002.04.044

17. Sanchez-Abarca LI, Gutierrez-Cosio S, Santamaria C, Caballero-Velazquez T, Blanco B, Herrero-Sanchez C, García JL, Carrancio S, Hernández-Campo P, González FJ et al. Immunomodulatory effect of 5-azacytidine (5-azaC): potential role in the transplantation setting. Blood 2010; 115:107-21; PMID:19887673; http://dx.doi.org/10.1182/blood-2009-03-210393

18. Goodyear OC, Dennis M, Jilani NY, Loke J, Siddique S, Ryan G, Nunnick J, Khanum R, Raghavan M, Cook M et al. Azacitidine augments expansion of regulatory T cells after allogeneic stem cell transplantation in patients with acute myeloid leukemia (AML). Blood 2012; 119:3361-9; PMID:22234690; http://dx.doi.org/10.1182/blood-2011-09-377044

19. Hubackova S, Novakova Z, Krejcikova K, Kosar M, Dobrovolna J, Duskova P, Hanzlikova H, Vancurova M, Barath P, Bartek J et al. Regulation of the PML tumor suppressor in drug-induced senescence of human normal and cancer cells by JAK/STAT-mediated signaling. Cell Cycle 2010; 9:3085-99; PMID:20699642; http://dx.doi.org/10.4161/cc.9.15.12521

20. Novakova Z, Hubackova S, Kosar M, Janderova-Rossmeislova L, Dobrovolna J, Vasicova P, Vancurova M, Horejsi Z, Hozak P, Bartek J et al. Cytokine expression and signaling in drug-induced cellular senescence. Oncogene 2010; 29:273-84; PMID:19802007; http://dx.doi.org/10.1038/onc.2009.318

21. Feng X, Scheinberg P, Wu CO, Samsel L, Nunez O, Prince C, Ganetzky RD, McCoy JP Jr, Maciejewski JP, Young NS. Cytokine signature profiles in acquired aplastic anemia and myelodysplastic syndromes. Haematologica 2011; 96:602-6; PMID:21160069; http://dx.doi.org/10.3324/haematol.2010.030536

22. Kornblau SM, McCue D, Singh N, Chen W, Estrov Z, Coombes KR. Recurrent expression signatures of cytokines and chemokines are present and are independently prognostic in acute myelogenous leukemia and myelodysplasia. Blood 2010; 116:4251-61; PMID:20679526; http://dx.doi.org/10.1182/blood-2010-01-262071

23. Pardanani A, Finke C, Lasho TL, Al-Kali A, Begna KH, Hanson CA, Tefferi A. IPSS-independent prognostic value of plasma CXCL10, IL-7 and IL-6 levels in myelodysplastic syndromes. Leukemia 2012; 26:693-9; PMID:21912394; http://dx.doi.org/10.1038/leu.2011.251

24. Curik N, Burda P, Vargova K, Pospisil V, Belickova M, Vlckova P, Savvulidi F, Necas E, Hajkova H, Haskovec C et al. 5-azacytidine in aggressive myelodysplastic syndromes regulates chromatin structure at PU.1 gene and cell differentiation capacity. Leukemia 2012; 26:1804-11; PMID:22343522; http://dx.doi.org/10.1038/leu.2012.47

25. Mund C, Hackanson B, Stresemann C, Lubbert M, Lyko F. Characterization of DNA demethylation effects induced by 5-Aza-2'-deoxycytidine in patients with myelodysplastic syndrome. Cancer Res 2005; 65:7086-90; PMID:16103056; http://dx.doi.org/10.1158/0008-5472.CAN-05-0695

26. Gore SD, Baylin S, Sugar E, Carraway H, Miller CB, Carducci M, Grever M, Galm O, Dauses T, Karp JE et al. Combined DNA methyltransferase and histone deacetylase inhibition in the treatment of myeloid neoplasms. Cancer Res 2006; 66:6361-9; PMID:16778214; http://dx.doi.org/10.1158/0008-5472.CAN-06-0080

27. Palii SS, Van Emburgh BO, Sankpal UT, Brown KD, Robertson KD. DNA methylation inhibitor 5-Aza-2′-deoxycytidine induces reversible genome-wide DNA damage that is distinctly influenced by DNA methyltransferases 1 and 3B. Mol Cell Biol 2008; 28:752-71; PMID:17991895; http://dx.doi.org/10.1128/MCB.01799-07

28. Fandy TE, Herman JG, Kerns P, Jiemjit A, Sugar EA, Choi SH, Yang AS, Aucott T, Dauses T, Odchimar-Reissig R et al. Early epigenetic changes and DNA damage do not predict clinical response in an overlapping schedule of 5-azacytidine and entinostat in patients with myeloid malignancies. Blood 2009; 114:2764-73; PMID:19546476; http://dx.doi.org/10.1182/blood-2009-02-203547

29. Acosta JC, O'Loghlen A, Banito A, Guijarro MV, Augert A, Raguz S, Fumagalli M, Da Costa M, Brown C, Popov N et al. Chemokine signaling via the CXCR2 receptor reinforces senescence. Cell 2008; 133:1006-18; PMID:18555777; http://dx.doi.org/10.1016/j.cell.2008.03.038

30. Kuilman T, Michaloglou C, Vredeveld LC, Douma S, van Doorn R, Desmet CJ, Aarden LA, Mooi WJ, Peeper DS. Oncogene-induced senescence relayed by an interleukin-dependent inflammatory network. Cell 2008; 133:1019-31; PMID:18555778; http://dx.doi.org/10.1016/j.cell.2008.03.039

31. Rodier F, Coppe JP, Patil CK, Hoeijmakers WA, Munoz DP, Raza SR, Freund A, Campeau E, Davalos AR, Campisi J. Persistent DNA damage signalling triggers senescence-associated inflammatory cytokine secretion. Nat Cell Biol 2009; 11:973-9; PMID:19597488; http://dx.doi.org/10.1038/ncb1909

32. Hsu HC, Lee YM, Tsai WH, Jiang ML, Ho CH, Ho CK, Wang SY. Circulating levels of thrombopoietic and inflammatory cytokines in patients with acute myeloblastic leukemia and myelodysplastic syndrome. Oncology 2002; 63:64-9; PMID:12187073; http://dx.doi.org/10.1159/000065722

33. Scapini P, Lapinet-Vera JA, Gasperini S, Calzetti F, Bazzoni F, Cassatella MA. The neutrophil as a cellular source of chemokines. Immunol Rev 2000; 177:195-203; PMID:11138776; http://dx.doi.org/10.1034/j.1600-065X.2000.17706.x

34. Desterke C, Martinaud C, Ruzehaji N, Le Bousse-Kerdiles MC. Inflammation as a keystone of bone marrow stroma alterations in primary myelofibrosis. Mediators of inflamm 2015; 2015:415024; PMID:26640324; http://dx.doi.org/10.1155/2015/415024

35. Tefferi A, Vaidya R, Caramazza D, Finke C, Lasho T, Pardanani A. Circulating interleukin (IL)-8, IL-2R, IL-12, and IL-15 levels are independently prognostic in primary myelofibrosis: a comprehensive cytokine profiling study. J Clin Oncol 2011; 29:1356-63; PMID:21300928; http://dx.doi.org/10.1200/JCO.2010.32.9490

36. Schinke C, Giricz O, Li W, Shastri A, Gordon S, Barreyro L, Bhagat T, Bhattacharyya S, Ramachandra N, Bartenstein M et al. IL8-CXCR2 pathway inhibition as a therapeutic strategy against MDS and AML stem cells. Blood 2015; 125:3144-52; PMID:25810490; http://dx.doi.org/10.1182/blood-2015-01-621631

37. Blazkova H, Krejcikova K, Moudry P, Frisan T, Hodny Z, Bartek J. Bacterial Intoxication Evokes Cellular Senescence with Persistent DNA Damage and Cytokine Signaling. J Cell Mol Med 2010; 14:357-67; PMID:19650831; http://dx.doi.org/10.1111/j.1582-4934.2009.00862.x

38. Hubackova S, Krejcikova K, Bartek J, Hodny Z. IL1- and TGFbeta-Nox4 signaling, oxidative stress and DNA damage response are shared features of replicative, oncogene-induced, and drug-induced paracrine 'Bystander senescence'. Aging (Albany NY) 2012; 4:932-51; PMID:23385065; http://dx.doi.org/10.18632/aging.100520

39. Kastelein RA, Hunter CA, Cua DJ. Discovery and biology of IL-23 and IL-27: related but functionally distinct regulators of inflammation. Annu Rev Immunol 2007; 25:221-42; PMID:17291186; http://dx.doi.org/10.1146/annurev.immunol.22.012703.104758

40. Seita J, Asakawa M, Ooehara J, Takayanagi S, Morita Y, Watanabe N, Fujita K, Kudo M, Mizuguchi J, Ema H et al. Interleukin-27 directly induces differentiation in hematopoietic stem cells. Blood 2008; 111:1903-12; PMID:18042804; http://dx.doi.org/10.1182/blood-2007-06-093328

41. Guzzo C, Che Mat NF, Gee K. Interleukin-27 induces a STAT1/3- and NF-kappaB-dependent proinflammatory cytokine profile in human monocytes. J Biol Chem 2010; 285:24404-11; PMID:20519510; http://dx.doi.org/10.1074/jbc.M110.112599

42. Wong CK, Chen da P, Tam LS, Li EK, Yin YB, Lam CW. Effects of inflammatory cytokine IL-27 on the activation of fibroblast-like synoviocytes in rheumatoid arthritis. Arthritis Res Ther 2010; 12:R129; PMID:20604932; http://dx.doi.org/10.1186/ar3067

43. Kim KS, Kang KW, Seu YB, Baek SH, Kim JR. Interferon-gamma induces cellular senescence through p53-dependent DNA damage signaling in human endothelial cells. Mech Ageing Dev 2009; 130:179-88; PMID:19071156; http://dx.doi.org/10.1016/j.mad.2008.11.004

44. Hubackova S, Kucerova A, Michlits G, Kyjacova L, Reinis M, Korolov O, Bartek J, Hodny Z. IFN[gamma] induces oxidative stress, DNA damage and tumor cell senescence via TGF[beta]/SMAD signaling-dependent induction of Nox4 and suppression of ANT2. Oncogene 2015; 35:1236-49; PMID:25982278; http://dx.doi.org/10.1038/onc.2015.162

45. Iannello A, Thompson TW, Ardolino M, Lowe SW, Raulet DH. p53-dependent chemokine production by senescent tumor cells supports NKG2D-dependent tumor elimination by natural killer cells. J Exp Med 2013; 210:2057-69; PMID:24043758; http://dx.doi.org/10.1084/jem.20130783

46. Ejaeidi AA, Craft BS, Puneky LV, Lewis RE, Cruse JM. Hormone receptor-independent CXCL10 production is associated with the regulation of cellular factors linked to breast cancer progression and metastasis. Exp Mol Pathol 2015; 99:163-72; PMID:26079660; http://dx.doi.org/10.1016/j.yexmp.2015.06.002

47. Wang YY, Cen JN, He J, Shen HJ, Liu DD, Yao L, Qi XF, Chen ZX. Accelerated cellular senescence in myelodysplastic syndrome. Exp Hematol 2009; 37:1310-7; PMID:19748549; http://dx.doi.org/10.1016/j.exphem.2009.09.002

48. Xiao Y, Wang J, Song H, Zou P, Zhou D, Liu L. CD34+ cells from patients with myelodysplastic syndrome present different p21 dependent premature senescence. Leuk Res 2013; 37:333-40; PMID:23219618; http://dx.doi.org/10.1016/j.leukres.2012.11.006

49. Novotna B, Bagryantseva Y, Siskova M, Neuwirtova R. Oxidative DNA damage in bone marrow cells of patients with low-risk myelodysplastic syndrome. Leuk Res 2009; 33:340-3; PMID:18687469; http://dx.doi.org/10.1016/j.leukres.2008.07.005

50. Grosjean-Raillard J, Tailler M, Ades L, Perfettini JL, Fabre C, Braun T, De Botton S, Fenaux P, Kroemer G. ATM mediates constitutive NF-kappaB activation in high-risk myelodysplastic syndrome and acute myeloid leukemia. Oncogene 2009; 28:1099-109; PMID:19079347; http://dx.doi.org/10.1038/onc.2008.457

51. Novotna B, Neuwirtova R, Siskova M, Bagryantseva Y. DNA instability in low-risk myelodysplastic syndromes: refractory anemia with or without ring sideroblasts. Hum Mol Genet 2008; 17:2144-9; PMID:18430715; http://dx.doi.org/10.1093/hmg/ddn113

52. Sallmyr A, Fan J, Rassool FV. Genomic instability in myeloid malignancies: increased reactive oxygen species (ROS), DNA double strand breaks (DSBs) and error-prone repair. Cancer Lett 2008; 270:1-9; PMID:18467025; http://dx.doi.org/10.1016/j.canlet.2008.03.036

53. Boehrer S, Ades L, Tajeddine N, Hofmann WK, Kriener S, Bug G, Ottmann OG, Ruthardt M, Galluzzi L, Fouassier C et al. Suppression of the DNA damage response in acute myeloid leukemia versus myelodysplastic syndrome. Oncogene 2009; 28:2205-18; PMID:19398952; http://dx.doi.org/10.1038/onc.2009.69

54. Orjalo AV, Bhaumik D, Gengler BK, Scott GK, Campisi J. Cell surface-bound IL-1alpha is an upstream regulator of the senescence-associated IL-6/IL-8 cytokine network. Proc Natl Acad Sci U S A 2009; 106:17031-6; PMID:19805069; http://dx.doi.org/10.1073/pnas.0905299106

55. Takacova S, Slany R, Bartkova J, Stranecky V, Dolezel P, Luzna P, Bartek J, Divoky V. DNA Damage Response and Inflammatory Signaling Limit the MLL-ENL-Induced Leukemogenesis In Vivo. Cancer Cell 2012; 21:517-31; PMID:22516260; http://dx.doi.org/10.1016/j.ccr.2012.01.021

56. Klammer H, Mladenov E, Li F, Iliakis G. Bystander effects as manifestation of intercellular communication of DNA damage and of the cellular oxidative status. Cancer Lett 2013; PMID:24370566; http://dx.doi.org/10.1016/j.canlet.2013.12.017

57. Martin OA, Redon CE, Nakamura AJ, Dickey JS, Georgakilas AG, Bonner WM. Systemic DNA damage related to cancer. Cancer Res 2011; 71:3437-41; PMID:21558390; http://dx.doi.org/10.1158/0008-5472.CAN-10-4579

58. Bartkova J, Rezaei N, Liontos M, Karakaidos P, Kletsas D, Issaeva N, Vassiliou LV, Kolettas E, Niforou K, Zoumpourlis VC et al. Oncogene-induced senescence is part of the tumorigenesis barrier imposed by DNA damage checkpoints. Nature 2006; 444:633-7; PMID:17136093; http://dx.doi.org/10.1038/nature05268

59. Di Micco R, Fumagalli M, Cicalese A, Piccinin S, Gasparini P, Luise C, Schurra C, Garre' M, Nuciforo PG, Bensimon A et al. Oncogene-induced senescence is a DNA damage response triggered by DNA hyper-replication. Nature 2006; 444:638-42; PMID:17136094; http://dx.doi.org/10.1038/nature05327

60. Nelson G, Wordsworth J, Wang C, Jurk D, Lawless C, Martin-Ruiz C, von Zglinicki T. A senescent cell bystander effect: senescence-induced senescence. Aging Cell 2012; 11:345-9; PMID:22321662; http://dx.doi.org/10.1111/j.1474-9726.2012.00795.x

61. Martin OA, Redon CE, Dickey JS, Nakamura AJ, Bonner WM. Para-inflammation mediates systemic DNA damage in response to tumor growth. Commun Integr Biol 2011; 4:78-81; PMID:21509186; http://dx.doi.org/10.4161/cib.13942

62. Redon CE, Dickey JS, Nakamura AJ, Kareva IG, Naf D, Nowsheen S, Kryston TB, Bonner WM, Georgakilas AG, Sedelnikova OA. Tumors induce complex DNA damage in distant proliferative tissues in vivo. Proc Natl Acad Sci U S A 2010; 107:17992-7; PMID:20855610; http://dx.doi.org/10.1073/pnas.1008260107

63. Bartek J, Mistrik M, Bartkova J. Long-distance inflammatory and geno-toxic impact of cancer in vivo. Proc Natl Acad Sci 2010; 107:17861-2; PMID:20926747; http://dx.doi.org/10.1073/pnas.1013093107

64. Kitagawa M, Saito I, Kuwata T, Yoshida S, Yamaguchi S, Takahashi M, Tanizawa T, Kamiyama R, Hirokawa K. Overexpression of tumor necrosis factor (TNF)-alpha and interferon (IFN)-gamma by bone marrow cells from patients with myelodysplastic syndromes. Leukemia 1997; 11:2049-54; PMID:9447819; http://dx.doi.org/10.1038/sj.leu.2400844

65. Bartek J, Hodny Z, Lukas J. Cytokine loops driving senescence. Nat Cell Biol 2008; 10:887-9; PMID:18670449; http://dx.doi.org/10.1038/ncb0808-887

66. Tugues S, Burkhard SH, Ohs I, Vrohlings M, Nussbaum K, Vom Berg J, Kulig P, Becher B. New insights into IL-12-mediated tumor suppression. Cell Death Differ 2015; 22:237-46; PMID:25190142; http://dx.doi.org/10.1038/cdd.2014.134

67. Wang Z, Tang X, Xu W, Cao Z, Sun L, Li W, Li Q, Zou P, Zhao Z. The different immunoregulatory functions on dendritic cells between mesenchymal stem cells derived from bone marrow of patients with low-risk or high-risk myelodysplastic syndromes. PLoS One 2013; 8:e57470; PMID:23469196; http://dx.doi.org/10.1371/journal.pone.0057470

68. Velimezi G, Liontos M, Vougas K, Roumeliotis T, Bartkova J, Sideridou M, Dereli-Oz A, Kocylowski M, Pateras IS, Evangelou K et al. Functional interplay between the DNA-damage-response kinase ATM and ARF tumour suppressor protein in human cancer. Nat Cell Biol 2013; 15:967-77; PMID:23851489; http://dx.doi.org/10.1038/ncb2795

69. Muller-Tidow C, Metzelder SK, Buerger H, Packeisen J, Ganser A, Heil G, Kügler K, Adigüzel G, Schwäble J, Steffen B et al. Expression of the p14ARF tumor suppressor predicts survival in acute myeloid leukemia. Leukemia 2004; 18:720-6; PMID:14973498; http://dx.doi.org/10.1038/sj.leu.2403296

70. Cheson BD, Greenberg PL, Bennett JM, Lowenberg B, Wijermans PW, Nimer SD, Pinto A, Beran M, de Witte TM, Stone RM et al. Clinical application and proposal for modification of the International Working Group (IWG) response criteria in myelodysplasia. Blood 2006; 108:419-25; PMID:16609072; http://dx.doi.org/10.1182/blood-2005-10-4149

71. Tvedt TH, Rye KP, Reikvam H, Brenner AK, Bruserud O. The importance of sample collection when using single cytokine levels and systemic cytokine profiles as biomarkers—a comparative study of serum versus plasma samples. J Immunol Methods 2015; 418:19-28; PMID:25637409; http://dx.doi.org/10.1016/j.jim.2015.01.006

72. Rudek MA, Zhao M, He P, Hartke C, Gilbert J, Gore SD, Carducci MA, Baker SD. Pharmacokinetics of 5-azacitidine administered with phenylbutyrate in patients with refractory solid tumors or hematologic malignancies. J Clin Oncol 2005; 23:3906-11; PMID:15851763; http://dx.doi.org/10.1200/JCO.2005.07.450

Supplementary Information:

Supplementary Table 1. Estimation of cytokine transcript levels in HeLa and HS-5 cells after 5-AC treatment using Human common cytokines PCR array. (A) HeLa cells were treated with 2 µM 5-AC for 7 days and then the levels of 84 common cytokines were estimated with qRT-PCR. As differentially expressed genes were considered genes with > 2 log fold change in the gene expression compared to untreated control. The samples were measured in duplicates. **(B)** HS-5 cells were treated with 0.5 µM 5-AC for 7 days and then the levels of 84 common cytokines were estimated using qRT-PCR. As differentially expressed genes were considered genes with > 2 log fold change in the gene expression compared to untreated control. The samples were measured in duplicates.

Supplementary Table 1.

A) Human common cytokines PCR array for HeLa after 5-AC treatment.

	fold induction	std.dev.	p-value
IL6	123,95	0,90	0,100
IL8	48,56	0,89	0,204
IL24	36,91	3,51	0,175
IL11	26,78	0,53	0,343
OSM	26,50	0,00	0,403
IL20	21,98	0,97	0,341
INHBA	8,94	0,11	0,587
TGFA	7,10	0,54	0,604
SPP1	5,09	0,00	0,653
CSF2	4,91	0,00	0,660
GDF5	4,64	0,51	0,696
FAM3B	3,82	0,00	0,709
TNF	3,68	3,42	0,539
CSF1	3,41	0,19	0,698
IL17B	3,37	0,00	0,734
IL1B	3,30	1,62	0,656
TNFSF14	2,83	1,28	0,798
IL23A	2,60	0,00	0,788
BMP4	2,60	0,01	0,810
IL1A	2,53	0,11	0,792
TNFSF4	2,32	0,26	0,807
IL12A	2,31	0,89	0,746
LTB	2,22	0,01	0,822
PDGFA	2,19	1,17	0,750
CSF3	2,17	0,00	0,827
IL1RN	2,07	0,00	0,837
THPO	2,02	0,00	0,842
IL3	-2,24	0,000	0,820
IFNA4	-2,34	0,00	0,806
BMP5	-4,94	0,46	0,650

B) Human common cytokines PCR array for HS-5 after 5-AC treatment.

	fold induction	std.dev.	p-value
OSM	32,27	0,75	0,005
IL20	19,27	1,03	0,051
IL24	6,95	0,43	0,028
GDF5	6,04	1,12	0,158
IL18	5,92	1,28	0,145
IL23A	5,88	0,07	0,007
BMP7	5,83	0,95	0,039
PDGFA	5,52	0,57	0,070
IL1RN	5,39	0,54	0,163
IL5	5,23	0,08	0,015
TNF	4,5	0,07	0,026
INHBA	4,42	0,72	0,025
CSF2	4,37	0,14	0,017
TGFB2	4,3	0,03	0,018
IL11	3,97	0,02	0,059
IL7	3,5	0,68	0,028
IL17B	3,44	1,05	0,138
TGFA	3,38	0,16	0,014
IL10	3,33	1,56	0,307
TNFSF13	3,29	0,28	0,036
IL21	3,24	0,03	0,042
GDF9	3,16	0,11	0,024
BMP5	3,01	0,18	0,001
BMP1	2,83	0,05	0,032
VEGFA	2,75	0,71	0,051
BMP3	2,71	1,94	0,399
IL15	2,68	0,45	0,053
FAM3B	2,61	0,76	0,065
LTB	2,59	0,06	0,117
IL12A	2,5	0,16	0,046
IFNG	2,46	0,30	0,077
IL16	2,46	0,002	0,070
IL6	2,42	0,20	0,005
TXLNA	2,19	0,41	0,021
IFNA2	2,18	0,70	0,072
IFNB1	2,08	0,11	0,092
TNFSF14	2,05	0,33	0,127
TNFSF13B	-2,10	0,27	0,1197
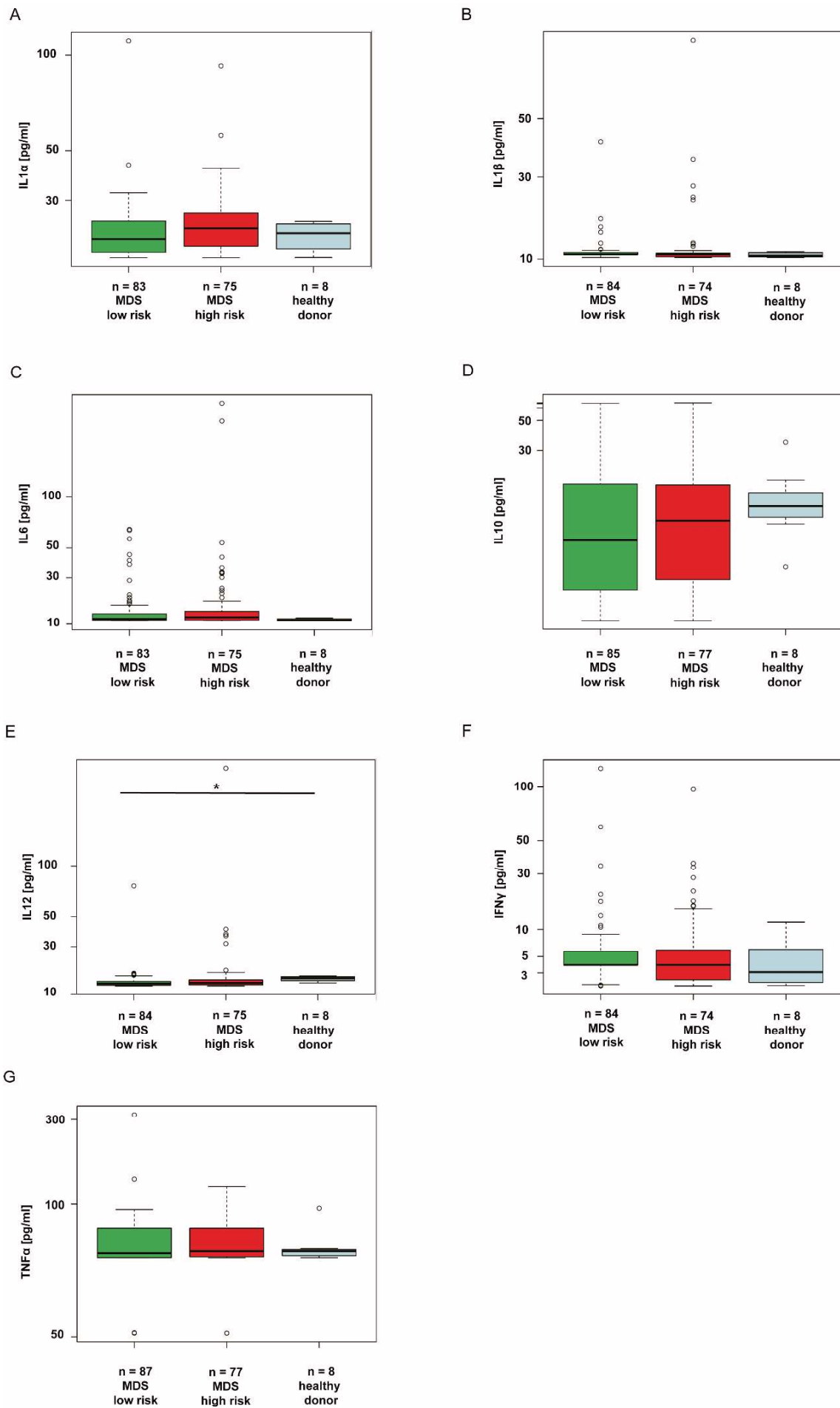
Supplementary Figure 1. Comparison of changes in cytokine levels among low-risk MDS, high-risk MDS and/or AML and healthy donors

Supplementary Figure 1. Comparison of changes in cytokine levels among low-risk MDS, high-risk MDS and/or AML and healthy donors. The data set was analyzed by robust linear mixed effects model at the 95% confidence interval. The box plot graphs demonstrate the upper and lower quartiles, and the median is represented by a short black line within the box for each group. The empty circles represent numerically distant measurements for individual patients (outliers; outside 1.5 times the interquartile range above the upper quartile and bellow the lower quartile). The p-value signifies the difference for the given cytokine measurements between all 3 groups. IL1a ($p = 0.72$); IL1b ($p = 0.43$); IL6 ($p = 0.18$); IL10 ($p = 0.38$); IL12p70 ($p = 0.02$); IFNg ($p = 0.41$); TNFa ($p = 0.36$).
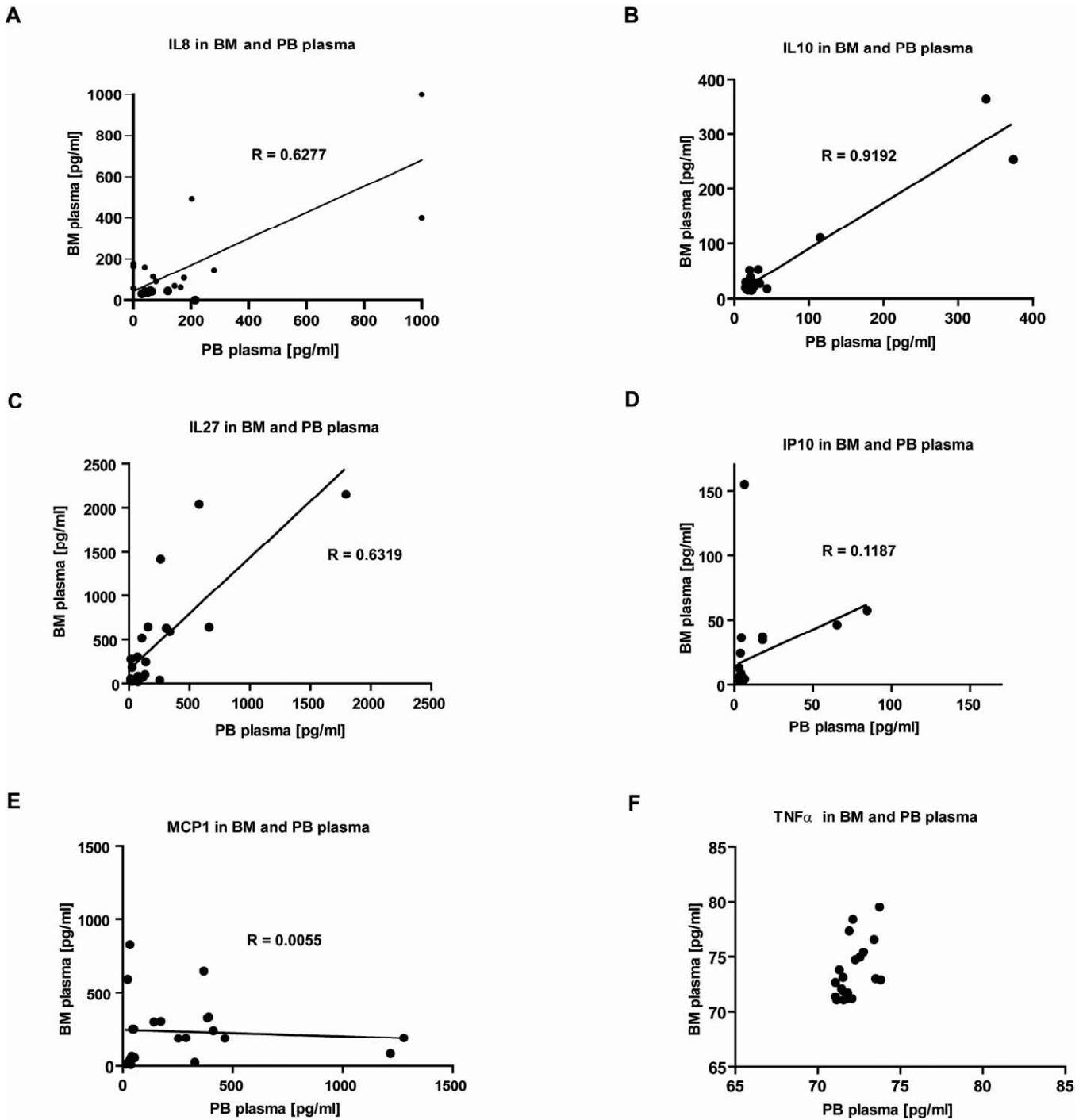
Supplementary Figure 2. Simultaneous estimation of cytokine levels in PB and BM plasma. BM and PB plasma collected at the same time point for the given patient was analyzed for IL8 (A), IL10 (B), IL27 (C), IP10 (D), MCP1 (E), and TNFα (F). In order to minimize the inter-sample variability, the corresponding samples were handled together and measured on the same 11-plex plate.

*NQO1*2* polymorphism predicts overall survival in MDS patients

The myelodysplastic syndromes (MDS) are a heterogenous group of clonal diseases of haematopoietic stem cells characterized by ineffective haemopoiesis with various clinical presentations of peripheral cytopenias and a tendency to progress to acute myeloid leukaemia (AML). The molecular pathogenesis of MDS and why it evolves to AML remains unclear. NAD(P)H quinone dehydrogenase 1 (NQO1) is an enzyme that detoxifies quinones and reduces oxidative stress. The naturally occurring germline polymorphism of *NQO1*

(*NQO1*2*) with a cytosine–to-thymidine (C → T) substitution at nucleotide position 609 of the *NQO1* cDNA (*NQO1^{C609T}*) results in the loss of NQO1 activity and rapid degradation of the protein encoded by *NQO1*2* due to an unstable structure (Lienhart *et al*, 2014). Here we examined how the presence of *NQO1*2* polymorphism affects the development and progression of MDS and assessed the correlation between *NQO1*2* and the overall survival (OS, calculated from the date of diagnosis), presence of karyotypic
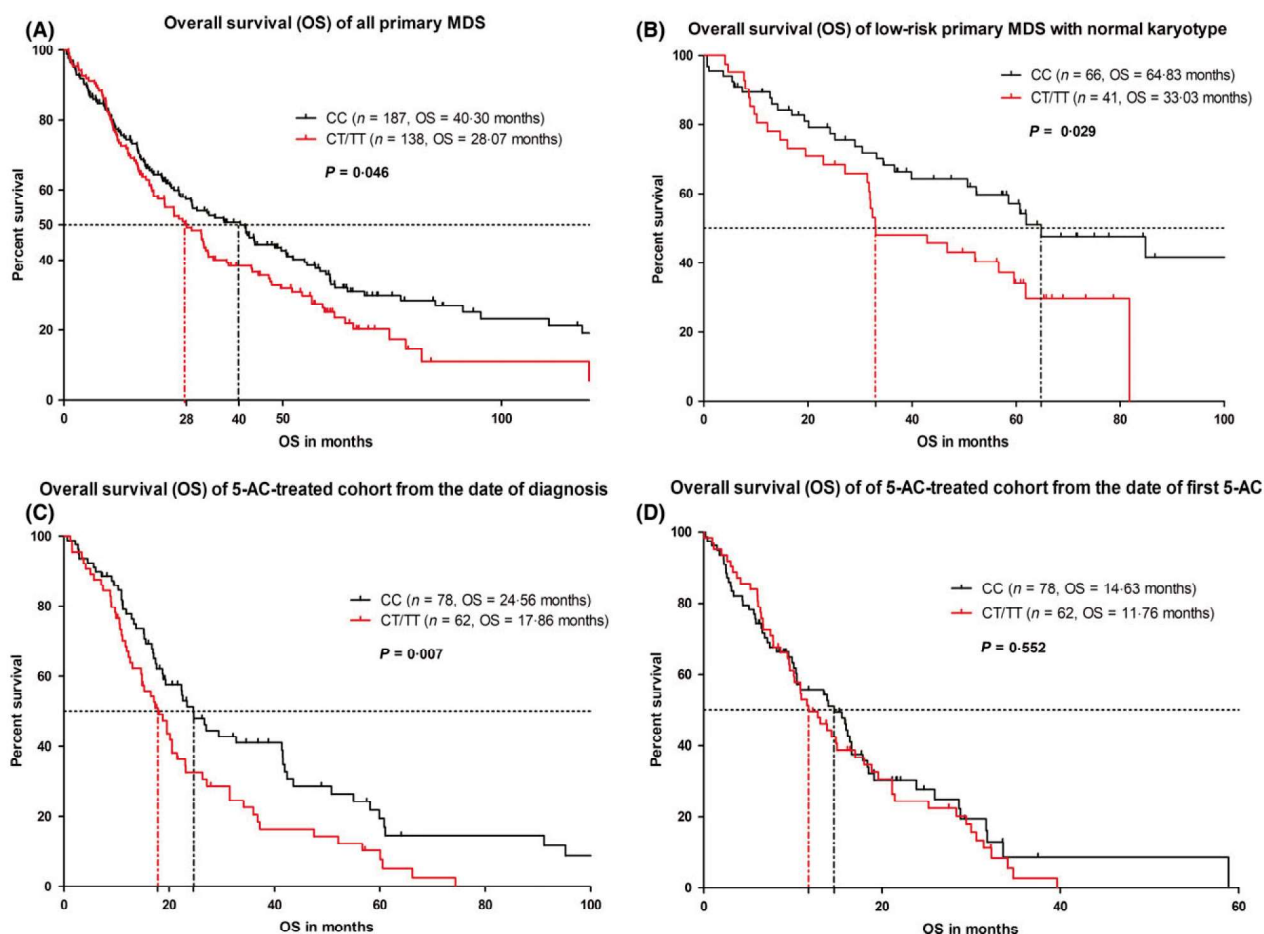
Fig 1. (A) *NQO1*2* genotypes are associated with decreased overall survival (OS) in all primary MDS. 187 CC and 138 CT/TT myelodysplastic syndrome (MDS) patients were analysed for overall survival (OS). Median survival for CC and CT/TT was 40·30 months and 28·07 months, respectively. The difference in median OS between these groups was 12·23 months (*P* = 0·046). (B) *NQO1*2* genotypes are associated with decreased OS in all primary low risk MDS patients with normal karyotype. 66 CC and 41 CT/TT patients were analysed for OS. Median survival for CC and CT/TT was 64·83 and 33·03 months, respectively. The difference in OS between groups was 31·8 months (*P* = 0·029). (C) *NQO1*2* genotype is associated with decreased OS in high risk MDS patients treated with 5-azacytidine (5-AC). OS of high-risk MDS patients treated with 5-AC estimated according to the date of first MDS diagnosis (C) or the date of first application of 5-AC (D).

abnormalities, and response to hypomethylating therapy in MDS patients.

We calculated the occurrence of NQO1*2 among the Caucasian population from a cohort of previously published healthy controls that included 22 734 individuals (Table S1) and compared it to the incidence of NQO1*2 among MDS patients (Table S2). The methodology is described in Appendix S1. Our cohort, consisting of 211 CC and 155 CT/TT patients (Table S3), demonstrated a significant increase in the occurrence of MDS among individuals with NQO1*2 ($P < 0.001$), this trend being more pronounced among men ($n = 191$; $P < 0.001$) than women ($n = 175$; $P = 0.077$). The presence of 17-β estradiol-regulated electrophile response elements in the NQO1 promoter, resulting in higher NQO1 expression in women, probably accounts for the higher MDS prevalence in men (Sanchez et al, 2003).

When the patients were divided according to their International Prognostic Scoring System risk score (low and intermediate-1 versus intermediate-2 and high), the apparent abundance of the NQO1*2 group compared to Hardy-Weinberg equilibrium in healthy controls remained in both groups. Moreover, the NQO1*2 proportion was enhanced in primary MDS ($n = 325$; $P < 0.001$), but not in therapy-related MDS (t-MDS; $n = 41$; $P = 0.226$), probably reflecting the smaller size of the t-MDS group.

However, when we compared the allelic frequencies within the diagnostic subcategories against their expected values, there was increased percentage of NQO1*2 patients among groups with a myeloblast count above 10% (i.e. refractory anaemia with excess blasts, type 2, MDS/AML with less than 30% myeloblasts, $n = 114$), suggesting a shorter expected OS among MDS patients with the non-functioning allele(s) of NQO1 ($P < 0.001$). This relative enlargement of the NQO1*2 group was apparent even after we compared the allelic frequencies present to their expected values according to the actual patient allele distribution ($P = 0.015$) (Table S4).

When we compared the OS of all MDS patients (Kaplan-Meier estimation), we found that patients with the NQO1*2 polymorphism showed a trend ($P = 0.095$) for shorter OS than those with the NQO1*1 allele (CC); the median OS was 33.16 months for CC and 27.86 months for CT/TT (data not shown). By excluding the t-MDS cases ($n = 41$) the difference in OS between patients with NQO1*1 (40.30 months) and NQO1*2 (28.07 months) reached significance ($P = 0.046$; Fig 1A).

Due to negative correlation between the presence of NQO1*2 and OS in MDS patients, we ascertained whether the occurrence of NQO1*2 correlates with the karyotype abnormalities. Indeed, the distribution of alleles among the group of patients with abnormal karyotype was skewed towards NQO1*2 ($n = 179$; $P = 0.002$), compared to patients with a normal karyotype ($n = 163$; $P = 0.069$). Moreover, a higher percentage of NQO1*2 patients was affected by prognostically worse karyotypic abnormalities, either intermediate ($n = 39$; $P = 0.032$) or poor karyotypes ($n = 55$; $P = 0.004$) (Schanz et al, 2012), reflecting the increased occurrence of NQO1*2 among worse prognostic subgroups and more advanced disease stages (Table S4).
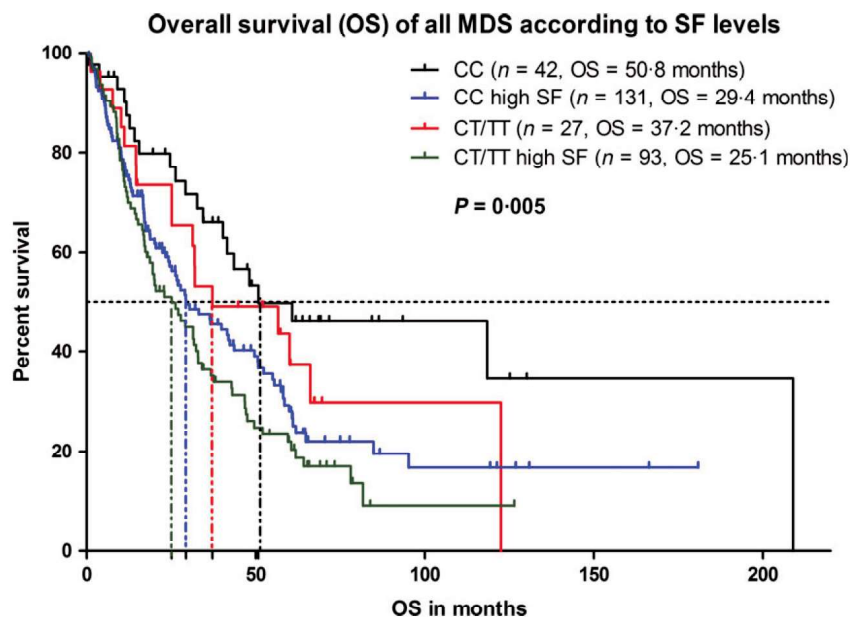
Fig 2. NQO1*2 genotype is associated with higher sensitivity to increased ferritin levels. The overall survival (OS) of all myelodysplastic syndrome (MDS) patients was analysed according to serum ferritin (SF) level. The cohort consisted of 42 CC and 27 CT/TT patients with normal range of SF and 131 CC and 93 CC/CT patients with SF levels ≥300 µg/l (high SF) at the time of diagnosis or at 6 months follow-up; median values at the time of diagnosis were 1104 µg/l for CC with iron overload (IO) and 996 µg/l for CT with IO. The calculated median OS for this cohort was 50.8 months for CC, 37.2 months for CT/TT, 29.4 months for CC with iron overload and 25.1 months for CT/TT with IO ($P = 0.005$).

The median OS for all primary low risk MDS patients with normal karyotype was 64·83 months for CC *versus* 33·03 months for CT/TT *NQO1* ($P = 0·029$; Fig 1B), but there was no impact of dysfunctional alleles on OS in high-risk MDS with normal karyotype ($P = 0·616$). Therefore, the presence of *NQO1*2* polymorphism could be used as an indicator of expected OS, especially among low risk patients with normal karyotype.

Further, we determined the impact of *NQO1*2* on OS in patients treated with 5-azacytidine (5-AC). 140 patients from our cohort who received 5-AC therapy (78 CC *versus* 62 CT/TT) were analysed. The median OS was 24·56 months for CC and 17·86 months for the CT/TT group ($P = 0·007$), showing a significant difference of 6·7 months (Fig 1C). Further, the median OS from date of first 5-AC dose was 14·63 months for CC patients ($n = 78$) and 11·76 months for the CT/TT group ($n = 62$; $P = 0·552$; Fig 1D); these results were within the expected range of OS for 5-AC-treated patient cohorts (Yun *et al*, 2016).

Our results indicate that the progression of MDS is faster among the patients with *NQO1*2* polymorphism, given that the median timeframe between diagnosis and the first application of 5-AC therapy is 3·83 months shorter in CT/TT group (9·93 months for CC *versus* 6·1 months for CT/TT). Nevertheless, presence of the *NQO1*2* polymorphism does not seem to negatively impact the OS of MDS patients in 5-AC therapy, in contrast to some previously examined therapeutic approaches that were affected by this polymorphism (Fagerholm *et al*, 2008).

Next, we analysed whether the decreased protection against superoxide radical formation caused by the *NQO1*2* polymorphism further worsens the OS in patients with iron overload (IO) caused by frequent blood transfusions, given that IO is associated with shortened OS in MDS (Pileggi *et al*, 2017). The threshold for potential IO was based on a serum ferritin (SF) level ≥ 300 µg/l at the time of the first contact or at 6 months follow-up. The median value of SF at the first contact was approximately 1000 µg/l for both CC and CT/TT patients. Notably, the expected OS in patients affected by both increased SF and *NQO1*2* polymorphism was significantly shorter than that of other groups ($P = 0·005$; Fig 2) indicating that functional NQO1 plays a protective role in MDS patients with increased SF and IO.

Funding

Author contributions

AM performed the research, analysed the data and wrote the paper, LM analysed the data, MV processed the bone marrow samples, AJ, ZH and JB designed the study, analysed and interpreted the data and wrote the paper.

Alena Moudra[1] iD
Lubomir Minarik[2]
Marketa Vancurova[1]
Jiri Bartek[1,3,4] iD
Zdenek Hodny[1] iD
Anna Jonasova[2] iD

[1]*Department of Genome Integrity, Institute of Molecular Genetics of the Czech Academy of Sciences,* [2]*1st Department of Medicine – Department of Haematology, First Faculty of Medicine, Charles University in Prague and General University Hospital, Prague, Czech Republic,* [3]*Danish Cancer Society Research Centre, Copenhagen, Denmark and* [4]*Division of Genome Biology, Department of Medical Biochemistry and Biophysics, Karolinska Institutet, Stockholm, Sweden.*
E-mails: alena.moudra@img.cas.cz; atjonas@hotmail.com

Supporting Information

Additional Supporting Information may be found in the online version of this article:

Table S1. NQO1*1/NQO1*2 meta-analysis pool for Caucasians

Table S2. Genotype distribution and allele frequencies of the NQO1*2 polymorphism in MDS cohort and Caucasian population

Table S3. Clinical characteristics of MDS/AML patients genotyped for NQO1*2 polymorphism

Table S4. Comparison between expected and actual number of patients in each sub-group of MDS based on NQO1*2 genotype.

Appendix S1. Supplementary methods.

References

Fagerholm, R., Hofstetter, B., Tommiska, J., Aaltonen, K., Vrtel, R., Syrjakoski, K., Kallioniemi, A., Kilpivaara, O., Mannermaa, A., Kosma, V.- M., Uusitupa, M., Eskelinen, M., Kataja, V., Aittomaki, K., von Smitten, K., Heikkila, P., Lukas, J., Holli, K., Bartkova, J., Blomqvist, C., Bartek, J. & Nevanlinna, H. (2008) NAD(P)H:quinone oxidoreductase 1 NQO1[ast]2 genotype (P187S) is a strong prognostic and predictive factor in breast cancer. *Nature Genetics*, **40**, 844–853.

Lienhart, W.D., Gudipati, V., Uhl, M.K., Binter, A., Pulido, S.A., Saf, R., Zangger, K., Gruber, K. & Macheroux, P. (2014) Collapse of the native

structure caused by a single amino acid exchange in human NAD(P)H:quinone oxidoreductase(1.). *FEBS Journal*, **281**, 4691–4704.

Pileggi, C., Di Sanzo, M., Mascaro, V., Marafioti, M.G., Costanzo, F.S. & Pavia, M. (2017) Role of serum ferritin level on overall survival in patients with myelodysplastic syndromes: results of a meta-analysis of observational studies. *PLoS ONE*, **12**, e0179016.

Sanchez, R.I., Mesia-Vela, S. & Kauffman, F.C. (2003) Induction of NAD(P)H quinone oxidoreductase and glutathione S-transferase activities in livers of female August-Copenhagen Irish rats treated chronically with estradiol: comparison with the Sprague-Dawley rat. *Journal of Steroid Biochemistry and Molecular Biology*, **87**, 199–206.

Schanz, J., Tuchler, H., Sole, F., Mallo, M., Luno, E., Cervera, J., Granada, I., Hildebrandt, B., Slovak, M.L., Ohyashiki, K., Steidl, C., Fonatsch, C., Pfeilstocker, M., Nosslinger, T., Valent, P., Giagounidis, A., Aul, C., Lubbert, M., Stauder, R., Krieger, O., Garcia-Manero, G., Faderl, S., Pierce, S., Le Beau, M.M., Bennett, J.M., Greenberg, P., Germing, U. & Haase, D. (2012) New comprehensive cytogenetic scoring system for primary myelodysplastic syndromes (MDS) and oligoblastic acute myeloid leukemia after MDS derived from an international database merge. *Journal of Clinical Oncology*, **30**, 820–829.

Yun, S., Vincelette, N.D., Abraham, I., Robertson, K.D., Fernandez-Zapico, M.E. & Patnaik, M.M. (2016) Targeting epigenetic pathways in acute myeloid leukemia and myelodysplastic syndrome: a systematic review of hypomethylating agents trials. *Clinical Epigenetics*, **8**, 68.

Supplementary Table S1. NQO1*1/NQO1*2 meta-analysis pool for Caucasians

publication PMID	1st author	Journal	Year published	Nationality	Disease type	CONTROL population only CC	CT	TT	Total
15184245	Alexandrie AK	Cancer Epidemiology, Biomarkers & Prevention	2004	Sweden	LC	368	153	9	530
15611867	Aston CE	Human Genetics	2005	USA	BC	824	347	41	1212
9696930	Bartsch H	European Journal of Cancer Prevention	1998	USA/Europe	PaC	46	24	6	76
16054862	Begleiter A	Oral Oncology	2005	USA/Canada	HNC	249	106	11	366
18676018	Begleiter A	Leukemia Research	2009	Canada	CLL	196	96	7	299
17164365	Begleiter A	Cancer Epidemiology, Biomarkers & Prevention	2006	Canada	CRC	239	102	8	349
23886315	Benhamou AV	Biomarkers	2001	Finland	HNC/LC	105	62	5	172
17339179	Bolufer P	Haematologica	2007	Spain	AML	268	160	19	447
22200898	Bonaventure A	Cancer causes and control	2012	France	AML/ALL pediatric	345	161	26	532
15746160	Broberg K	Carcinogenesis	2005	Sweden	BLC	107	46	3	156
10397241	Chen H	Cancer Research	1999	USA	LC	105	62	4	171
16284498	Clavel J	European Journal of Cancer Prevention	2005	France	ALL pediatric	68	33	3	104
19174490	Cote ML	Carcinogenesis	2009	USA	LC	271	119	15	405
17575500	di Martino E	Genetics in medicine	2007	UK	EC	55	33	5	93
19027952	Fabiani E	Leukemia Research	2009	Italy	MDS	106	47	6	159
15198733	Fern L	British Journal of Haematology	2004	UK	tAML	56	22	7	85
21480392	Goode EL	Molecular carcinogenesis	2011	USA	OC	695	308	32	1035
18061941	Gra OA	Americal Journal of Hematology	2007	Russia	CML	119	52	6	177
17476281	Guillem VM	Leukemia	2007	Spain	tAML	41	34	5	80
10663383	Harth V	Archives of toxicology	2000	Germany	CRC	135	62	8	205
18569591	Harth V	Journal of toxicology and environmental health	2008	Germany	HNC	197	87	12	296
20878130	Hlavata I	Oncology reports	2010	Czech	CRC	344	138	13	495
17726138	Hong CC	Cancer Epidemiology, Biomarkers & Prevention	2007	USA	BC	323	151	21	495
15731166	Hou L	Carcinogenesis	2005	USA	CRA	468	228	12	708
14729580	Hung RJ	Carcinogenesis	2004	Italy	BLC	135	66	13	214
15590400	Kracht T	Haematologica	2004	Germany	ALL pediatric	126	61	3	190
12041882	Krajinovic M	Reviews of environmental health	2002	Canada	ALL pediatric	195	84	25	304
26987799	Kurfurstova D	Molecular Oncology	2016	Czech	PrC	149	64	6	219
11023538	Lafuente MJ	Carcinogenesis	2000	Spain	CRC	189	98	9	296
23021489	Lautner-Csorba	BMC medical genomics	2012	Hungary	ALL pediatric	355	155	19	529
11679176	Lewis SJ	Lung cancer	2001	UK	LC	111	32	2	145
15824189	Li G	Cancer Epidemiology, Biomarkers & Prevention	2005	USA	HNC	805	388	33	1226
16949155	Lincz LF	Leukemia Research	2007	Australia	MM	142	56	3	201
10383153	Longuemaux S	Cancer Research	1999	France	RCC	136	66	8	210
21755707	Lozic B	Collegium Anthropologicum	2011	Croatia	AML pediatric	30	8	0	38
18061666	Maggini V	Leukemia Research	2008	Italy	MM	77	40	7	124
15138483	Menzel HJ (Austria)	British Journal of Cancer	2004	Austria	BC	290	126	8	424
15138483	Menzel HJ	British Journal of Cancer	2004	Czech	BC	175	53	3	231
17082176	Mitrou PN	Carcinogenesis	2007	UK	CRC	646	266	24	936
20966810	Mohelnikova-Duchonova B	Pancreas	2011	Czech	PaC	187	71	7	265
20375710	Northwood EL	Pharmacogenetics and genomics	2010	UK	CRA	198	89	9	296
15694256	Okada S	Neuroscience letters	2005	USA	PD	172	90	7	269
15196853	Olson SH	Gynecologic Oncology	2004	USA	OC	120	55	7	182
12694753	Park SJ	Mutation Research	2003	USA	BLC	163	66	10	239
12419832	Sachse C	Carcinogenesis	2002	UK	CRC	398	173	22	593
15781212	Saldivar SJ	Mutation Research	2005	USA	LC	480	186	17	683
14688016	Sanyal S	Carcinogenesis	2004	Sweden	BLC	83	34	7	124
14506737	Sarbia M	International Journal of Cancer	2003	Germany	GC/EC	185	63	4	252
12393447	Sarmanova J	European Journal of Human Genetics	2004	Czech	BC	221	83	6	310
9241663	Schulz WA	Pharmacogenetics	1997	Germany	RCC/BLC	195	61	4	260
12393447	Seedhouse C	Blood	2002	UK	tAML	110	53	12	175
12476637	Siegelmann-Danieli N	Harefuah	2002	USA	BC	168	61	6	235
15808404	Sorensen M	Cancer Letters	2005	Denmark	LC	176	80	11	267
20568895	Soucek P	Neoplasma	2010	Czech	HNC	83	35	3	121
20056632	Steinbrecher A	Cancer Epidemiology, Biomarkers & Prevention	2010	Germany	PrC	333	133	26	492
10077223	Steiner M	Cancer Letters	1999	Germany	PrC	67	31	2	100
23109831	Stoehr CG	International Journal of Molecular Sciences	2012	Germany	PrC	166	60	6	232
15767364	Terry PD	Cancer Epidemiology, Biomarkers & Prevention	2005	USA	BLC	150	58	6	214
18074351	Tijhuis MJ	International journal of cancer	2008	Spanish	CRA	490	185	23	698
16039674	Van der Logt EM	Mutation Research	2006	Netherlands	CRC	292	112	11	415
15455349	von Rahden BJ	International Journal of Cancer	2005	Germany	EC	185	65	10	260
17761709	Voso MT	Annals of Oncology	2007	Italy	AML	108	40	7	155
10463613	Wiemels JL	Cancer Research	1999	UK	AML pediatric	67	32	1	100
11319169	Xu LL	Cancer Epidemiology, Biomarkers & Prevention	2001	USA	LC	715	341	40	1096
20962519	Yamaguti GG	Acta Hematologica	2010	Brazil	ALL	73	26	0	99
23643325	Zachaki S	Leukemia Research	2013	Greece	MDS	259	147	10	416
12771035	Zhang J	Carcinogenesis	2003	Germany	EC	185	63	4	252

	CONTROL population only					frequency of alleles	
	CC	CT	TT	total		C	T
Caucasian	15320	6689	725	22734	Caucasian	0.821	0.179
	67.39%	29.42%	3.19%				

List of abbreviations

ALL	acute lymphoid leukemia
AML	acute myeloid leukemia
BC	breast cancer
BLC	bladder cancer
CLL	chronic lymphoid leukemia
CML	chronic myeloid leukemia
CRA	colorectal adenoma
CRC	colorectal cancer
EC	esophageal cancer
GC	gastric cancer
HNC	head and neck cancer
LC	lung cancer
MM	multiple myeloma
OC	ovarian cancer
PaC	pancreatic carcinoma
PD	Parkinson disease
PrC	prostate carcinoma
RCC	renal cell carcinoma
tAML	therapy related acute myeloid leukemia

Supplementary Table S2. Genotype distribution and allele frequencies of the NQO1*2 polymorphism in MDS cohort and Caucasian population

Group	no.	CC	CT	TT	C	T
		NQO1 genotype frequency (%)			Allele frequency	
MDS patients	366	211 (0.57)	150 (0.41)	5 (0.01)	0.781	0.219
Caucassian population*	23645	15918 (0.67)	6889 (0.29)	739 (0.03)	0.819	0.177

* based on meta-analysis (see **Supplementary Table S2** for details)

Supplementary Table S3. Clinical characteristics of MDS/AML patients genotyped for NQO1*2 polymorphism

MDS low risk group	n	CC	CT + TT
number of patients	366	211	155
patient age at diagnosis (years), median (range)	71 (45-88)	71 (45-88)	71 (46-87)
males/females	191 / 175	104 / 107	87 / 68
primary/secondary MDS/AML	325 / 41	187 / 24	138 / 17
Sample distribution according to WHO 2008			
MDS 5q	27	16	11
RCMD	91	54	37
RARS	8	3	5
MDS RA	19	11	8
MDS RN	2	0	2
RAEB I	48	32	16
RAEB II	88	42	46
CMLD	2	1	1
CMML I	35	25	10
CMML II	6	5	1
MDS/MPN-u	5	4	1
MDS/AML <30% MB	26	15	11
de novo AML	9	3	6
IPSS risk group			
low + intermediate I	193	113	80
intermediate II + high	160	90	70
not applicable	13		
Karyotype			
normal	163	99	64
abnormal	179	101	78
good	248	153	95
intermediate	39	20	19
poor	55	27	28
not determined	24		

Supplementary Table S4. Comparison between expected and actual number of patients in each sub-group of MDS based on NQO1*2 genotype.

	Actual number of individuals in each sub-group of patients			Expected number of individuals in each sub-group as if normal Caucasian distribution		
	total	CC	CT/TT	CC	CT/TT	p value for χ^2
allele frequency		0.6105	0.3895	0.6740	0.3260	
IPSS risk group						
low + intermediate I	193	113	80	130.09	62.91	0.009
intermediate II + high	160	90	70	107.85	52.15	0.003
not applicable	13					
total	**366**	**211**	**155**	**246.70**	**119.30**	**0.000**
gender (%)						
male	191	104	87	128.74	62.26	0.000
female	175	107	68	117.96	57.04	0.077
Karyotype						
normal	163	99	64	109.87	53.13	0.069
abnormal	179	101	78	120.65	58.35	0.002
good	248	153	95	167.16	80.84	0.055
intermediate	39	20	19	26.29	12.71	0.032
poor	55	27	28	37.07	17.93	0.004
not determined	24					
not good karyotype (int+poor)	94	47	47	63.36	30.64	0.000
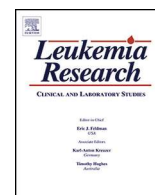
Research paper

Lenalidomide treatment in lower risk myelodysplastic syndromes—The experience of a Czech hematology center. (Positive effect of erythropoietin ± prednisone addition to lenalidomide in refractory or relapsed patients)

Anna Jonasova[a],[*],[1], Radana Neuwirtova[a], Helena Polackova[a], Magda Siskova[a], Tomas Stopka[a], Eduard Cmunt[a], Monika Belickova[b], Alena Moudra[c], Lubomir Minarik[a], Ota Fuchs[b], Kyra Michalova[d], Zuzana Zemanova[d]

[a] 1st Department of Medicine and Biocev, 1st Faculty of Medicine, Charles University and General University Hospital, Prague, U Nemocnice 2, Prague 2, 128 08, Czech Republic
[b] Institute of Hematology and Blood Transfusion, U Nemocnice 1, 128 00 Prague, Czech Republic
[c] Department of Genome Integrity, Institute of Molecular Genetics, Academy of Sciences of the Czech Republic, 14220 Prague, Czech Republic
[d] Center of Oncocytogenetic, Institute of Medical Biochemistry and Laboratory Diagnostics, First Faculty of Medicine, Charles University and General University Hospital, U Nemocnice 2, 128 00 Prague, Czech Republic

ARTICLE INFO

ABSTRACT

Lenalidomide therapy represents meaningful progress in the treatment of anemic patients with myelodysplastic syndromes with del(5q). We present our initial lenalidomide experience and the positive effect of combining erythropoietin and steroids with lenalidomide in refractory and relapsed patients. We treated by lenalidomide 55 (42 female; 13 male; median age 69) chronically transfused lower risk MDS patients with del(5q) (45) and non-del(5q) (10). Response, meaning transfusion independence (TI) lasting ≥ eight weeks, was achieved in 38 (90%) of analyzed patients with del(5q), of whom three achieved TI only by adding erythropoietin ± prednisone. Another five patients responded well to this combination when their anemia relapsed later during the treatment. In the non-del(5q) group only one patient with RARS-T reached TI. Cytogenetic response was reached in 64% (32% complete, 32% partial response). The *TP53* mutation was detected in 7 (18%) patients; four patients progressed to higher grade MDS or acute myeloid leukemia (AML). All seven RAEB-1 patients cleared bone marrow blasts during lenalidomide treatment and reached complete remission (CR); however, three later progressed to higher grade MDS or AML. Lenalidomide represents effective treatment for del(5q) group and combination with prednisone and erythropoietin may be used for non-responders or therapy failures.

1. Introduction

The most common cytogenetic abnormality of MDS is the deletion of the long arm of chromosome 5 (del(5q)), which occurs in nearly 30% of MDS patients [1]. The group of patients with this aberration is relatively heterogeneous with regard to clinical manifestation, although this depends on other factors such as bone marrow myeloblast count, additional cytogenetic aberrations, and the presence of mutations and cytopenias (especially thrombocytopenia) [2–5]. A special categorization is reserved among the subgroups of MDS for patients with isolated del(5q) without increased blasts. In this group, patients are predominantly those with 5q- syndrome, which, with regard to survival, is one of the most prognosticly favorable syndromes of MDS [6,7]. Unfortunately, within a few years the majority of these patients develop transfusion dependency, along with all its negative consequences, such as the organ siderosis, deterioration of quality of life, worsening morbidity, and decrease overall survival (OS). For these patients, the primary therapeutic aims consist of reaching a normalized blood count and eliminating transfusion dependency. In recent years, new therapeutic approach, immunomodulation therapy, represented by lenalidomide have been instituted in MDS treatment [8,9]. Lenalidomide have a significant effect, specifically in MDS patients with del(5q)

* Corresponding author at: 1st Department of Medicine, 1st Faculty of Medicine, Charles University and General University Hospital, Prague, U Nemocnice 2, Prague 2, 128 08, Czech Republic.
E-mail address: anna.jonasova@vfn.cz (A. Jonasova).
[1] http://int1.lf1.cuni.cz/

[10,11]. Lenalidomide treatment leads to normalized blood count and, in some patients, to the minimization (or, less often, the disappearance) of the pathological clone, which is detectable by standard cytogenetic examination. Response to lenalidomide therapy occurs in about 60–70% lower-risk MDS patients with del(5q) and in about 90% of patients that meet the criteria of typical 5q- syndrome [11,12]. Particular caution needs to be taken with patients who have other cytogenetic aberrations, higher blast counts, the *TP53* mutation, and thrombocytopenia. These patients are at greater risk of earlier disease progression, and thus it is necessary, in their cases, to consider more aggressive therapy [13,14,3]. However, only about 25–27% of non-del (5q) patients treated by lenalidomide reach red blood cell transfusion independence (RBC-TI) [15,16]. The response rate in these non-del(5q) patients could be increased by combining EPO with lenalidomide. A randomized phase III study in 131 RBC transfusion-dependent (RBC-TD) lower-risk erythropoietin (EPO)-refractory non-del(5q) MDS patients who were treated by lenalidomide alone or in combination with EPO showed positive effect of adding EPO [17]. RBC-TI was reached in 13.8 and 24.2% of the patients in the lenalidomide versus lenalidomide + EPO arm. Low baseline serum EPO level and a G polymorphism of CRBN gene in this study predicted erythroid response. Nevertheless, additional clinical research is further required to determine who might be the potential lenalidomide responder within the non-del(5q) group. In our recent study, we have analyzed the mRNA level of Cereblon (CRBN) in MDS patients with del(5q), non-del (5q) MDS patients, and controls and found statistically significant higher levels in del(5q) patients, as well as amongst the lenalidomide responders [18].

In our work, we herein present one Czech University center's experience with lenalidomide treatment in lower risk del(5q) and non-del (5q) MDS patients and point to some specific clinical observations, namely the positive effect of the erythropoietin and prednisone addition to lenalidomide therapy in refractory and relapsed patients.

2. Patients and methods

Since 2007 we have provided lenalidomide treatment for 55 (42F/ 13M) MDS patients, median age 69 (range 51–83 years). The patients' characteristics are summarized in the Table 1. All patients belong to the International Prognostic Scoring System (IPSS) low or intermediate group 1. They represent two groups: 45 patients with del(5q) [36 cases (82%) with isolated del(5q), nine cases (18%) with del(5q) and one additional cytogenetic aberration] with classic sex distribution 39F/ 6M, and 10 non-del(5q) patients (3F/7M). Six out of these 10 patients were treated with lenalidomide when accepted into MDS 005 trial, which was approved by the Institutional Review Board and conducted according to the Declaration of Helsinki. Written informed consent was obtained from all patients prior to enrollment.

WHO 2008 (World Health Organization) diagnoses are listed in Table 1. All patients were examined by conventional G-banding and by FISH with appropriate Vysis locus-specific DNA probes (Abbott Molecular). Six out of nine patients with a single additional aberration to del (5q) had an unrelated clone with trisomy of chromosome 8 and represent a specific group. We have repeatedly collected bone marrow samples for cytogenetic analysis and for other studies every six months of therapy, then at 12 months, and then every other 12 months thereafter. Thirty-nine patients (70%) were tested for *TP53* mutations before lenalidomide treatment. In order to determine the mutational status of the *TP53* gene, we analyzed the patients' DNA isolated from the bone marrow mononuclear cells, and applied the method of new generation sequencing (454 GS Junior, Roche).

All studied MDS patients were red blood cell transfusion dependent (RBC-TD), with a median hemoglobin (Hb) level 80 g/l (51–100) at the beginning of treatment. RBC-TD was defined as the requirement of at least two transfusions per month for at least eight weeks prior to the initiation of therapy. Forty-four patients received erythropoietin (EPO) prior to lenalidomide treatment (34 del(5q)), 10 non-del(5q) with just

Table 1
Characteristics of lenalidomide treated patients.

Patients characteristics (No = 55)	Value
Age (years)	
median	69
range	51–83
Sex	
F	42
M	13
WHO 2008 in 5q- group	
Isolated del(5q) (true 5q- syndrome)	28
RCMD	9
RAEB 1	7
MDS/MPN-U	1
WHO 2008 in non 5q- group	
RCMD	7
RARS	1
RARS-T	2
IPSS (both groups)	
ISPP low	36
IPSS int I	16
Unclassified	3
Cytogenetic findings in 5q- group	
Isolated del(5q)	36
two unrelated clones with del(5q) and +8	6
del(5q),del(20q)	1
del(5q)der(19)t(1,19)	1
del(5q), t(2;11)	1
Cytogenetic findings in non 5q- group	
Normal karyotype	10
***TP53*mutation (39 tested)**	
5q- group	7 (18%)
Non 5q- group	0
Previous treatment	
EPO	44 (80%)
CyA + prednisone	1
Azacitidine	1
Transfusion dependency	55 (100%)
Hbg/l (median, range)	80 (51–100)
Thrombocytopenia($< 100 \times 10^9$/l)	1
Time from diagnosis to lenalidomide start (months)	
Median (range)	15 (2–199)

Abbreviations: CyA, cyclosporine, EPO, erythropoietin, Hb, hemoglobin F, female, IPSS, MDS/MPD-U, myelodysplastic/myeloproliferative neoplasm, M, male, unclassifiable international prognostic scoring system, RARS, refractory anemia with ring sideroblasts, RAEB-1, refractory anemia with excess of blasts, RARS-T refractory anemia with ring sideroblasts and thrombocytosis, RCMD, refractory cytopenia with multilineage dysplasia.

one intermittent responder. One of our patients also presented an interesting case, which following the diagnosis of RAEB2 with isolated del (5q) was treated by azacitidine (18 cycles, 7-day regime, 75 mg/m^2/ day) and reached bone marrow complete response with just transient transfusion independency (TI). This patient was switched to lenalidomide upon RBC-TD and reached until now more than 2 years lasting TI without any signs of disease progression.

The median time from diagnosis to the beginning of lenalidomide therapy was 15 months, with a range of 2–199 months. Lenalidomide was administered at a dose of 5 mg from the beginning of treatment in 26 patients, and at a dose of 10 mg in 29 patients (including all non-del (5q) patients). The median duration of lenalidomide therapy was 15.5 months, with a range of 2–70 months.

Nine patients, six with del(5q) and three non-del(5q), were treated by EPO or by EPO plus prednisone in addition to lenalidomide when the initial response to lenalidomide was inadequate. In seven patients, all with del(5q), EPO ± prednisone was administered in addition to the lenalidomide therapy when their anemia relapsed during the lenalidomide treatment. Prednisone was added to EPO only when the response to EPO was not satisfactory within two months. All these patients received EPO before lenalidomide initiation, and all were primarily refractory patients. Median serum EPO level of these patients before

lenalidomide treatment was 300 mU/ml (range 197–774).EPO added to lenalidomide was administered at a dose of 40–80,000 units/week. Prednisone was started with a dose of 20 mg/day. The dose was decreased to 5 mg/day in all responding patients. None of these refractory or relapsed patients were candidates for bone marrow transplantation.

The comparison of the overall survival (OS) from the date of the first lenalidomide treatment of each group was evaluated using the Kaplan-Meier estimation. P-values < 0.05 were considered as statistically significant. The Log-rank test was used to compare the survival distributions between each patient group. Analyses were conducted using the GraphPad Prism version 5.00 for Windows, GraphPad Software, San Diego California USA (www.graphpad.com).

3. Results

In regards to response, we evaluated 52 patients (42 del(5q) and 10 non-del(5q)) with known RBC-TD. In the del(5q) group, we evaluated 42 patients who had been treated with lenalidomide longer than three months, of whom 38 (90.4%) reached RBC-TI. From these 38 del(5q) responders, two patients reached TI only after adding EPO and one patient after EPO plus prednisone. The characteristics of these EPO ± prednisone treated patients are summarized in Table 2. Three del(5q) patients did not respond even after EPO or EPO + prednisone. Among four del(5q) non-responders, there were two patients with the *TP53* mutation, and two patients with del(5q) and one additional cytogenetic aberration der(19)(q21.2;p13.3) and t(2;11)(p21;q23). On the other hand, all patients with two cytogenetically unrelated clones (del(5q) and trisomy 8) belonged among well responding patients and showed features very similar to patients with low risk MDS with isolated del(5q) as reported by Neuwirtova et al. [19]. There was only one responder diagnosed with RARS-T, out of the 10 non-del(5q) patients.

Once again, this patient reached TI with lenalidomide but experienced a further increase of Hb (> 90 g/l) by combining the lenalidomide with EPO.

Response to lenalidomide treatment in all del(5q) patients was well demonstrated by increased erythropoiesis in the bone marrow. Response, as previously described in the literature, usually began at 2–8 weeks of therapy (median 4 weeks). Responses (RBC-TI) are detailed in the Table 3. The median duration of hematologic response (RBC-TI) was 35 months (3–79).

In terms of cytogenetic response in the del(5q) group, we evaluated consecutive bone marrow samples in 34 patients (75%) with ≥3 samples per patient in 23 of them (51%). Cytogenetic response was reached in altogether 64% of patients. Eleven (32%) patients achieved complete cytogenetic response (CCyR), but only in four of these patients did the response last longer throughout the course of the disease. Partial cytogenetic response (the shrinkage of pathological clones by more than 50%) was documented in 11 (32%) patients. Stable cytogenetic results were documented in six patients and an increase of the clone size was noted in two patients. However, all these patients are good clinical responders with TI. Four patients (12%) developed additional cytogenetic abnormalities, including complex karyotypes (≥3 aberrations) in three cases (two of them progressed). The median time to cytogenetic response was 12 months (range 6–23 months).

In terms of the dose/response relationship, we did not observe any correlative evidence between the cytogenetic response and the drug dosage. From 22 responding patients, 11 were treated with 5 mg daily and another 11 with 10 mg daily. CyCR was reached in six patients on 5 mg and in five patients on 10 mg of lenalidomide. Thanks to repeated BM collections we have documented 10 cytogenetic relapses amongst the patients who achieved cytogenetic response (CyCR + CyPR, 22 cases). Nine out of these 10 patients had stable complete hematological

Table 2
Basic characteristics and responses of lenalidomide plus EPO ± prednisone treated patients.

No	Age	Sex	WHO 2008	Cytogenetics	EPO level	Lenalidomide dose	EPO only	EPO + Prednisone	Response
A/responders									
Refractory or unsatisfactory responding to lenalidomide									
1	82	F	RAEB I	del(5q)	55	10 mg	yes	no	RBC-TI
2	68	F	Isol.5q-	del(5q)	300	5 mg	yes	no	RBC-TI
3	65	F	RARS-T	46XX	287	10 mg	yes	no	RBC-TI
4	83	F	Isol.5q-	del(5q)	120	10 mg	no	yes	RBC-TI
Relapsed (transfusion dependency)									
5	74	F	Isol.5q-	del(5q),	255	5 mg	yes	no	RBC-TI
6	75	F	Isol.5q-	del(5q)	380	10 mg	yes	no	RBC-TI
7	79	F	Isol.5q-	del(5q)	774	10 mg	no	yes	RBC-TI
8	72	F	Isol.5q-	del(5q)	300	5 mg	no	yes	RBC-TI
9	78	F	RCMD	del(5q), +8	203	5 mg	no	yes	RBC-TI
B/non-responders									
Refractory or unsatisfactory responding to lenalidomide									
10	71	F	Isol.5q-	del(5q)	600	10 mg	no	yes	no
11	68	F	MDS/MPD	del(5q)	60	10 mg	no	yes	no
12	60	M	RCMD	46XY	769	10 mg	no	yes	no
13	60	M	RCMD	46XY	258	10 mg	no	yes	no
Relapsed (transfusion dependency)									
14	74	F	RCMD	del(5q),del(20q)	456	10 mg	no	yes	no
15	77	F	RCMD	del(5q), +8	ND	10 mg	no	yes	no
16	72	M	RCMD	del(5q),t(2;11)	400	10 mg	no	yes	no

A/Patients responding to lenalidomide and EPO alone, or EPO plus prednisone.
B/Patients non-responding to lenalidomide and EPO alone, or EPO plus prednisone.
We divide our responders and non-responders each into two groups:
Refractory or unsatisfactory responding patients: those who were treated by lenalidomide at least 3–4 months were still transfusion dependent or did not increased hemoglobin (Hb) above 90 g/l.
Relapsed patients: those who reached RBC-TI but became RBC-TD, or had Hb level ≤ 80 g/l at least in 2 consecutive samples, later during the course of lenalidomide treatment.
Patients, who were treated by 5 mg, did not tolerate higher dose of lenalidomide due to thrombocytopenia or neutropenia.
EPO only: patients treated by lenalidomide plus EPO.
EPO + prednisone: patients treated by lenalidomide plus EPO and prednisone.
Abbreviation: EPO, erythropoietin, ND, not done, RBC-TD, red blood cell transfusion dependence, RBC-TI, red blood cell transfusion independence.
EPO level units: mU/ml.

Table 3
Erythroid response evaluation in relation to lenalidomide dosage.

Variable (No,%)	Lenalidomide 10 mg	Lenalidomide 5 mg	All patients
A/5q- group	No = 19	No = 23	No = 42
Transfusion independence (TI)	17 (89%)	21 (91%)	38 (90%)
Time to TI, median (range) (weeks)	4,2 (2–18)	4,4 (3–20)	4,3 (2–20)
Hb (g/l) baseline, median (range)	78 (60–104)	79 (51–97)	80 (51–104)
Hb (g/l) first response, median (range)	96 (90–120)	95 (92–125)	95 (90–125)
B/non5q- group	No = 10	No = 0	No = 10
Transfusion independence (TI)	1 (10%)	none	1 (10%)
Time to TI (weeks)	8		8
Hb (g/l) baseline, median (range)	79 (51–88)		79 (51–88)
Hb (g/l) first response	90 (single responder)		90 (single responder)

response without any clinical signs of progression, had lasting complete TI at the time of the BM examination, and were on a stable lenalidomide dosage. The *TP53* mutation was detected in seven patients (18%), two of who carried two mutations simultaneously. The median of variant allele frequency (VAF) of detected mutations was 14.7% with a range of 1.1–44.2%. Four of these seven *TP53* mutation positive patients progressed to the higher risk MDS during the lenalidomide treatment.

The relapse of anemia (TD or decrease of Hb below 90 g/l) in patients still treated by lenalidomide was observed in seven del(5q) patients. All of these patients were further treated with a combination of lenalidomide and EPO $\pm$ prednisone. Five of these patients responded: three with just EPO, two to EPO + prednisone. We saw a positive effect of combining lenalidomide with EPO $\pm$ prednisone in nine out of 16 patients (four patients with initial insufficient response to lenalidomide and five patients with relapse of anemia). Moreover, two of our well-responding patients had an acute attack of polymyalgia rheumatica during the course of lenalidomide, both accompanied by a profound decrease of Hb and requirement of RBC transfusions. Both reacted promptly to a high dose of prednisone with an increase of hemoglobin and restoring TI.

Lenalidomide was interrupted/discontinued in six well-responding and transfusion independent patients with del(5q) (4 with CyCR, 2 with CyPR). One of them relapsed after 12 months and responded well after resumption of lenalidomide treatment. Median duration of TI in this group is 38 months (12–54).

Interestingly, six patients with del(5q) (13%) but none of the non-del(5q) patients progressed to higher risk MDS or AML. These del(5q) patients' characteristics at the time of diagnosis, before lenalidomide treatment, were noted as follows: three patients with RAEB 1 and three patients with *TP53* mutation. Only one patient is currently alive and is on the azacitidine treatment. Consequent treatment of the six progressing patients included subcutaneous azacitidine (3 patients), allogeneic stem cell transplantation (1 patient), low dose of cytosine arabinoside (1 patient), and best supportive care (1 patient).

Nine del(5q) patients were no longer alive at the time of analysis; of these, five died from disease progression and transformation to acute leukemia (AML), while the other four died as a result of comorbidity. Four patients from the non-del(5q) group also died as a consequence of comorbidity.

In terms of median overall survival; we separate our patients into four subgroups. Median OS since the start of lenalidomide treatment was not reached in low risk MDS patients with isolated del(5q) (patients with features of 5q- syndrome) and in the group of patients with del(5q) and one additional aberration and was reached at 36 months for non-del(5q) patients and 28 months for RAEB1 (all with del(5q)). The median OS, much like the median of response duration (35 months, range 3–79), is influenced by a relatively recent treatment initiation. Regardless, we present the OS curves for various groups in Fig. 1.

Concerning adverse effects (we have evaluated all 55 patients together), the most frequent were hematological, with such as
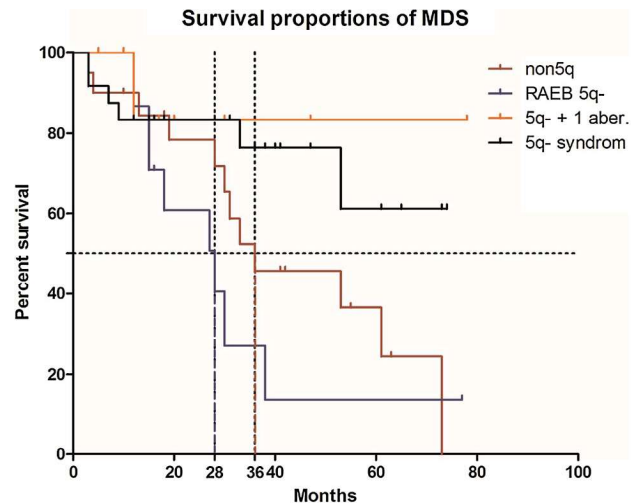
Legend

Lenalidomide treated patients are divided into four groups: 10 non5q- patients, 7 RAEB 1 patients, 9 patients with del(5q) plus 1 cytogenetic aberration, and 28 low risk MDS patients with isolated del(5q) (5q- syndrome). P-value for Log-rank (Mantel-Cox) Test = 0.04; P-value for Logrank test for trend = 0.03.

Fig. 1. Patients' survival proportions represented as Kaplan Meyer curves. Lenalidomide treated patients are divided into four groups: 10 non5q- patients, 7 RAEB 1 patients, 9 patients with del(5q) plus 1 cytogenetic aberration, and 28 low risk MDS patients with isolated del(5q) (5q- syndrome). P-value for Log-rank (Mantel-Cox) Test = 0.04; P-value for Logrank test for trend = 0.03.

neutropenia occurring in 94% (in 70,6% toxicity grade 3,4), and thrombocytopenia in 88% (23,5% with grade 3,4). Later, throughout the course of therapy, we observed a gradual increase of neutrophils and thrombocytes. Nevertheless, hematologic toxicity was the primary reason for the reduction of the initial dosage from 10 mg to 5 mg per day, and in some cases even to 2.5 mg daily. Non-hematological toxicity occurred in 70% of patients, typically of grades 1 or 2 and well manageable. Most frequent were dermatological side effects, which usually presented as transient reactions such as dry skin, itching, and rashes. Fourteen percent of patients experienced gastrointestinal symptomatology (nausea, obstipation, diarrhea) not exceeding grade 2 toxicity. Unlike previous reports, we observed a higher number of thrombotic events. Five patients (9%) experienced venous thrombosis of the lower extremities. None were on steroid therapy at the time of thrombosis. One received lenalidomide plus EPO. All continued on lenalidomide treatment with anticoagulation therapy after the short lenalidomide discontinuation. We never terminated the therapy for reasons relating to adverse side effects.

4. Discussion

The introduction of immunomodulation therapy, represented by

lenalidomide, has been of great benefit for treating anemia in MDS patients. This treatment's high efficacy is, however, specifically tied to a smaller subgroup of MDS: patients with the del(5q). As stated above, previous large studies demonstrated a response in the form of transfusion independence in 60–70% of patients [10,11]. We observe an even higher response rate reaching 90% in our set of 42 evaluated patients with del(5q). This is likely because we predominantly treat patients with 'true' 5q- syndrome (63% of our del(5q) patients) with superior response to lenalidomide. Furthermore, for those patients not responding to lenalidomide we were able to improve the response significantly by the addition of EPO, or EPO plus prednisone. This combination improved further the clinical results and lead to a better response in eight del(5q) patients (19%) and one out of ten non-del(5q) MDS patients. The positive effect of the EPO addition to lenalidomide therapy was previously reported in non-del(5q) patients by Toma et al. [17]. Possible mechanisms are explored in Basiorka et al. [20], which suggest that lenalidomide is potentially involved in the up-regulation of expression and stability of the EPO receptor (EpoR) and in enhancing the JAK2-STAT 5 signaling pathway. Lenalidomide has E3 ubiquitin ligase inhibitory effects that extend to RNF41. The inhibition of RNF41 auto-ubiquitination promotes membrane accumulation of signaling competent JAK2/EpoR complexes that augment EPO responsiveness. It is important to note that those patients who improved their Hb levels after combining EPO with lenalidomide were EPO-refractory before the lenalidomide treatment, much like our group of patients.

The additional positive effect of administering steroids together with lenalidomide is explained by Narla et al. [21]. Corticosteroids increase the proliferation of erythroid progenitor cells *in vitro* and improve burst-forming units-erythroid (BFU-E) colony formation, whereas lenalidomide specifically increases colony-forming unit-erythroid (CFU-E) [21,22]. The author's findings indicate that dexamethasone and lenalidomide promote different stages of erythropoiesis and thus the combination of steroids plus lenalidomide might possess a synergistic clinical effect. Narla et al. described the effects of dexamethasone and lenalidomide, individually and in combination, on the cell differentiation of primary human bone marrow progenitors *in vitro*. Both agents promoted erythropoiesis by increasing the absolute number of erythroid cells produced from normal CD34$^+$ cells. Authors also found that lenalidomide with dexamethasone promotes erythropoiesis in *RPS14*- and *RPS19*-deficient cells and suggested that lenalidomide and dexamethasone, individually or in combination, have the potential to increase red blood cell production in erythroid disorders of ribosome dysfunction, such as MDS with del(5q).

Among the excellent responders to lenalidomide in our set of patients is a specific group with two cytogenetically unrelated clones with del(5q) and trisomy 8, that was previously described by us in Neuwirtova et al. [19]. This group has striking similarities to real 5q-syndrome. We even observed in one patient the disappearance of both clones (del(5q) and +8). On the other hand, two patients with different additional aberrations in one clone with del(5q) were refractory to the lenalidomide therapy.

Even patients with the RAEB 1 subtype reached surprisingly positive results. All seven patients were very good responders in terms of reaching transfusion independence and all cleared the bone marrow blasts; but later, during the course of therapy, three patients relapsed and their disease progressed. Interestingly, the decrease of bone marrow blasts was not always accompanied by cytogenetic response. We thus suggest that these patients should be carefully and more frequently monitored, and have regular bone marrow examinations to detect early progression to a more advanced stage of disease.

We found just one responder in the non-del(5q) group with a WHO 2008 diagnosis RARS-T, a disease rather similar in terms of peripheral blood findings and OS to 5q- syndrome. We know of only a few case reports in the literature with positive responses to lenalidomide in these patients [23]. Our one RARS-T patient reached TI after lenalidomide and also showed further increase of hemoglobin following the addition

of EPO therapy.

Our results support previous studies that document the high sensitivity of cells with 5q deletion to lenalidomide and the relatively high percentage of cytogenetic response. Cytogenetic response was recorded in 64% of patients. In comparison to larger studies, however, we report a lower percentage of complete cytogenetic response (11% in our study compared to 25% in MDS 004) supporting the possibility that lenalidomide may not completely eliminate the malignant clone/s. As of now, this can be explained by a shorter duration of therapy, given the recent authorization of lenalidomide in the Czech Republic and the use of generally lower doses of lenalidomide (the prevailing dose is 5 mg, even 2.5 mg in some long-term schedules). On the other hand, the dosing does not affect the number of hematological responses and leads to excellent drug tolerance without any further discontinuations of treatment because of side effects. The very good profile of adverse side effects from lenalidomide thus contributes to the likability of this oral medication. Although hematological toxicity is higher in the first few months of treatment, in most cases it gradually disappears and does not indicate more serious problems in lenalidomide therapy. Furthermore, the Sekeres' study demonstrates a positive correlation of the depth of thrombocytopenia and neutropenia in the first cycles of treatment with the quality of response [24]. The only exception in terms of side effects in our group is strikingly higher occurrence of deep vein thrombotic events.

It remains unclear why patients with del(5q) have such a high sensitivity to lenalidomide and how to identify the proper responders from non- del(5q) group. Our recent work demonstrates a connection between the specific sensitivity to lenalidomide and the mRNA levels of CRBN, a protein that is part of ubiquitin ligase E and the binding site for immunomodulation drugs, and whose expression, for reasons yet unknown, is significantly higher in patients with 5q- syndrome [18]. CRBN is a primary target of immunomodulating drugs in MM and MDS and is required for the activity of these drugs [25–27]. In our previous study, we also analyzed several del(5q) patients treated by lenalidomide and found high levels of CRBN mRNA in both the bone marrow and the peripheral blood mononuclear cells of the responders. Moreover, we found that patients who stopped responding to lenalidomide and whose disease progressed showed a sudden decrease of mRNA CRBN expression [18]. The new analysis of a larger group of low risk MDS lenalidomide-treated patients is just being prepared for publication. Our work also indicate that patients with del(5q) especially those carrying mutations in *TP53* gene progress to high risk MDS or MDS/ AML. Interestingly, our other work recently showed that preceding isolated single del(5q) state represents rather strong positive predictor of longer overall survival and response duration in high risk MDS patients treated with azacitidine [28]. This implies that progression of del (5q) might be a result of different pathogenetic mechanisms as compared to those without del(5q) and that acquired resistance to lenalidomide might be involved in this process.

In conclusion, data from our set of MDS patients with del(5q) and transfusion dependence confirm a high efficacy of lenalidomide and a very good tolerance of this drug. Inadequate response or the relapse of anemia during lenalidomide treatment can be alleviated by combining lenalidomide with EPO or EPO plus steroids. We plan to confirm these clinical observations by means of a clinical study with a larger patient cohort, conducted in cooperation with other hematology centers in the Czech Republic.

Conflicts of interests

None.

Funding

References

[1] (a) D. Haase, U. Germing, J. Schanz, M. Pfeilstöcker, T. Nösslinger, B. Hildebrandt, A. Kundgen, M. Lübbert, R. Kunzmann, A.A. Giagounidis, C. Aul, L. Trümper, O. Krieger, R. Stauder, T.H. Müller, F. Wimazal, P. Valent, C. Fonatsch, C. Steidl, New insights into the prognostic impact of the karyotype in MDS and correlation with subtypes: evidence from a core dataset of 2124 patients, Blood 110 (2007) 4385–4395;
(b) A. List, S. Kurtin, D.J. Roe, A. Buresh, D. Mahadevan, D. Fuchs, L. Rimsza, R. Heaton, R. Knight, J.B. Zeldis, Efficacy of lenalidomide in myelodysplastic syndromes, N. Engl. J. Med. 352 (February (6)) (2005) 549–557.

[2] J. Brezinova, Z. Zemanova, D. Bystricka, J. Sarova, L. Lizcova, E. Malinova, J. IzakovaE. Sajdova, D. Sponerova, A. Jonasova, J. Cermak, K. Michalva, Deletion of the long arm but not the 5q31 region of chromosome 5 in myeloid malignancies, Leuk. Res. 36 (2012) 43–45.

[3] A. Jonasova, J. Cermak, J. Vondrakova, M. Siskova, I. Hochova, E. Kadlckova, O. Cerna, M. Sykora, V. Vozobulova, N. Seifertova, K. Michalova, Z. Zemanova, J. Brezinova, P. Belohlavkova, A. Kostecka, R. Neuwirtova, Thrombocytopenia at diagnosis as an important negative prognostic marker in isolated 5q- MDS (IPSS low and intermediate-1), Leuk. Res. 36 (December (12)) (2012) 222–224.

[4] M. Mallo, J. Cervera, J. Schanz, E. Such, G. García-Manero, E. Luño, C. Steidl, B. Espinet, T. Vallespí, U. Germing, S. Blum, K. Ohyashiki, J. Grau, M. Pfeilstöcker, J.M. Hernández, T. Noesslinger, A. Giagounidis, C. Aul, M.J. Calasanz, M.L. Martín, P. Valent, R. Collado, C. Haferlach, C. Fonatsch, M. Lübbert, R. Stauder, B. Hildebrandt, O. Krieger, C. Pedro, L. Arenillas, M.Á. Sanz, A. Valencia, L. Florensa, G.F. Sanz, D. Haase, F. Solé, Impact of adjunct cytogenetic abnormalities for prognostic stratification in patients with myelodysplastic syndrome and deletion 5q, Leukemia 25 (2011) 110–120.

[5] A.G. Kulasekararaj, A.E. Smith, S.A. Mian, A.M. Mohamedali, P. Krishnamurthy, N.C. Lea, J. Gäken, C. Pennaneach, R. Ireland, B. Czepulkowski, S. Pomplun, J.C. Marsh, G.J. Mufti, TP53 mutations in myelodysplastic syndrome are strongly correlated with aberrations of chromosome 5, and correlate with adverse prognosis, Br. J. Haematol. 160 (2013) 660–672.

[6] H. Van den Berghe, J.J. Cassiman, G. David, J.P. Fryns, J.L. Michaux, G. Sokal, Distinct haematological disorder with deletion of the long arm of no. 5 chromosome, Nature 251 (1974) 437–438.

[7] H. Van den Berghe, The 5q- syndrome, Scand. J. Haematol. Suppl. 45 (1986) 78–81.

[8] A. List, S. Kurtin, D.J. Roe, A. Buresh, D. Mahadevan, D. Fuchs, L. Rimsza, R. Heaton, R. Knight, J.B. Zeldis, Efficacy of lenalidomide in myelodysplastic syndromes, N. Engl. J. Med. 352 (February (6)) (2005) 549–557.

[9] A. Jonasova, Myelodysplastic syndromes—therapy progress over the last two decades, Vnitr. Lek. 59 (2013) 635–640. Article in Czech.

[10] A. List, G. Dewald, J. Bennett, A. Giagounidis, A. Raza, E. Feldman, B. Powell, P. Greenberg, D. Thomas, R. Stone, C. Reeder, K. Wride, J. Patin, M. Schmidt, J. Zeldis, R. Knight, Myelodysplastic syndrome-003 study investigators. Lenalidomide in the myelodysplastic syndrome with chromosome 5q deletion, N. Engl. J. Med. 355 (October (14)) (2006) 1456–1465.

[11] P. Fenaux, A. Giagounidis, D. Selleslag, O. Beyne-Rauzy, G. Mufti, M. Mittelman, P. Muus, P. Te Boekhorst, G. Sanz, C. Del Cañizo, A. Guerci-Bresler, L. Nilsson, U. Platzbecker, M. Lübbert, B. Quesnel, M. Cazzola, A. Ganser, D. Bowen, B. Schlegelberger, C. Aul, R. Knight, J. Francis, T. Fu, E. Hellström-Lindberg, MDS-004 Lenalidomide del5q Study Group, A randomized phase 3 study of lenalidomide versus placebo in RBC transfusion-dependent patients with Low-/Intermediate-1-risk myelodysplastic syndromes with del5q, Blood 118 (October (14)) (2011) 3765–3776.

[12] A. Jonasova, L. Cervinek, P. Belohlavkova, J. Cermak, M. Belickova, P. Rohon, O. Cerna, I. Hochova, M. Siskova, K. Kacmarova, E. Janousova, Lenalidomide treatment in myelodysplastic syndrome with 5q deletion–Czech MDS group experience, Vnitr. Lek. 61 (December (12)) (2015) 1028–1033. Article in Czech.

[13] M. Jädersten, L. Saft, A. Smith, A. Kulasekararaj, S. Pomplun, G. Göhring, A. Hedlund, R. Hast, B. Schlegelberger, A. Porwit, E. Hellström-Lindberg, G.J. Mufti, TP53 mutations in low-risk myelodysplastic syndromes with del(5q) predict disease progression, J. Clin. Oncol. 29 (May (15)) (2011) 1971–1979.

[14] U. Germing, M. Lauseker, B. Hildebrandt, A. Symeonidis, J. Cermak, P. Fenaux, C. Kelaidi, M. Pfeilstöcker, T. Nösslinger, M. Sekeres, J. Maciejewski, D. Haase, J. Schanz, J. Seymour, M. Kenealy, R. Weide, M. Lübbert, U. Platzbecker, P. Valent, K. Götze, R. Stauder, S. Blum, K.A. Kreuzer, R. Schlenk, A. Ganser, W.K. Hofmann, C. Aul, O. Krieger, A. Kündgen, R. Haas, J. Hasford, A. Giagounidis, Survival, prognostic factors and rates of leukemic transformation in 381 untreated patients with MDS and del(5q): a multi-center study, Leukemia 26 (2012) 1286–1292.

[15] A. Raza, J.A. Reeves, E.J. Feldman, G.W. Dewald, J.M. Bennett, H.J. Deeg, L. Dreisbach, C.A. Schiffer, R.M. Stone, P.L. Greenberg, P.T. Curtin, V.M. Klimek, J.M. Shammo, D. Thomas, R.D. Knight, M. Schmidt, K. Wride, J.B. Zeldis, A.F. List, Phase 2 study of lenalidomide in transfusion-dependent, low-risk, and intermediate-1 risk myelodysplastic syndromes with karyotypes other than deletion 5q, Blood 111 (January (1)) (2008) 86–93.

[16] V. Santini, A. Almeida, A. Giagounidis, S. Gröpper, A. Jonasova, N. Vey, G.J. Mufti, R. Buckstein, M. Mittelman, U. Platzbecker, O. Shpilberg, R. Ram, C. Del Cañizo, N. Gattermann, K. Ozawa, A. Risueño, K.J. MacBeth, J. Zhong, F. Séguy, A. Hoenekopp, C.L. Beach, P. Fenaux, Randomized phase III study of lenalidomide versus placebo in RBC transfusion-dependent patients with lower-risk non-del(5q) myelodysplastic syndromes and ineligible for or refractory to erythropoiesis-stimulating agents, J. Clin. Oncol. 34 (September (25)) (2016) 2988–2996.

[17] A. Toma, O. Kosmider, S. Chevret, J. Delaunay, A. Stamatoullas, C. Rose, O. Beyne-Rauzy, A. Banos, A. Guerci-Bresler, S. Wickenhauser, D. Caillot, K. Laribi, B. De Renzis, D. Bordessoule, C. Gardin, B. Slama, L. Sanhes, B. Gruson, P. Cony-Makhoul, B. Chouffi, C. Salanoubat, R. Benramdane, L. Legros, E. Wattel, G. Tertian, K. Bouabdallah, F. Guilhot, A.L. Taksin, S. Cheze, K. Maloum, S. Nimuboma, C. Soussain, F. Isnard, E. Gyan, R. Petit, J. Lejeune, V. Sardnal, A. Renneville, C. Preudhomme, M. Fontenay, P. Fenaux, F. Dreyfus, Lenalidomide with or without erythropoietin in transfusion-dependent erythropoiesis-stimulating agent-refractory lower-risk MDS without 5q deletion, Leukemia 30 (April (4)) (2016) 897–905.

[18] A. Jonasova, R. Bokorova, J. Polak, M. Vostry, A. Kostecka, H. Hajkova, R. Neuwirtova, M. Siskova, D. Sponerova, J. Cermak, D. Mikulenkova, L. Cervinek, J. Brezinova, K. Michalova, O. Fuchs, High level of full length cereblon mRNA in lower risk myelodysplastic syndromes with isolated 5q deletion is connected with the efficacy of lenalidomide, Eur. J. Haematol. 95 (July (1)) (2015) 27–34.

[19] R. Neuwirtová, Z. Zemanová, J. Brezinová, M. Belickova, P. Dvorak, A. Oltova, A. Jonasova, J. Cermak, D. Sponerova, J. Ullrichova, Z. Maskova, L. Cervinek, Y. Smelikova, V. Vozobulova, E. Polonyova, M. Svoboda, K. Michalova, Are we justified to classify patients with two unrelatd clones with del(5q) and trisomy 8 as a subgroup of myelodysplastic syndrome of the type of 5q- syndrome? Transfuze Hematol. Dnes 20 (2014) 25–31. Article in Czech.

[20] A.A. Basiorka, K.L. McGraw, L. De Ceuninck, L.N. Griner, L. Zhang, J.A. Clark, G. Caceres, L. Sokol, R.S. Komrokji, G.W. Reuther, S. Wei, J. Tavernier, A.F. List, Lenalidomide stabilizes the erythropoietin receptor by inhibiting the E3 ubiquitin ligase RNF41, Cancer Res. 76 (June (12)) (2016) 3531–3540.

[21] A. Narla, S. Dutt, J.R. McAuley, F. Al-Shahrour, S. Hurst, M. McConkey, D. Neuberg, B.L. Ebert, Dexamethasone and lenalidomide have distinct functional effects on erythropoiesis, Blood 118 (2011) 2296–2304.

[22] M. von Lindern, W. Zauner, G. Mellitzer, P. Steinlein, G. Fritsch, K. Huber, B. Löwenberg, H. Beug, The glucocorticoid receptor cooperates with the erythropoietin receptor and c-Kit to enhance and sustain proliferation of erythroid progenitors in vitro, Blood 94 (2) (1999) 550–559.

[23] G. Huls, A.B. Mulder, S. Rosati, A.A. van de Loosdrecht, E. Vellenga, J.T. de Wolf, Efficacy of single-agent lenalidomide in patients with JAK2 (V617F) mutated refractory anemia with ring sideroblasts and thrombocytosis, Blood 116 (July (2)) (2010) 180–182.

[24] M.A. Sekeres, J.P. Maciejewski, A.A. Giagounidis, K. Wride, R. Knight, A. Raza, A.F. List, Relationship of treatment-retated cytopenias and response to lenalidomide in patients with lower-risk myelodysplastic syndromes, J. Clin Oncol. 26 (December (36)) (2008) 5943–5949.

[25] T. Ito, H. Ando, T. Suzuki, T. Ogura, K. Hotta, Y. Imamura, Y. Yamaguchi, H. Handa, Identification of a primary target of thalidomide teratogenicity, Science 327 (2010) 1345–1350.

[26] A. Lopez-Girona, D. Mendy, T. Ito, K. Miller, A.K. Gandhi, J. Kang, S. Karasawa, G. Carmel, P. Jackson, M. Abbasian, A. Mahmoudi, B. Cathers, E. Rychak, S. Gaidarova, R. Chen, P.H. Schafer, H. Handa, T.O. Daniel, J.F. Evans, R. Chopra, Cereblon is a direct protein target for immunomodulatory and antiproliferative activities of lenalidomide and pomalidomide, Leukemia 26 (2012) 2326–2335.

[27] J. Krönke, E.C. Fink, P.W. Hollenbach, K.J. MacBeth, S.N. Hurst, N.D. Udeshi, P.P. Chamberlain, D.R. Mani, H.W. Man, A.K. Gandhi, T. Svinkina, R.K. Schneider, M. McConkey, M. Järås, E. Griffiths, M. Wetzler, L. Bullinger, B.E. Cathers, S.A. Carr, R. Chopra, B.L. Ebert, Lenalidomide induces ubiquitination and degradation of CK1α in del(5q) MDS, Nature 523 (July (7559)) (2015) 183–188.

[28] K. Polgarova, K. Vargova, V. Kulvait, N. Dusilkova, L. Minarik, Z. Zemanova, M. Pesta, A. Jonasova, T. Stopka, Somatic mutation dynamics in MDS patients treated with azacitidine indicate clonal selection in patients-responders, Oncotarget 8 (December (67)) (2017) 111966–111978.

Article

Strong homeostatic TCR signals induce formation of self-tolerant virtual memory CD8 T cells

Ales Drobek[1,†] ID, Alena Moudra[1,†], Daniel Mueller[2], Martina Huranova[1] ID, Veronika Horkova[1], Michaela Pribikova[1], Robert Ivanek[2,3], Susanne Oberle[4,‡], Dietmar Zehn[4,5], Kathy D McCoy[6,§], Peter Draber[1] & Ondrej Stepanek[1,2,*] ID

Abstract

Virtual memory T cells are foreign antigen-inexperienced T cells that have acquired memory-like phenotype and constitute 10–20% of all peripheral CD8^{+} T cells in mice. Their origin, biological roles, and relationship to naïve and foreign antigen-experienced memory T cells are incompletely understood. By analyzing T-cell receptor repertoires and using retrogenic monoclonal T-cell populations, we demonstrate that the virtual memory T-cell formation is a so far unappreciated cell fate decision checkpoint. We describe two molecular mechanisms driving the formation of virtual memory T cells. First, virtual memory T cells originate exclusively from strongly self-reactive T cells. Second, the stoichiometry of the CD8 interaction with Lck regulates the size of the virtual memory T-cell compartment via modulating the self-reactivity of individual T cells. Although virtual memory T cells descend from the highly self-reactive clones and acquire a partial memory program, they are not more potent in inducing experimental autoimmune diabetes than naïve T cells. These data underline the importance of the variable level of self-reactivity in polyclonal T cells for the generation of functional T-cell diversity.

Introduction

Immunological memory is one of the hallmarks of adaptive immunity. During infection, pathogen-specific naïve T cells differentiate into short-lived effector and memory T cells. The latter facilitate long-standing protection against a secondary infection of the same pathogen. CD8^{+} CD44^{+} CD62L^{+} central memory (CM) T cells have the capability of expansion, self-renewal, and generation of cytotoxic effector T cells upon repeated encountering of their cognate antigen (Graef et al, 2014).

Interestingly, some T cells with an apparent memory phenotype are specific to antigens which the host organism has not been exposed to (Haluszczak et al, 2009; Su et al, 2013). There are two possible explanations of their origin: (i) They could be cross-reactive T cells that have encountered another foreign cognate antigen previously (Su et al, 2013) or (ii) they are generated via homeostatic mechanisms independently of the exposure to any foreign antigens (Haluszczak et al, 2009). The strong evidence for the role of homeostatic mechanisms in generation of CD8^{+} memory-like T cells was provided by the detection of these cells in germ-free mice. Since these T cells had limited prior exposure to foreign antigens, they were called virtual memory (VM) T cells (Haluszczak et al, 2009).

Generation and/or maintenance of VM T cells depends on transcription factors Eomes and IRF4, type I interferon signaling, IL-15 and/or IL-4 signaling, and CD8α^{+} dendritic cells (Akue et al, 2012; Sosinowski et al, 2013; Kurzweil et al, 2014; Tripathi et al, 2016; White et al, 2016). It has been shown that VM T cells express slightly higher levels of CD122 (IL-2Rβ) and lower levels of CD49d (integrin α4, a subunit of VLA-4) than true (i.e., foreign antigen-experienced) CM T cells (Sosinowski et al, 2013). Based on these markers, VM T cells constitute for a majority of memory-phenotype CD8^{+} T cells in unimmunized mice and around 10–20% of total CD8^{+} T cells in lymphoid organs. Moreover, it has been proposed that memory-phenotype T cells, that accumulate in aged mice, are VM T cells (Chiu et al, 2013). However, with the notable exception of the very initial study that identified CD44^{+} CD62L^{+} CM T cells in germ-free mice (Haluszczak et al, 2009), all other published

1 Laboratory of Adaptive Immunity, Institute of Molecular Genetics of the Czech Academy of Sciences, Prague, Czech Republic
2 Department of Biomedicine, University Hospital and University of Basel, Basel, Switzerland
3 Swiss Institute of Bioinformatics, Basel, Switzerland
4 Swiss Vaccine Research Institute, Epalinges, Switzerland
5 Division of Animal Physiology and Immunology, School of Life Sciences Weihenstephan, Technical University of Munich, Freising, Germany
6 Department of Clinical Research (DKF), Inselspital, University of Bern, Bern, Switzerland
*Corresponding author. Tel.: +420 241062155; E-mail: ondrej.stepanek@img.cas.cz
†These authors contributed equally to this work
‡Present address: Sanofi Genzyme, Baar, Switzerland
§Present address: Department of Physiology and Pharmacology, Cumming School of Medicine, University of Calgary, Calgary, AB, Canada

experiments used specific pathogen-free (SPF) mice that have significant exposure to microbial antigens. There are three major hypothesis of how virtual memory T cells might be formed in a homeostatic manner: (i) The differentiation into VM T cells occurs purely on a stochastic basis, (ii) lymphopenic environment in newborns induces differentiation of the first wave of thymic emigrants into VM T cells (Akue *et al*, 2012), or (iii) the VM T cells are generated from relatively highly self-reactive T cells that receive strong homeostatic TCR signals at the periphery (White *et al*, 2016). However, none of these hypotheses has been addressed in detail.

Although VM T cells form a large CD8$^+$ T cell population, their biological role is still unknown. VM T cells share some functional properties with true CM cells, including rapid production of IFNγ upon stimulation with a cognate antigen or cytokines (Haluszczak *et al*, 2009; Lee *et al*, 2013). On a per cell basis, ovalbumin-specific VM T cells provide a protection to ovalbumin-expressing *Listeria monocytogenes* (Lm), comparable to true CM T cells, and surpass naïve T cells with the same specificity (Lee *et al*, 2013). In addition, it has been proposed that VM T cells are capable of by-stander protection against infection, i.e., independently of their cognate antigen exposure (Chu *et al*, 2013; White *et al*, 2016). Altogether, these data pointed toward the superior role of VM T cells in protective immunity to infection. In a marked contrast to the above-mentioned findings, Decman *et al* showed that CD44$^+$ CD8$^+$ T-cell receptor (TCR) transgenic T cells isolated from unprimed mice (i.e., putative VM T cells) expand less than CD44$^-$ CD8$^+$ T cells expressing the same TCR upon antigenic stimulation *in vivo* (Decman *et al*, 2012). Likewise, VM T cells from aged mice were shown to be hyporesponsive to their cognate antigens in comparison with their naïve counterparts, mostly because of their susceptibility to apoptosis (Decman *et al*, 2012; Renkema *et al*, 2014).

As VM T cells develop independently of infection, the understanding of mechanisms that guide their development is critical in order to elucidate their biological roles. One hint is the observation that levels of CD5 (a marker of self-reactivity) on naïve T cells correlate with their ability to differentiate into VM T cells (White *et al*, 2016). In this study, we demonstrate that virtual memory T cells originate exclusively from relatively highly self-reactive T-cell clones and acquire only a partial memory gene expression program. Moreover, the interaction between CD8 and Lck (and possibly the overall intrinsic sensitivity of the TCR signaling machinery) determines the size of the virtual memory compartment. These data highlight the virtual memory T-cell formation as a T-cell fate decision checkpoint, when the intensity of TCR signals induced by self-antigens plays a central role in the decision-making process. Although virtual memory T cells show augmented responses to their foreign cognate antigen in some experimental setups in comparison with naïve T cells, the potency of VM T cells to induce pathology in an experimental model of autoimmune diabetes is not higher than that of naïve T cells.

Results

Strong homeostatic TCR signaling induces virtual memory T cells

In this work, we aimed to understand why some mature CD8$^+$ T cells differentiate into VM T cells and some maintain their naïve

phenotype. The peripheral T-cell pool of polyclonal mice consists of clones with different level of self-reactivity. To test the hypothesis that the level of self-reactivity plays a role in the formation of virtual memory T cells, we took advantage of previous observations that coupling frequency (or stoichiometry) of CD8 coreceptor to Lck kinase is a limiting factor for the TCR signaling in thymocytes (Erman *et al*, 2006; Stepanek *et al*, 2014). We used T cells from CD8.4 knock-in mouse strain, that express a chimeric CD8.4 coreceptor, consisting of the extracellular portion of CD8α fused to the intracellular part of CD4 (Erman *et al*, 2006). In comparison with WT CD8α, the chimeric CD8.4 coreceptor is more strongly binding Lck, a kinase initiating the TCR signal transduction. As a consequence, higher fraction of CD8.4 coreceptors molecules than CD8 coreceptors are loaded with Lck (Erman *et al*, 2006; Stepanek *et al*, 2014). Because the self-antigen triggered TCR signaling is stronger in CD8.4 T cells than CD8WT T cells (Park *et al*, 2007; Kimura *et al*, 2013; Stepanek *et al*, 2014), we use the CD8.4 T cells as a model to address the role of self-reactivity in virtual memory T-cell formation.

First, we compared monoclonal F5 Rag$^{-/-}$ T cells (henceforth CD8WT F5) and CD8.4 knock-in F5 Rag$^{-/-}$ T cells (henceforth CD8.4 F5) from unimmunized animals. The F5 TCR is specific for influenza NP68 and has been shown to have a very low level of self-reactivity (Ge *et al*, 2004; Hogan *et al*, 2013). We observed that CD8.4 F5 T cells had lower levels of CD8 and TCR and elevated levels of CD5 and IL-7R in comparison with CD8WT F5 T cells (Fig EV1A). Because the downregulation of CD8 and expression of CD5 and IL-7R correlate with the intensity of homeostatic TCR signaling (Park *et al*, 2007), we could conclude that CD8.4 indeed enhances homeostatic TCR signaling. However, we did not detect upregulation of memory markers, CD44, CD122, and LFA-1 on CD8.4 F5 T cells (Figs 1A and EV1A). CD8.4 F5 T cells showed slightly stronger antigenic responses, measured as CD25 and CD69 upregulation, than CD8WT F5 T cells *in vitro* upon activation with the cognate antigen, NP68, or a lower affinity antigen, NP372E (Shotton & Attaran, 1998; Fig 1B). Accordingly, CD8.4 F5 T cells expanded more than CD8WT F5 T cells after the immunization with NP68 peptide (Fig 1C). Infection with transgenic *Listeria monocytogenes* expressing NP68 (Lm-NP68) induced stronger expansion and formation of larger KLRG1$^+$IL-7R$^-$ short-lived effectors and KLRG1$^-$IL-7R$^+$ memory-precursor subsets in CD8.4 F5 than in CD8WT F5 T cells (Figs 1D and EV1B). Collectively, these data showed that CD8-Lck coupling frequency sets the sensitivity of peripheral T cells to self-antigens during homeostasis and to foreign cognate antigens during infection. However, supraphysiological CD8-Lck coupling in CD8.4 F5 T cells does not induce differentiation into memory-phenotype T cells in unimmunized mice.

Whereas the level of self-reactivity of F5 T cells is very low, transgenic OT-I T cells, specific for chicken ovalbumin (OVA), exhibit a relatively high level of self reactivity (Ge *et al*, 2004; Hogan *et al*, 2013). We tested whether a combination of a relatively highly self-reactive OT-I TCR and supraphysiological CD8-Lck coupling is sufficient to induce VM T cells. For this reason, we compared monoclonal OT-I Rag$^{-/-}$ T cells (henceforth CD8WT OT-I) and CD8.4 knock-in OT-I Rag$^{-/-}$ T cells (henceforth CD8.4 OT-I) from unimmunized animals. As expected, CD8.4 OT-I T cells exhibited signs of stronger homeostatic TCR signaling than CD8WT OT-I
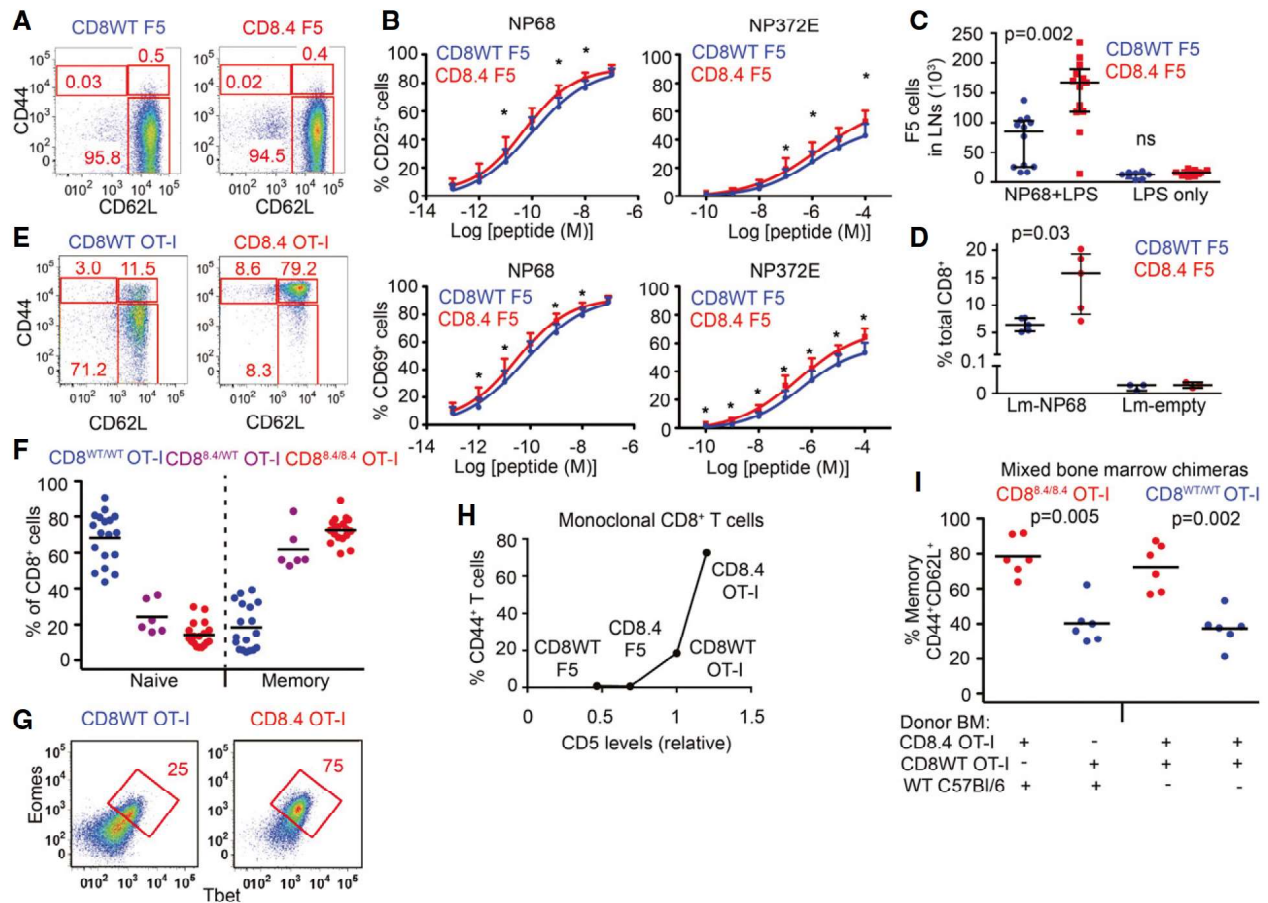
Figure 1. Supraphysiological CD8-Lck coupling induces differentiation into VM T cells in a clone-specific manner.

A LN cells isolated from CD8WT F5 and CD8.4 F5 mice were analyzed by flow cytometry (gated as viable CD8⁺CD4⁻). A representative experiment out of 4 in total.

B LN cells isolated from CD8WT F5 and CD8.4 F5 mice were stimulated with antigen-loaded DCs overnight and CD69 or CD25 expression was analyzed by flow cytometry. Mean + SEM. $n = 7$ independent experiments. *$P < 0.05$.

C 2×10^6 CD8WT F5 or CD8.4 F5 LN T cells were adoptively transferred into Ly5.1 WT host 1 day prior to immunization with NP68 peptide and LPS or LPS only. Three days after the immunization, donor Ly5.2⁺ Ly5.1⁻ CD8⁺ T cells from LN of the host mice were analyzed by flow cytometry and counted. Median ± interquartile range. $n = 8$–13 mice from seven independent experiments.

D 1×10^5 CD8WT F5 or CD8.4 F5 LN T cells were adoptively transferred into Ly5.1 WT hosts and immunized with WT Lm (empty) or Lm-NP68. Six days after the immunization, the percentage of donor Ly5.2⁺ Ly5.1⁻ CD8⁺ T cells among all CD8⁺ T cells was determined. Median ± interquartile range. $n = 3$–5 mice from three independent experiments.

E, F LN cells isolated from CD8WT OT-I, CD8.4 OT-I, and heterozygous CD8^{WT/8.4} mice were analyzed by flow cytometry (gated as viable CD8⁺ CD4⁻). Percentages of naïve (CD44⁻ CD62L⁺) and memory (CD44⁻ CD62L⁺) CD8⁺ T cells were determined. $n = 6$–18 mice per group from at least five independent experiments.

G Expression of Eomes and Tbet in CD8⁺ LN T cells isolated from CD8WT OT-I and CD8.4 OT-I mice was determined by flow cytometry. A representative experiment out of 3 in total.

H Relationship between relative CD5 levels (CD5 on CD8WT OT-I was arbitrarily set as 1) percentage of VM T cells (CD44⁺ CD62L⁺) using the data from indicated TCR transgenic strains. Mean value of $n = 5$–8 mice per group from at least five independent experiments.

I Irradiated Rag2⁻/⁻ host mice were transplanted with B-cell and T-cell depleted bone marrow from Ly5.1 C57Bl/6 together with CD8.4 OT-I or CD8WT OT-I bone marrow in 1:1 ratio (first two datasets) or, with bone marrow from CD8.4 OT-I and CD8WT OT-I mice in 1:1 ratio (last two datasets). Eight weeks later, LN cells were isolated and analyzed by flow cytometry. $n = 6$ mice per group from three independent experiments.

Data information: Statistical significance was determined using two-tailed Wilcoxon signed-rank test (B) and Mann Whitney test (C, D, I).

Source data are available online for this figure.

T cells, including downregulation of TCR, CD8, and increased levels of CD5 and CD127 (Fig EV1C and D). Interestingly, the majority of the CD8.4 OT-I T cells exhibited CM phenotype including CD44⁺ CD62L⁺ double positivity, increased levels of CD122 and LFA-1, increased forward-scatter signal, and expression of transcription factors Tbet and Eomes (Figs 1E–G and EV1C), which was in a striking contrast with analogical experiments with CD8WT/CD8.4 F5 T

cells (Figs 1A and EV1A). The CD8^{WT/CD8.4} heterozygous OT-I T cells showed an intermediate frequency of memory T cells (Fig 1F). Because CD8.4 OT-I T cells exhibited features of memory T cells without encountering their foreign cognate antigen, we concluded that CD8.4 induced a differentiation of OT-I T cells into VM cells. When we compared monoclonal T cells from all four transgenic mouse strains tested, we identified a relationship between surface

levels of CD5, a commonly used marker of self-reactivity, and the frequency of VM T-cell formation. However, the dependency was not linear, but showed a threshold behavior, indicating that only the most self-reactive T cells have the potential to develop into VM T cells (Figs 1H and EV1E).

To address whether CD8.4 induces VM T-cell formation in OT-I T cells in a T-cell intrinsic manner, we generated mixed bone marrow chimeric animals where both CD8.4 and CD8WT populations were present. We transplanted bone marrow cells from Ly5.1 WT mouse together with bone marrow cells from either Ly5.2 CD8WT OT-I or Ly5.2 CD8.4 OT-I mice into an irradiated Rag2$^{-/-}$ recipient. CD8.4 OT-I T cells generated substantially more VM T cells than CD8WT OT-I T cells (Fig 1I). In an alternative setup, we cotransferred mixed bone marrow cells from Ly5.1 CD8WT OT-I and Ly5.2 CD8.4 OT-I animals into an irradiated Rag2$^{-/-}$ recipient to compare these two subsets in a single mouse. Again, CD8.4 OT-I T cells generated significantly more VM T cells than CD8WT OT-I T cells (Fig 1I). These experiments showed that CD8.4 OT-I T cells intrinsically trigger the memory differentiation program.

CD8-Lck coupling frequency regulates the size of virtual memory compartment in polyclonal repertoire

In a next step, we addressed how the CD8-Lck stoichiometry regulates the size of virtual memory compartment in a polyclonal T-cell pool. Interestingly, CD8.4 polyclonal mice showed significantly higher frequency of VM CD8$^+$ T cells than CD8WT control animals, although most CD8.4 T cells still showed a naïve phenotype (Fig 2A and B). Thus, CD8.4 induced the VM T-cell formation only in a subset of polyclonal CD8$^+$ T cells, implying that enhanced CD8-Lck coupling has clone-specific effects. The VM T cells from both CD8WT and CD8.4 mice rapidly produced IFNγ after stimulation with PMA/ionomycin, showing that CD8WT and CD8.4 VM T cells are indistinguishable in this functional trait, typical for memory T cells (Fig EV2A). Importantly, the analysis of mice in germ-free condition showed elevated frequency of CD44$^+$ and Tbet/Eomes double-positive T cells in CD8.4 mice when compared to CD8WT (Fig 2C and D), demonstrating that supraphysiological CD8-Lck coupling indeed promotes formation of VM T cells independently of the exposure to foreign antigens.

Although the VM and true CM T cells are very similar in many aspects, VM T cells were previously reported to express lower levels of CD49d and slightly higher levels of CD122 than true CM T cells (Haluszczak *et al*, 2009; Chiu *et al*, 2013; Sosinowski *et al*, 2013; White *et al*, 2016). However, CD49d as a marker discriminating VM and true CM T cells has not been validated using T cells from germ-free animals. For the first time, we could show that CD49d$^-$ and CD49d$^+$ T cells within the CD44$^+$ compartment of SPF and germ-free mice occur at comparable frequencies (Fig 2E). Only the CD49d$^-$ CD44$^+$, but not the CD49d$^+$ CD44$^+$, subset was expanded in the CD8.4 mouse, indicating that these subsets are not related (Fig 2E). Accordingly, CD122^{HI} CD49d$^-$ CD44$^+$ T cells, but not CD122^{LOW} CD49d$^+$ CD44$^+$ T cells, were more abundant in germ-free CD8.4 mouse than in germ-free CD8WT mouse (Figs 2F and G, and EV2B). Collectively, these data implied that CD122^{HI} CD49d$^-$ memory T cells represent the CD8$^+$ VM T-cell population, which originates from naïve T cells with a relatively strong level of self-reactivity independently of foreign antigens.

Virtual memory T cells use distinct TCR repertoire than naïve T cells

Based on the previous data, generation of VM T cells can be understood as a fate decision checkpoint of individual naïve T cells (staying naïve vs. becoming VM), where the decision is based on the level of self-reactivity of the T cell's TCR. This hypothesis predicts that naïve and VM T-cell compartments should contain different T-cell clones with distinct TCR repertoires. We analyzed the TCR repertoires by using a Vβ5 transgenic mouse with fixed TCRβ from the OT-I TCR (Fink *et al*, 1992). The advantage of this mouse is that it generates a polyclonal population of T cells, but the variability between the clones is limited to TCRα chains. Moreover, pairing of TCRα and TCRβ upon repertoire analyses is not an issue in this model. Last, but not least, this mouse has a relatively high frequency of oligoclonal T cells that recognize the ovalbumin antigen (Zehn & Bevan, 2006).

Unimmunized Vβ5 mice have a frequency of memory CD8$^+$ T cells around 10–15% which is comparable to wild-type mice (Fig 3A). When we analyzed the frequency of VM vs. naïve T cells among particular T-cell subsets defined by the expression of particular TCRVα segments, we observed that TCRVα3.2$^+$ T cells are comparable to the overall population, TCRVα2$^+$ T cells are slightly enriched for the VM T cells, and TCRVα8.3$^+$ T cells have lower frequency of VM T cells than the overall population (Fig 3A). These data suggested that naïve and VM T cells might have distinct TCR repertoires. However, the differences between the subsets were only minor, most likely because particular TCRVα subsets had still significant intrinsic diversity. To further reduce clonality in our groups, we gated on K^b-OVA-specific TCRVα3.2$^+$, TCRVα2$^+$, and TCRVα8.3$^+$ T cells (Fig 3B). Interestingly, around 50% of OVA-specific TCRVα2$^+$ clones exhibited VM phenotype, whereas vast majority of OVA-specific TCRVα8.3$^+$ T cells were naïve and OVA-specific TCRVα3.2$^+$ T cells had intermediate frequency of VM T cells in peripheral LN, mesenteric LN as well as in the spleen (Fig 3B and C). Accordingly, the frequency of TCRVα2$^+$ T cells is almost 10-fold higher in VM than in naïve OVA-specific T-cell population, whereas the frequency of TCRVα8.3$^+$ T cells is slightly lower in VM than in naïve OVA-specific T cells (Fig EV3A). Similar differences between total and OVA-specific TCRVα3.2$^+$, TCRVα2$^+$, and TCRVα8.3$^+$ CD8$^+$ T cell subsets were observed in germ-free Vβ5 mice (Fig 3D and E), confirming the VM identity of memory-phenotype T cells in the Vβ5 mice. In addition, OVA-specific TCRVα2$^+$ had higher levels of CD5 than TCRVα8.3$^+$ (Fig EV3B and C), suggesting that OVA-specific TCRVα2$^+$ clones are on average more self-reactive than TCRVα8.3$^+$ clones. This explains why more OVA-specific TCRVα2$^+$ T cells than TCRVα8.3$^+$ T cells acquire the VM phenotype in Vβ5 mice.

Based on the analysis of particular TCRVα subsets, we hypothesized that naïve and VM T cells would contain different TCR clonotypes. We cloned and sequenced genes encoding for TCRα chains from OVA-reactive CD8$^+$ VM and naïve T-cell subsets from germ-free Vβ5 mice using primers specific for TRAV14 (TCRVα2) and TRAV12 (TCRVα8) TCR genes (Table EV1). The distribution of the clonotypes as well as TRAJ usage was significantly different between VM and naïve subsets (Figs 3F and EV3D). We observed essentially two types of clonotypes that were captured in more than 1 experiment (Fig 3F). One type of clonotypes, called "VM clones",
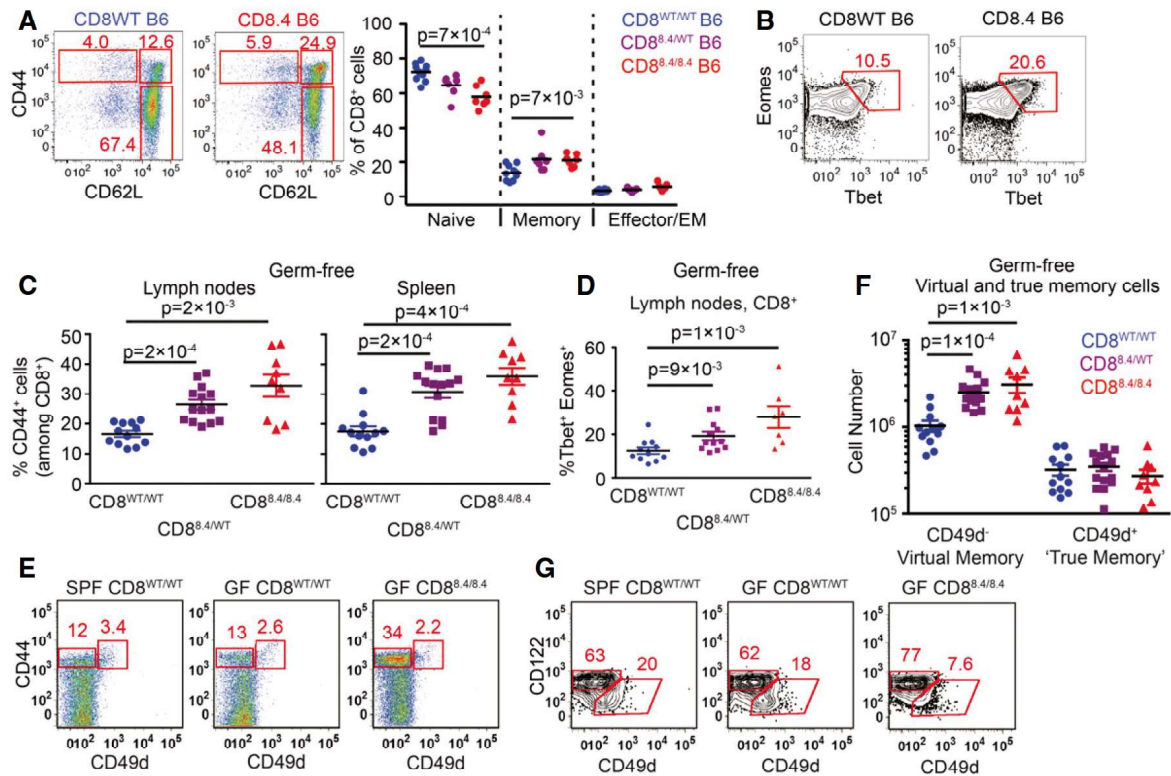
Figure 2. CD8-Lck coupling is a limiting factor for the size of the virtual memory T-cell compartment.

A, B   Percentages of naïve (CD44⁻ CD62L⁺), central memory (CD44⁺ CD62L⁻), and effector/effector memory (CD44⁺ CD62L⁻) (A) and Eomes⁺ Tbet⁺ (B) CD8⁺ LN T cells isolated from CD8WT and CD8.4 mice were determined by flow cytometry. Representative experiments out of seven (A) or five (B) in total.

C–F   LN cells and splenocytes were isolated from germ-free polyclonal CD8WT, CD8.4, and heterozygous CD8^WT/8.4 mice and CD8⁺ T cells were analyzed by flow cytometry. (C) Percentage of CD44⁺ T cells among CD8⁺ LN cells and splenocytes. Mean + SEM. n = 9–14 mice per group from four independent experiments. (D) Percentage of Tbet⁺ Eomes⁺ double-positive T cells. Mean ± SEM. n = 7–12 mice per group from three independent experiments. (E) Percentage of CD44⁺ CD49d⁻ VM and CD44⁺ CD49d⁺ true memory T cells in the spleen. A representative experiment out of four in total. (F) Absolute numbers of CD8⁺ CD44⁺ CD49d⁻ VM and CD8⁺ CD44⁺ CD49d⁺ true memory T cells in LN and the spleen were quantified. Mean + SEM. n = 9–14 mice from four independent experiments.

G   Percentage of CD122^HI CD49d⁻ VM and CD122^LOW CD49⁺ true CM cells among CD8⁺ CD44⁺ CD62L⁺ CM T cells isolated from LN. A representative experiment out of three in total.

Data information: Statistical significance was determined using two-tailed Mann–Whitney test.
Source data are available online for this figure.

was enriched among VM T cells and was also present in naïve T cells. The other type, "naïve clones", was almost exclusively detected in naïve T cells. These data demonstrate that naïve and VM T-cell population contain different T-cell clones.

To directly investigate whether TCR is the main factor that determines whether a particular T cell has the potential to differentiate into VM T cells, we established a protocol to generate monoclonal T-cell populations using transduction of a particular TCRα-encoding gene in a retrogenic vector into immortalized hematopoietic stem cells (Ruedl *et al*, 2008). We transduced immortalized Vβ5 Rag2⁻/⁻ hematopoietic stem cells with expression vectors encoding for two VM TCRα clones (V14 C1 and V14 C2), three naïve TCRα clones (V14-C6, V14-C7, and V14-C17), or OT-I TCRα as a control (Fig EV3F). At least 8 weeks after the transplantation of the progenitors into a Ly5.1 recipient, we analyzed the cell fate of the donor monoclonal T-cell populations. T cells expressing VM TCR clones formed a significant VM T-cell population, whereas T cells expressing naïve TCR clones formed a homogenous naïve population (Figs 3G and EV3F). These data demonstrate that the virtual

memory T cells are formed only from certain T-cell clones and that the TCR sequence determines whether a T cell differentiates into a VM T cell or stays naïve.

In a next step, we addressed whether "VM clones" are more self-reactive than "naïve clones". We compared levels of CD5, a commonly used reporter for self-reactivity, on naïve (CD44⁻) populations of retrogenic monoclonal T cells. "VM clones" expressed significantly higher CD5 levels than "naïve clones", indicating that "VM clones" are indeed T cells with a relatively high level of self-reactivity (Figs 3H and EV3G). Interestingly, retrogenic OT-I T cells represented an intermediate VM population, which corresponds to their level of self reactivity (Figs 1H, 3G, and EV3F and G). Moreover, the relative size of retrogenic OT-I VM population well corresponded to the frequency of VM T cells in conventional transgenic OT-I TCR mice (Fig 1E and H), indicating that the protocol for generation of retrogenic monoclonal T cells itself does not have a strong effect on VM formation. Overall, these results document that only relatively highly self-reactive clones form VM T cells.
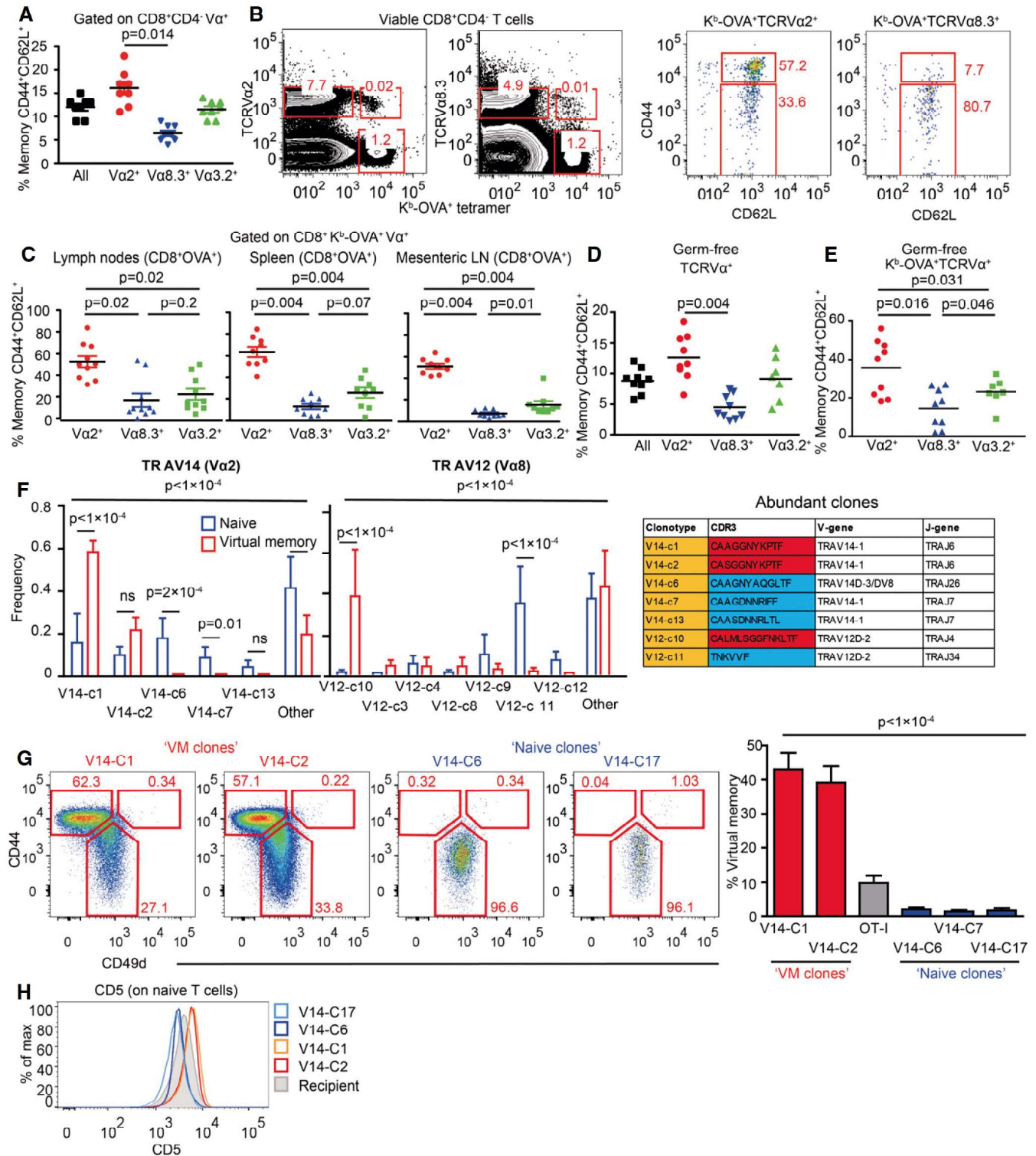
Figure 3.

Virtual memory T cells represent an intermediate stage between naïve and memory T cells

The relationship of the differentiation programs of naïve, VM, and true CM T cells is unclear. So far, CD49d and, to a lesser extent, CD122 were the only known markers discriminating between true CM memory and VM T cells (Haluszczak *et al*, 2009; Chiu *et al*, 2013; Sosinowski *et al*, 2013; White *et al*, 2016). To compare their gene expression profiles, we performed deep RNA sequencing of the transcripts from sorted CD8$^+$ naïve (CD44$^-$ CD62L$^+$) and VM (CD44$^+$ CD62L$^+$ CD49d$^-$) T cells isolated from germ-free animals and from true antigen-specific CM T cells (TM) (K^b-OVA$^+$ CD44$^+$

Figure 3. Virtual memory and naïve T cells use different TCR repertoires.

A   LN cells isolated from Vβ5 mice were stained for CD8, CD4, CD44, CD62L, and Vα2 or Vα8.3 or Vα3.2. CD8$^+$ T cells were gated as CD8$^+$ CD4$^-$ and then the percentage of CD44$^+$ CD62L$^+$ memory T cells among CD8$^+$ Vα2$^+$ or CD8$^+$ Vα8.3$^+$ or CD8$^+$ Vα3.2$^+$ T cells was determined by flow cytometry. Mean, n = 8 mice from eight independent experiments.

B, C   Cells isolated from peripheral LN (B, C), mesenteric LN (C), and the spleen (C) were stained as in (A) with the addition of OVA tetramer. The OVA-reactive Vα-specific CD8$^+$ T cells were gated and the percentage of CD44$^+$ CD62L$^+$ memory T cells was determined by flow cytometry. n = 9–10 mice from five independent experiments.

D   The same experiment as in (A) was performed using germ-free Vβ5 mice. Mean, n = 7–9 mice from four independent experiments.

E   The same experiment as in (B, C) was performed using a mixture of T cells isolated from LNs and the spleen from germ-free Vβ5 mice. Mean, n = 7–9 from 2 to 3 independent experiments.

F   RNA was isolated from memory (CD44$^+$CD62L$^+$) and (CD44$^+$CD62L$^+$) K^b-OVA$^+$ 4mer$^+$ T cells sorted from LNs and the spleen of germ-free Vβ5 mice. TCRα encoding genes using either TRAV12 (corresponding to Vα8) or TRAV14 (corresponding to Vα2) were cloned and sequenced. 12–20 clones were sequenced in each group/experiment. Clonotypes identified in at least two experiments are shown. Mean frequency + SEM, n = 4 independent experiments. Statistical significance was determined by chi-square test (global test) and paired two-tailed t-tests as a post-test (individual clones). CDR3 sequences of clonotypes enriched in naïve or VM compartments are shown in the table.

G, H   Retroviral vectors encoding selected TCRα clones were transduced into immortalized Rag2$^{-/-}$ Vβ5 bone marrow stem cells. These cells were transplanted into an irradiated Ly5.1 recipient. (G) At least 8 weeks after the transplantation, frequency of virtual memory T cells among LN donor T cells (CD45.2$^+$ CD45.1$^-$ GFP$^+$) was analyzed. Mean + SEM; n = 10–21 mice from 2 to 7 independent experiments. Statistical significance was tested using Kruskal–Wallis test. (H) CD5 levels on naïve monoclonal T cells were detected by flow cytometry. Representative mice out of 9–14 in total from two to four independent experiments.

Data information: (A, C–E) Statistical significance was determined by two-tailed Wilcoxon signed-rank test.
Source data are available online for this figure.

CD62L$^+$), generated by infecting Vβ5 mice with Lm expressing OVA (Lm-OVA). The data showed that naïve, VM, and TM T cells represent three distinct T-cell populations (Fig EV4A and B). We identified genes differently expressed in VM T cells in comparison with naïve or TM T cells (Tables EV2–EV5). Based on previously published data (Kaech *et al*, 2002; Luckey *et al*, 2006; Wherry *et al*, 2007), we established lists of memory signature and naïve signature genes. As expected, memory signature genes were enriched in TM T cells and naïve signature genes were enriched in naïve T cells (Figs 4A and EV4C). Interestingly, VM T cells exhibited an intermediate gene expression profile (Figs 4A and EV4C). Pairwise rotation gene set tests revealed the hierarchy in the enrichment for memory signature genes and for naïve signature genes as TM > VM > naïve, and naïve > VM > TM, respectively (Fig 4B). VM T cells also showed an intermediate expression of cytokine and chemokine encoding genes (Figs 4C and EV4D). The transcription of genes encoding for cytokine and chemokine receptors in VM T cells seemed to be also somewhat half-way between naïve and true CM T cells (Fig EV4E and F).

We further investigated selected differentially expressed genes between VM and true CM cells on a protein level. RNA encoding for CX3CR1 and NRP1 showed enrichment in TM vs. VM T cells. For this reason, we compared surface levels of CX3CR1 and NRP1 on naïve and VM T cells from unprimed mice and on TM and effector/effector memory T cells from LM-OVA infected mouse during the memory phase (Fig 4D and E). In contrast to VM T cells, a significant percentage of effector and TM T cells expressed CX3CR1 and NRP1, confirming the transcriptomic data and suggesting that VM T cells can be characterized as CX3CR1 and NRP1 negative.

Differentiation into virtual memory T cells does not break self-tolerance

VM T cells provide better protection against Lm than naïve T cells and respond to proinflammatory cytokines IL-12 and IL-18 by producing IFNγ (Haluszczak *et al*, 2009; Lee *et al*, 2013; White *et al*, 2016). Moreover, VM T cells express higher levels of several killer lectin-like receptors than naïve T cells (Table EV4 and White *et al*,

2016). The combination of a hyperresponsive differentiation state with the expression of highly self-reactive TCRs suggests that VM CD8$^+$ T cells could be less self-tolerant than naïve T cells and might represent a risk for inducing autoimmunity. We used CD8WT OT-I T cells (mostly naïve) and CD8.4 OT-I T cells (mostly VM) for a functional comparison of naïve and VM T cells with the same TCR specificity. VM CD8.4 OT-I T cells, but not naïve OT-I T cells, rapidly produced IFNγ after the stimulation by PMA/ionomycin or cognate antigen (Fig 5A), supporting the idea of an autoimmune potential of VM T cells. We directly tested this hypothesis using an experimental model of autoimmune diabetes (King *et al*, 2012). We transferred CD8WT OT-I or CD8.4 OT-I T cells into RIP.OVA mice expressing OVA under the control of rat insulin promoter (Kurts *et al*, 1998) and primed them with Lm-OVA or Lm-Q4H7 (King *et al*, 2012). Q4H7 is an antigen that binds to the OT-I TCR with a low affinity and does not negatively select OT-I T cells in the thymus (Daniels *et al*, 2006; Stepanek *et al*, 2014). Thus, Q4H7 resembles a self-antigen that positively selected peripheral T cells might encounter at the periphery. Surprisingly, CD8.4 OT-I T cells were not more efficient in inducing the autoimmune diabetes than CD8WT OT-I T cells in any tested condition (Figs 5B and EV5A). Adoptively transferred naïve OT-I, CD8.4 OT-I, and even TM OT-I T cells did not promote clearance of Lm-Q4H7 in this experimental setup (relatively low number of injected CFUs, low antigen affinity; Fig EV5B), excluding the possibility that the bacterial burden differs between experimental groups.

To further analyze the functional responses of VM T cells, we stimulated CD8.4 OT-I and CD8WT OT-I T cells with dendritic cells loaded with OVA or suboptimal cognate antigens T4 or Q4H7 *ex vivo*. No significant difference in the upregulation of CD69 or CD25 between naïve and VM cells was observed in the case of high-affinity OVA stimulation. However, the responses to antigens with suboptimal affinity to the TCR differed between these two cell types. Interestingly, although CD8.4 OT-I T cells showed stronger CD69 upregulation than naïve T cells when stimulated with low antigen dose, when the antigen dose was high, the response of VM T cells was lower than that of naïve T cells (Fig 5C). Upregulation of CD25 was lower in CD8.4 OT-I T cells than in naïve T cells, when activated with the low-affinity antigens (Fig 5D).
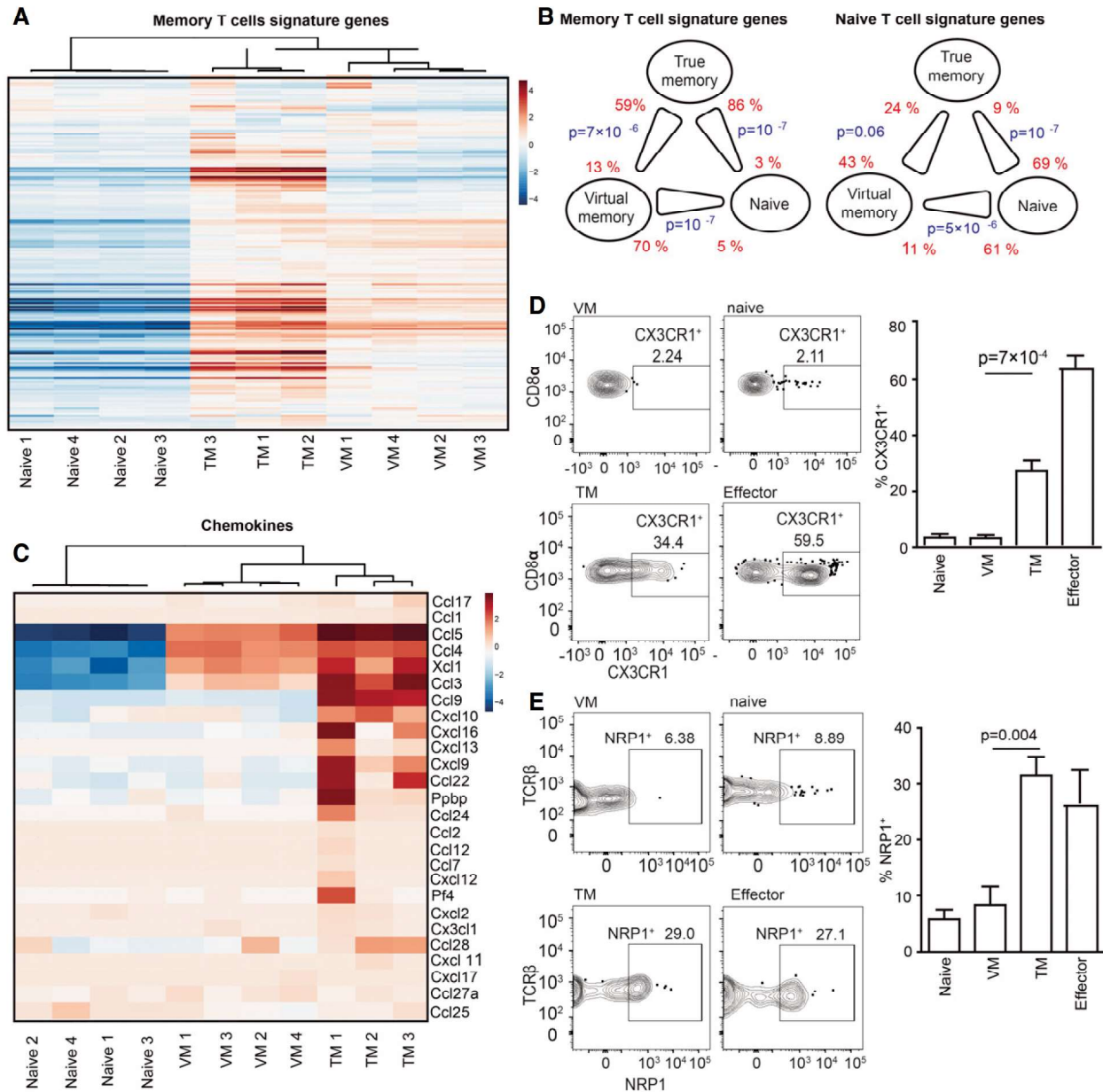
Figure 4. Virtual memory T cells represent an intermediate stage between naïve and true memory T cells.

A–C   Transcriptomes of naive ($n = 4$), VM ($n = 4$), and TM ($n = 3$) CD8$^+$ T cells were analyzed by deep RNA sequencing. (A) Enrichment of CD8$^+$ memory signature genes (as revealed by previous studies) in naïve, virtual memory, and true memory T cells. (B) Pairwise comparisons between naïve, VM, and TM CD8$^+$ cells for the overall enrichment of the memory signature and naïve signature gene sets by a method ROAST. The thick end of the connecting line between the populations indicates the population with the overall relative enrichment of the gene set, the percentage of the genes from the gene set that are more expressed in the indicated population (z-score > sqrt(2)) over the opposite population is indicated. (C) The relative enrichment of chemokine encoding transcripts in the samples is shown.

D, E   Surface staining for CX3CR1 (D) and NRP1 (E) was performed on naïve (gated as CD62L$^+$CD44$^-$CD49d^{low}) and VM (CD62L$^+$CD44$^+$CD49d^{low}) K^b-OVA-4mer$^+$ CD8$^+$ T cells isolated from unprimed Vβ5 mouse and on true CM memory (gated as CD62L$^+$CD44$^+$CD49d^{high}) and effector/effector memory (CD62L$^-$CD44$^+$CD49d^{high}) K^b-OVA-4mer$^+$ CD8$^+$ T cells isolated from Vβ5 mouse 30–45 days after Lm-OVA infection. A representative experiment out of five (D) or four (E) in total is shown. Mean percentage + SEM of CX3CR1$^+$ and NRP1$^+$ cells within the particular population is shown. (D) $n = 10$ immunized mice and five unprimed mice from five independent experiments. (E) $n = 8$ immunized mice and four unprimed mice from four independent experiments. Statistical analysis was performed by two-tailed Mann–Whitney test.

Source data are available online for this figure.

Next, we examined antigenic responses of naïve and VM T cells *in vivo*. CD8WT and CD8.4 OT-I T cells show comparable expansion when primed by Lm-OVA or Lm-Q4H7 (Fig EV5C). However, CD8.4 OT-I formed significantly less memory precursors (IL-7R$^+$KLRG1$^-$), more IL-7R$^+$KLRG1$^+$ double-positive cells, and slightly more short-lived effector cells (IL-7R$^-$KLRG1$^+$) than CD8WT OT-I T cells upon
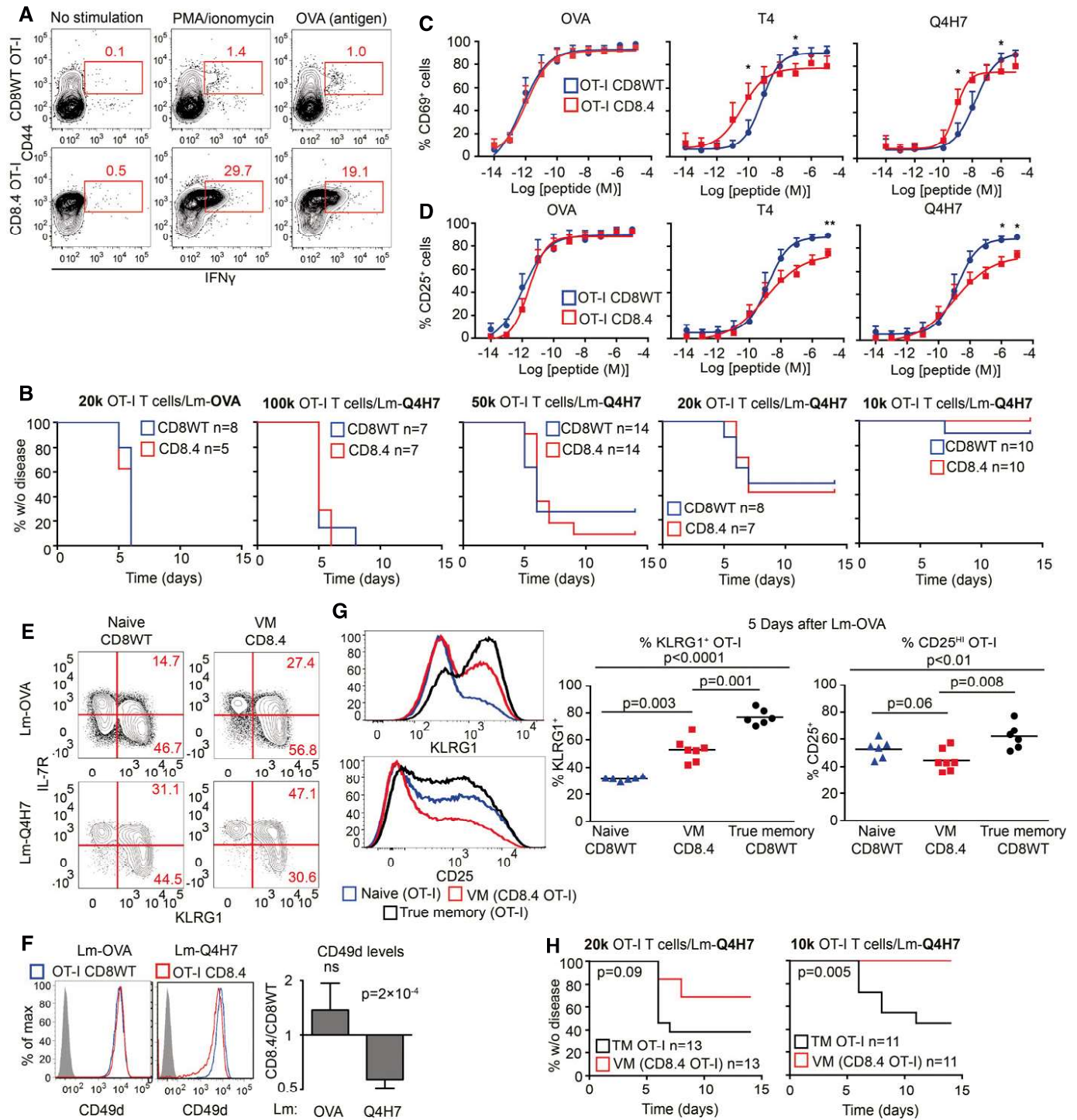
Figure 5.

priming with Lm-OVA (Figs 5E and EV5C). Interestingly, upon priming with low-affinity Lm-Q4H7, VM T cells formed less short-lived effector cells and more IL-7R$^+$KLRG1$^+$ double-positive cells (Figs 5E and EV5C). Moreover, CD8.4 OT-I T cells did not upregulate CD49d (a subunit of VLA-4) to the same extent as CD8WT OT-I upon immunization with Lm-Q4H7 (Fig 5F). Collectively, VM T cells exhibited several signs of hyporesponsiveness in comparison with naïve T cells upon low-affinity antigenic stimulation: lower

upregulation of CD25 *in vitro*, lower frequency of short-lived effector cells, and lower CD49d upregulation.

Subsequently, we compared responses of VM CD8.4 T cells to naïve and true memory OT-I T cells *in vivo*. True memory showed stronger upregulation of KLRG1 and CD25 than VM T cells upon Lm-OVA challenge (Fig 5G). Importantly, true memory OT-I T cells were more potent in inducing the autoimmune diabetes in our RIP.OVA model (Figs 5H and EV5D). Collectively, these data

◀

Figure 5. Virtual memory T cells are as self-tolerant as naïve T cells.

A   LN cells isolated from CD8WT OT-I and CD8.4 OT-I mice were stimulated with PMA and ionomycin or OVA peptide in the presence of BD GolgiStop for 5 h and the production of IFNγ was analyzed by flow cytometry (gated as CD8⁺). A representative experiment out of four in total.

B   Indicated number of CD8WT OT-I or CD8.4 OT-I T cells were adoptively transferred into RIP.OVA hosts, which were infected with Lm-OVA or -Q4H7 1 day later. The glucose in the urine was monitored for 14 days. The percentage of non-diabetic mice in time is shown. Differences between OTI-I and CD8.4 were not significant by log-rank test. *n* = 5–11 (indicated) mice per group in 3–6 independent experiments.

C, D   CD8WT OT-I or CD8.4 OT-I LN T cells were stimulated *ex vivo* with dendritic cells loaded with varying concentrations of OVA, Q4R7, Q4H7 peptides overnight and the expression of CD69 (C) and CD25 (D) on CD8⁺ T cells was analyzed. Mean + SEM. *n* = 3–5 independent experiments. Statistical significance was determined paired two-tailed Student's *t*-test (C, D). *$P < 0.05$, **$P < 0.01$.

E, F   CD8WT OT-I or CD8.4 OT-I LN T cells were adoptively transferred to polyclonal Ly5.1 host mice, which were infected 1 day later with transgenic Lm-OVA or -Q4H7. Six days after the infection, splenocytes from the hosts were isolated and analyzed for the expression of IL-7R, KLRG1 (E) or CD49d (F). (F) A representative experiment out of four (7–9 mice per group in total). (E) *n* = 7 (Lm-OVA) or 9 (Lm-Q4H7) from four independent experiments. Statistical significance was determined using a one-value two-tailed *t*-test (for the ratio of CD49d MFI between the subsets). Normality of the data was tested using Shapiro–Wilk normality test (passing threshold $P < 0.01$).

G 1×10^4 naïve CD8WT OT-I, VM CD8.4 OT-I, or true memory OT-I T cells loaded with 5 μM CellTrace Violet were injected into Ly5.1 recipients followed by immunization with Lm-OVA 1 day later. Five days after the immunization, splenocytes were isolated and donor cells were examined for the expression of KLRG1 and CD25 by flow cytometry. *n* = 6 from three independent experiments. Statistical significance was performed by Kruskal–Wallis test, and selected pairs of groups were compared by Mann–Whitney test.

H   Indicated number of CD8.4 OT-I or true memory OT-I T cells were adoptively transferred into RIP.OVA hosts, which were infected with Lm-Q4H7 1 day later. The glucose in the urine was monitored for 14 days. The percentage of non-diabetic mice in time is shown. Statistical significance was calculated by log-rank test. *n* = 11 (1×10^4 transferred cells) or 13 (2×10^4 transferred cells) mice per group in four independent experiments.

Source data are available online for this figure.

suggest that virtual memory T cells are less efficient in their responses to the antigen *in vivo* and in inducing the autoimmune tissue pathology than true memory T cells.

We wondered whether CD8.4 OT-I T cells do respond to endogenous self-antigens Catnb and Mapk8 that were previously proposed as positive selecting antigens for OT-I T cells (Santori *et al*, 2002). In agreement with previous reports (Salmond *et al*, 2014; Oberle *et al*, 2016), we could not detect a substantial response of peripheral OT-I T cells to these antigens *in vitro* using antigen-loaded dendritic cells and *in vivo* using Lm-Catnb (Fig EV5E and F). CD8.4 OT-I T cells showed no significant response to these self-peptides as well (Fig EV5E and F). Although we could see that Lm infection induced proliferation of VM CD8.4 T cells (probably via cytokines), expression of the positive selecting self-antigen Catnb in the *Listeria* did not enhance this response at all (Fig EV5F). These experiments suggest that VM T cells are tolerant to self-antigens that have previously triggered their conversion to VM T cells.

Retrogenic T cells as a model for functional differences between naïve and VM T cells

To complement our data from CD8.4 OT-I VM model, we used sorted naïve and VM T cells from the OVA-specific clones V14-C1 and V14-C2 (Fig 3F–H). The advantage of this approach is that both naïve and VM express the same TCR and CD8 coreceptor and any differences between these populations can be attributed solely to their different developmental programs. We adoptively transferred these cells into RIP.OVA mice followed by infection with Lm-OVA. Naïve T cells were more efficient in inducing the autoimmune diabetes than VM T cells in case of both clones, but only the clone V14-C1 showed a statistically significant difference (Fig 6A). When we adoptively transferred naïve or VM T cells expressing V14-C1 or V14-C2 TCRs into Ly5.1 recipients followed by immunization with dendritic cells loaded with OVA or lower affinity antigen Q4R7, we observed that VM clones showed significantly lower level of upregulation of CD49d, a subunit of VLA4 important for tissue infiltration (Fig 6B). These observations were in agreement with the results

obtained with the CD8.4 OT-I model of monoclonal VM T cells, demonstrating that VM T cells are not inherently less self-tolerant than naïve T cells.

Although others and we showed that VM T cells elicit stronger responses than naïve T cells in some assays (Fig 5A and Lee *et al*, 2013), they do not show a stronger potency than naïve T cells to induce autoimmune pathology in our diabetic model. Most likely VM T cells acquire mechanisms to suppress their responses to antigens, infiltration of the tissue, and/or their effector functions. One such mechanism, contributing to the self-tolerance of VM T cells, can be lower expression of CD49d and CD25 upon activation. Collectively, these data establish that relatively strongly self-reactive T-cell clones differentiate into VM T cells and trigger a specific developmental program that enables them to efficiently response to infection, but does not increase their autoimmune potential (Fig 7).

Discussion

We observed that CD8-Lck coupling frequency regulates intensity of TCR homeostatic signals. For the first time, we showed that the intrinsic sensitivity of the TCR signaling machinery sets the frequency of VM CD8⁺ T cells. We also showed that only relatively strongly self-reactive T-cell clones have the potential to form VM T cells. We identified the gene expression profile of VM T cells and showed that they represent an intermediate stage between naïve and true CM T cells. Although the combination of relatively strong self-reactivity and acquisition of the partial memory program could represent a potential risk for autoimmunity, we observed that VM T cells are not more potent than naïve T cells in a model of experimental type I diabetes.

It is well established that some memory-phenotype T cells respond to an antigen, and they have not been previously exposed to (Haluszczak *et al*, 2009; Lee *et al*, 2013; Sosinowski *et al*, 2013; Su *et al*, 2013; White *et al*, 2017). Some researchers call these cells as VM T cells and propose that they were generated in the absence of a foreign antigenic stimulation (Haluszczak *et al*, 2009; White
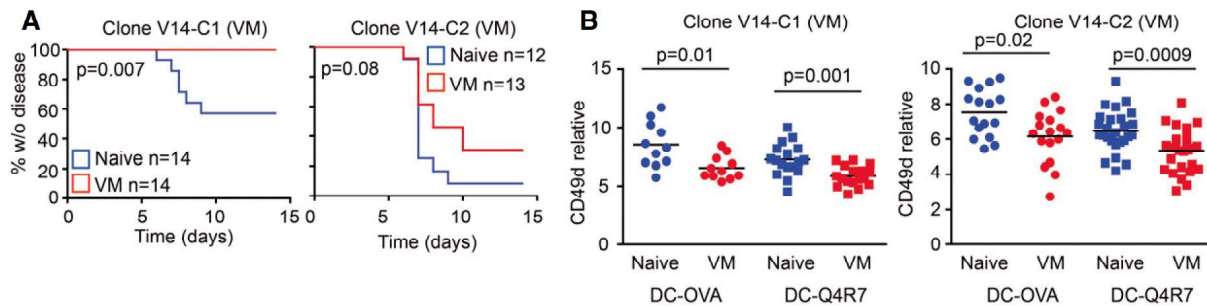
Figure 6.   Comparison of naïve and VM subsets generated from retrogenic T-cell clones.

A 5×10^3 FACS-sorted naïve (CD44⁻) or VM (CD44⁺) T cells from V14-C1 or V14-C2 T cells generated via bone marrow transfer (Fig EV3E) were adoptively transferred into RIP.OVA mice followed by immunization with Lm-OVA 1 day later. Glucose concentration in the urine was monitored for 14 days. Statistical significance was tested using log-rank test. *n* = 12–14 mice per group in 4–5 independent experiments.

B   FACS-sorted naïve (CD44⁻) or VM (CD44⁺) T cells from V14-C1 or V14-C2 T cells generated via bone marrow transfer (Fig EV3E) were adoptively transferred into RIP.OVA mice followed by immunization with OVA- or Q4R7-loaded bone marrow-derived dendritic cells. The number of adoptively transferred T cells was 1×10^3 and 3×10^3 for OVA- and Q4R7-loaded dendritic cells, respectively. *n* = 11–27 mice per group in 5–6 independent experiments. Mean is indicated. Statistical significance was tested using Mann–Whitney test.

Source data are available online for this figure.
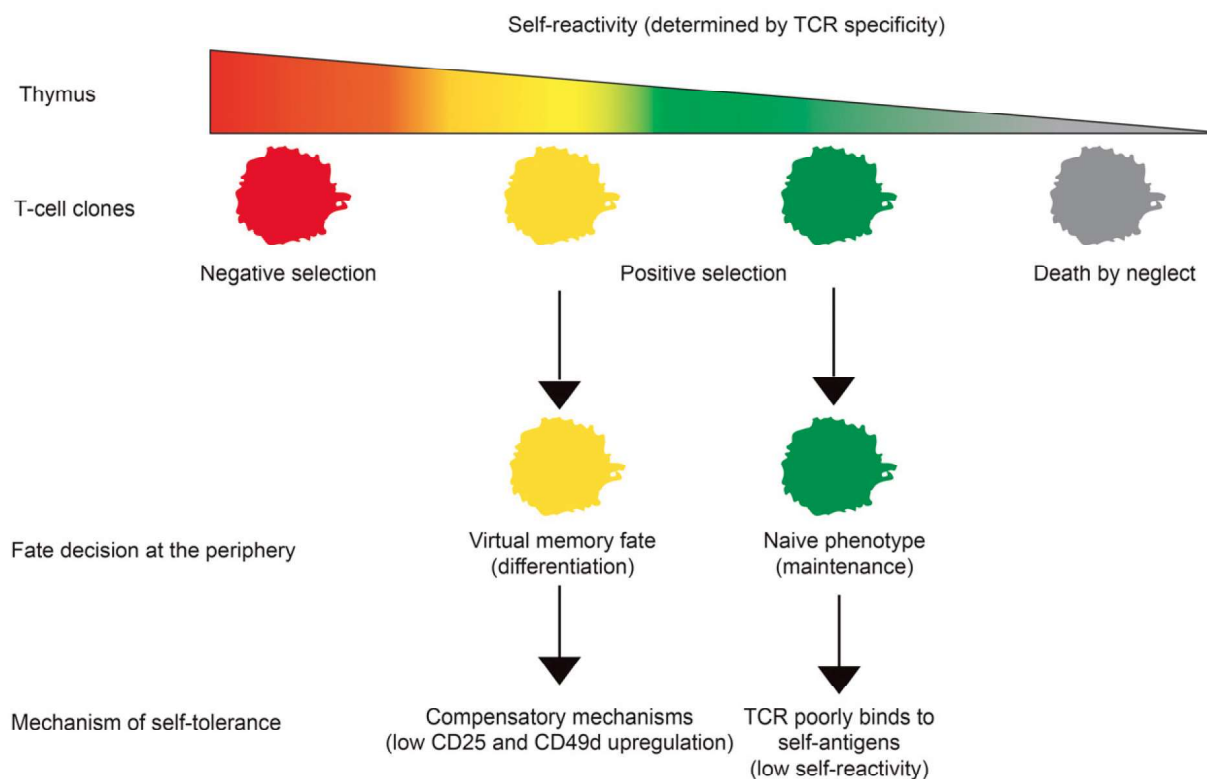
Figure 7.   Schematic representation of the role of self-reactivity in major cell fate decisions of conventional CD8⁺ T cells.

Our results establish a novel T-cell fate decision checkpoint, differentiation of positively selected T-cell clone with a relatively high level of self-reactivity into virtual memory T cells.

et al, 2017). The main argument supporting this hypothesis is that germ-free mice, with low levels of foreign antigenic exposure, contain comparable levels of CM-phenotype T cells as control mice (Haluszczak *et al*, 2009). However, in mice with normal microbiota, which were used for the subsequent characterization of VM T cells, it is difficult to exclude the existence of cross-reactive memory T

cells that were previously exposed to another foreign antigen (Su *et al*, 2013). Importantly, we show that CD8.4 knock-in mice with enhanced homeostatic TCR signaling exhibit larger VM compartment than CD8WT T cells in SPF and germ-free conditions. We confirmed that VM T cells have lower expression of CD49d than antigen-experienced cells using germ-free mice and confirmed that

antigen-inexperienced VM T cells can be defined as CD49$^-$CD122^{HI} T cells. Altogether these data established that the strength of homeostatic signals provided to T cells is a major factor leading to formation of VM compartment independently of stimulation with cognate foreign antigens.

It has been observed that IL-15 availability is a limiting factor regulating the size of the VM subset (Sosinowski *et al*, 2013; White *et al*, 2016). In this study, we showed that the intrinsic sensitivity of the TCR signaling machinery (specifically the CD8-Lck coupling frequency) is another major factor that sets the frequency of VM CD8$^+$ T cells in the secondary lymphoid organs. It has been suggested that the level of CD5, a marker of self-reactivity, is linked with the T-cell ability to form VM T cells (White *et al*, 2016). We investigated individual T-cell clones using transgenic cells with normal and hypersensitive TCR signaling machinery, comparing TCR repertoires of naïve and VM T cells, and analyzing retrogenic monoclonal T-cell populations. These complementary approaches revealed that VM T-cell formation absolutely depends on the level of self-reactivity of a particular T cell and exhibits a threshold behavior. Relatively highly self-reactive T cell clones frequently differentiate into VM T cells (~ 40–50%), whereas weakly self-reactive T cells completely lack this property. This finding characterizes the formation of VM T cells as a previously unappreciated T-cell fate decision check point, where the intensity of homeostatic TCR signals is the critical decisive factor. Our data also explain a previous observation that VM T cells are formed exclusively from T cells expressing endogenous recombined TCR chains in OT-I Rag$^+$ mice during aging (Renkema *et al*, 2014). Some of the T-cell clones that replaced the OT-I TCR with a variable endogenous one are probably more self-reactive than OT-I T cells, which drives their differentiation in VM T cells.

The functionality of a T-cell subset is determined by its gene expression profile. Whereas it is clear that VM T cells substantially differ from naïve T cells (Haluszczak *et al*, 2009; Lee *et al*, 2013; Sosinowski *et al*, 2013; White *et al*, 2016), the CD49d and CD122 were the only markers that can distinguish VM T cells from true memory (TM) T cells. In this study, we characterized gene expression of VM T cells and compared it to naïve T cells from germ-free mice and foreign antigen-specific TM T cells. Analysis focusing on previously established naïve and memory T-cell signature genes revealed that VM T cells have an intermediate gene expression profile between naïve and TM T cells. Accordingly, expression of chemokines and cytokines was generally lower in VM T cells than in TM T cells. These data suggest that VM T cells trigger a partial memory program. Alternatively, TM CD8$^+$ T cells might represent a heterogeneous population of two or more subsets with different degrees of similarity to VM T cells, as suggested by heterogeneous expression of CX3CR1 and NRP1, two genes that showed a large difference between TM and VM T cells. Indeed, CX3CR1 has been proposed as a marker that discriminates different subsets of memory T cells (Bottcher *et al*, 2015; Gerlach *et al*, 2016). Single cell gene expression profiling would show whether immune responses to foreign antigens generate any TM T cells identical to VM T cells.

VM T cells share some phenotypic traits with stem-like memory (SCM) T cells, including higher expression of CD122, CXCR3, and dependency on IL-15 (Zhang *et al*, 2005). However, unlike VM cells, SCM T cells are derived from CD44^{low} population and human SCM

T-cell counterparts are derived from the CD45RA$^+$ population (Gattinoni *et al*, 2011). Furthermore, SCM T cells express Sca-1 stemness marker which is not upregulated in the VM T cells as revealed by our RNAseq data. Thus, VM and SCM T cells represent two distinguishable subsets of CD8$^+$ T cells. However, because SCM T cells give rise to central memory, effector memory, and effector CD8$^+$ T cells (Gattinoni *et al*, 2011), we cannot exclude that VM T-cell population preferentially arise from SCM T cells.

VM T cells were shown to surpass naïve T cells in their response to inflammatory cytokines IL-12 and IL-18 (Haluszczak *et al*, 2009), in the rapid generation of short-lived effectors (Lee *et al*, 2013), rapid IFNγ production, and in the protection against Lm both in antigen-specific (Lee *et al*, 2013) and in by-stander manners (Wu *et al*, 2010). We demonstrated that VM T cells develop from relatively strongly self-reactive T-cell clone. Both the hyperresponsivness and self-reactivity of VM T cells might potentially enhance their capacity to break self-tolerance. We addressed the potency of VM T cells to induce experimental autoimmune pathology by using two monoclonal models for comparing naïve and VM T cells with the same TCR specificity. We observed that VM T cells were not more efficient than naïve T cells in inducing the experimental autoimmune diabetes on a per cell basis. This can be at least partially explained by the fact that VM T cells show lower upregulation of CD25 and VLA-4 than naïve T cells when activated with a suboptimal antigen. VLA-4 has been previously shown to be essential for the induction of the tissue pathology in the mouse experimental model of type I diabetes (King *et al*, 2012). We propose that VM T cells surpass naïve T cells in some kind of responses to promote rapid immunity to pathogens (Lee *et al*, 2013; White *et al*, 2016), but they also develop compensatory mechanisms that make these cells self-tolerant to an extent comparable to naïve T cells. We used an experimental model of autoimmune diabetes, a prototypic autoimmune pathology that involves self-reactive CD8$^+$ T cells. The important aspect of our model is that the adoptively transferred neoself-reactive T cells developed in the absence of the neoself antigen. We cannot exclude the possibility that VM T cells represent a major risk in other types of autoimmune diseases/conditions.

Based on pilot studies in the field (Pihlgren *et al*, 1996; Curtsinger *et al*, 1998; London *et al*, 2000), it was generally accepted that one feature of immunological memory is that a memory T cell elicits a faster and stronger response to cognate antigens than a naïve T cell. However, recent evidence showed that, at least under certain conditions, the response of naïve T cells to an antigen is stronger than the response of memory T cells (Knudson *et al*, 2013; Mehlhop-Williams & Bevan, 2014; Cho *et al*, 2016). We showed that true memory T cells surpass virtual memory T cells in the upregulation of KLRG1, CD25, and in their potency to induce experimental autoimmune pathology. These data correspond to a previous study showing stronger responses of TM T cells in comparison with lymphopenia induced memory T cells (Cheung *et al*, 2009), suggesting that virtual memory and lymphopenia-induced memory T cells might have similar functions. The physiological role of VM T cells needs to be further investigated, but it seems plausible that VM T cells have unique type of responses to pathogens and thus contribute to functional diversity of T-cell immunity, which might be required for efficient immune protection.

Recently, it has been proposed that human innate Eomes$^+$ KIR/NKG2A$^+$ CD8$^+$ T cells (Jacomet *et al*, 2015) represent counterparts of murine VM T cells, although expression of some markers including CD27 and CD5 substantially differed between these two subsets (White *et al*, 2016). It would be interesting to elucidate whether the human Eomes$^+$ KIR/NKG2A$^+$ CD8$^+$ subset shows similar gene expression pattern as mouse VM T cells, whether they originate from relatively highly self-reactive clones, and whether these cells acquire tolerance mechanisms as murine VM CD8$^+$ T cells do.

Materials Methods

Antibodies and reagents

Antibodies to following antigens were used for flow cytometry: CD69 (clone H1.2F3), CD11a (LFA-1) (clone M17/4), CD25 (PC61), CD3 (145-2C11), IFNγ (XMG1.2), TCRβ (H57-597), TCR Vα2 (B20.1), TCR Vα8.3 (B21.14), TCR Vα3.2 (R3-16), CD49d (R1-2), CD5 (53-7.3) (all BD Biosciences), Tbet (4B10), Eomes (Dan11mag), CD8α (53-6.7), CD8β (H35-17.2), CD127 (A7R34) (all eBioscience) CD44 (IM7), CD4 (RM-45), CD62L (MEL-14), CD122 (TM-beta1), KLRG1 (2F1), PD-1 (RMP1-30), CD19 (6D5) (all Biolegend), pErk1/2 (D13.14.4E, Cell Signaling). The antibodies were conjugated with various fluorescent dyes or with biotin by manufacturers. K^b-OVA PE tetramer was prepared as described previously (Stepanek *et al*, 2014). Peptides OVA$_{257-264}$ (SIINFEKL), Q4R7 (SIIRFERL), Q4H7 (SIIRFEHL), NP68 (ASNENMDAM), NP372E (ASNENMEAM), Mapk8$_{267-274}$ (AGYSFEKL), and Catnb$_{329-336}$ (RTYTYEKL) were purchased from Eurogentec or Peptides&Elephants. Proliferation dye CellTrace Violet was purchased from ThermoFisher Scientific (C34557).

Flow cytometry and cell counting

For the surface staining, cells were incubated with diluted antibodies in PBS/0.5% gelatin or PBS/2% goat serum on ice. LIVE/DEAD near-IR dye (Life Technologies) or Hoechst 33258 (Life Technologies) was used for discrimination of live and dead cells. For the intracellular staining, cells were fixed and permeabilized using Foxp3/Transcription Factor Staining Buffer Set (eBioscience, 00-5523-00). For some experiments, enrichment of CD8$^+$ T cells was performed using magnetic bead separation kits EasySep (STEMCELL Technologies) or Dynabeads (Thermo Fisher Scientific) according to manufacturer's instructions prior to the analysis or sorting by flow cytometry. Cells were counted using Z2 Coulter Counter (Beckman) or using AccuCheck counting beads (Thermo Fisher Scientific) and a flow cytometer. Flow cytometry was carried out with a FACSCantoII, LSRII, or a LSRFortessa (BD Bioscience). Cell sorting was performed using a FACSAria III or Influx (BD Bioscience). Data were analyzed using FlowJo software (TreeStar).

Experimental animals

All mice were 5–12 weeks old and had C57Bl/6j background. RIP.OVA (Kurts *et al*, 1998), OT-I Rag2$^{-/-}$ (Palmer *et al*, 2016), CD8.4, F5 Rag1$^{-/-}$ (Erman *et al*, 2006), and Vβ5 (Fink *et al*, 1992)

strains were described previously. Mice were bred in our facilities (SPF mice: University Hospital Basel and Institute of Molecular Genetics; germ-free mice: University of Bern, Switzerland) in accordance with Cantonal and Federal laws of Switzerland and the Czech Republic. Animal protocols were approved by the Cantonal Veterinary Office of Basel-Stadt, Switzerland, and Czech Academy of Sciences, Czech Republic. Transfer into germ-free conditions was performed using time-mating followed by transferring 2-cell embryos into germ-free foster mothers.

Males and females were used for the experiments. Age- and sex-matched pairs of animals were used in the experimental groups. If possible, littermates were equally divided into the experimental groups. The randomization for adoptive transfer experiments was done by assigning the experimental conditions to recipient mouse ID numbers by an experimenter who had no prior contact with the mice. Other experiments were not randomized. The experiments were not blinded since no subjective scoring method was used.

RNA sequencing

RNA was isolated using Trizol (Thermo Fisher Scientific) followed by in-column DNase treatment using RNA clean & concentrator kit (Zymo Research). The library preparation and RNA sequencing by HiSeq2500 (HiSeq SBS Kit v4, Illumina) were performed by the Genomic Facility of D-BSSE ETH Zurich in Basel. Obtained single-end RNAseq reads were mapped to the mouse genome assembly, version mm9, with RNA-STAR (Dobin *et al*, 2013), with default parameters except for allowing only unique hits to genome (outFilterMultimapNmax = 1) and filtering reads without evidence in spliced junction table (outFilterType = "BySJout"). All subsequent gene expression data analysis was done within the R software (R Foundation for Statistical Computing, Vienna, Austria). Raw reads and mapping quality were assessed by the qQCreport function from the R/Bioconductor software package QuasR (version 1.12.0; Gaidatzis *et al*, 2015). Using RefSeq mRNA coordinates from UCSC (genome.ucsc.edu, downloaded in July 2013) and the qCount function from QuasR package, we quantified gene expression as the number of reads that started within any annotated exon of a gene. The differentially expressed genes were identified using the edgeR package (version 3.14.0; Robinson *et al*, 2010). We generated lists of naïve and memory signature genes based on previously published studies [gene sets M3022, M5832, M3039 for memory, and M3020, M5831, M3038 for naïve T cells in the Molecular Signature Databases (Kaech *et al*, 2002; Subramanian *et al*, 2005; Luckey *et al*, 2006; Wherry *et al*, 2007)]. In our memory and naïve signature gene lists, we included only genes that were listed at least in two out of the above-mentioned three respective gene sets. For the global comparison of the expression of the signature genes in naïve, VM, and true CM T cells, we used self-contained gene set enrichment test called Roast, which is available in edgeR package (Wu *et al*, 2010).

DNA cloning and production and viruses

RNA was isolated using Trizol reagent (Thermo Fisher Scientific) and RNA clean & concentrator kit (Zymoresearch, R1013). Reverse transcription was performed using RevertAid (Thermo Fisher Scientific) according to the manufacturer's instructions. TCR sequences

were amplified using cDNA from sorted T cells by PCR using Phusion polymerase (New England Biolabs) and following primers: TRACrev (EcoRI) 5′-TCAGACgaattcTCAACTGGACCACAGCCTCA, TRAV14for (XhoI) 5′ GTAGCTctcgagATGGACAAGATCCTGACA GCA, TRAV12for (XhoI) 5′ GTAGCTctcgagATGCGTCCTGDCACCTG CTC and ligated into pBlueScript vector using T4 ligase (New England Biolabs) and sequenced by Sanger sequencing using T7 primer 5′ TAATACGACTCACTATAGGG. Selected clones were cloned into MSCV-GFP vector via EcoRI and XhoI (New England Biolabs).

Coding sequence of SCF, IL-3 and IL-6 was obtained from bone marrow cDNA with Phusion polymerase using these primers: SCFfor 5′-TTGGATCCGCCACCATGAAGAAGACACAAACTTGGATT ATC, SCFrev 5′-AACTCGAGTTACACCTCTTGAAATTCTCTCTCTTTC, IL-3for 5′-TTGAATTCGCCACCATGGTTCTTGCCAGCTCTACCACCAG, IL3rev 5′-AACTCGAGTTAACATTCCACGGTTCCACGGTTAGG, IL-6 for 5′-TTGAATTCGCCACCATGAAGTTCCTCTCTGCAAGAGACTT, IL6 rev 5′ AACTCGAGCTAGGTTTGCCGAGTAGATCTCAAAGTG. cDNA was cloned into pXJ41 expression vector using BamHI or EcoRI and XhoI restriction sites and sequenced. Cytokines were produced in HEK293 cells transfected with pXJ41 using polyethylenimine (PEI) transfection in ratio 2.5 µl PEI to 1 µg DNA). Supernatant was harvested 3 days after transfection. Titration against commercial recombinant cytokines of known concentration and their effect on BM cell proliferation *in vitro* was used to determine biological activity of cytokines in supernatant. Dilution of supernatant corresponding to concentration of 100 ng/ml SCF, 20 ng/ml IL-3 and 10 ng/ml IL-6 was used for cultivation of immortalized bone marrow cells.

Retroviral MSCV and pMYs particles were generated by transfection of the vectors into Platinum-E cells (Cell Biolabs) by PEI as described above.

Ex vivo activation assay

For the analysis of IFNγ production, T cells (1×10^6/ml in RPMI/ 10% FCS) were stimulated with 10 ng/ml PMA and 1.5 µM ionomycin or 1 µM OVA peptide in the presence of BD Golgi Stop for 5 h. For the CD69 and CD25 upregulation assay, dendritic cells differentiated from fresh or immortalized bone marrow stem cells were pulsed with indicated concentration of indicated peptides, mixed with T cells isolated from LNs in a 1:2 ratio, and analyzed after ~ 16 h of coculture as described previously (Palmer *et al*, 2016).

Bone marrow chimeras

Bone marrow cells were isolated from long bones of indicated mouse strains and lymphocytes were depleted using biotinylated antibodies to CD3 and CD19 and Dynabeads biotin binder kit (Thermo Fisher Scientific). In total, 6×10^6 cells (always a 1:1 mixture from two different donor strains) in 200 µl of PBS were injected into irradiated (300 cGy) Rag2$^{-/-}$ host mice i.v. The mice were analyzed 8 weeks after the transfer.

Monoclonal retrogenic T cells

Generation of immortalized bone marrow was described previously (Ruedl *et al*, 2008). Briefly, Vβ5 Rag2$^{-/-}$ mice were treated with

100 mg/kg 5-fluorouracil and bone marrow cells were harvested 5 days later. Cells were cultivated in complete IMDM (10% FCS) supplemented with SCF, IL-3, and IL-6. After 2 days, proliferating cells were virally transduced with a fusion construct NUP98-IIOXB4 in a retroviral vector pMYs. Viral infections were performed in the presence of 10 µg/ml polybrene by centrifugation (90 min, 1,250 *g*, 30°C). The transduced cells were selected for 2 days in puromycin (1 µg/ml). Selected immortalized cells were subsequently virally transduced with MSCV vector containing s TCRα-encoding gene and GFP as a selection marker. Two days after the transduction, GFP⁺ was FACS-sorted and transplanted into irradiated (7 Gy) congenic Ly5.1 recipients. At least 8 weeks after the transplantation, the recipient mice were sacrificed and donor LN T cells were used for cell fate analysis by flow cytometry or for adoptive transfers.

In vivo activation and a model for autoimmune diabetes

Indicated numbers of T cells were adoptively transferred into a host mouse i.v. On a following day, the host mice were immunized with indicated peptide (50 µg) and LPS (25 µg) in 200 µl of PBS i.p. or with 5,000 CFU of Lm. Lm strains expressing OVA, Q4R7, and Q4H7 have been described previously (King *et al*, 2012; Oberle *et al*, 2016). Lm expressing NP68 was produced by adding the ASNENMDAM epitope to ovalbumin encoding gene and introduced to Lm as previously described (Zehn *et al*, 2009). Dendritic cells for *in vivo* experiments were generated from full bone marrow isolated from long bones of 6- to 10-week-old mice. Cells were cultured for 10 days in complete Iscove's modified Dulbecco's medium (10% FCS) conditioned with 2% GM-CSF supernatant (Lutz cells). Medium was refreshed for new on day 4 and 7. Differentiated DCs were pulsed with corresponding peptide (10^{-7} M) in the presence of LPS (100 ng/ml) for 3 h and 1×10^6 antigen-loaded DCs were used for i.v. immunization. In the experimental model of autoimmunity, we monitored glucose in the urine of RIP.OVA mice on a daily basis using test strips (Diabur-Test 5000, Roche or GLUKO-PHAN, Erba Lachema, Czech Republic). The animal was considered to suffer from lethal autoimmunity when the concentration of glucose in the urine reached ≥ 1,000 mg/dl. We also measured blood glucose by contour blood glucose meter (Bayer) on day 7 post-infection. In the diabetic experiments, mice that died before the end of the monitored period (14 days) and before they reached 1,000 mg/dl glucose levels in the urine were excluded. Only one mouse in total was excluded based on this pre-established criterium.

Generation of true memory T cells

True memory T cells were generated by infecting Vβ5 mice with 5,000 CFU of Lm-OVA. After 60–90 days (for RNAseq) or 30 50 days (for FACS staining), CD8⁺ Kb OVA tetramer⁺ CD49d⁺ CD44⁺ CD62L⁺ from LNs and the spleen were sorted (or gated). TM OT-I T cells were generated by adoptive transfer of 1×10^6 T cells from OT-I Rag2$^{-/-}$ mouse into Ly5.1 recipient and subsequent infection with 5,000 CFU of Lm-OVA. At least 30 days after infection, CD8⁺ Ly5.2⁺ cells from LNs and the spleen were sorted and adoptively transferred into recipient mice.

Listeria clearance

FACS-sorted 1×10^4 naïve CD8WT OT-I, CD8.4 OT-I (VM), sorted true memory OT-I T cells, or no T cells were adoptively transferred into Ly5.1 C57Bl/6j mice followed by infection with 5,000 CFU Lm-Q4H7. The recipient mice were sacrificed on day 3 and 5 post-infection, and the spleen was homogenized and lysed in PBS with 0.1% Tergitol (Sigma-Aldrich). 1/20 of splenic lysate was plated onto brain–heart infusion agar (BHI, Sigma-Aldrich) plates with 200 μg/ml streptomycin and incubated at 37°C. The resulting number of colonies was quantified the following day.

Statistics

Statistical analysis was carried out using Prism (V5.04, GraphPad Software) or MS Excel. The statistical tests are indicated for each experiment. Whenever possible, we used nonparametric statistical tests. In one case, we use one-value *t*-test after the data passed Shapiro–Wilk normality test. In the *ex vivo* activation assays, we used paired Student's *t*-test (pairs = individual experiments). In this case, we tested the normality of differences using Shapiro–Wilk test, using pooled differences from two highest concentrations of peptides for each condition (because of too few data points for each peptide concentration). For comparing the abundance of individual TCR clones in different subsets, we use paired *t*-test as a post-test after using global chi-square test. Because of the very low $n = 3$, we could not test the normality of differences. All statistical tests were two-tailed.

Data availability

The data RNAseq data are deposited in the GEO database (GSE90522).

Expanded View for this article is available online.

Acknowledgements

Author contributions

Conflict of interest

The authors declare that they have no conflict of interest.

References

Akue AD, Lee JY, Jameson SC (2012) Derivation and maintenance of virtual memory CD8 T cells. *J Immunol* 188: 2516–2523

Bottcher JP, Beyer M, Meissner F, Abdullah Z, Sander J, Hochst B, Eickhoff S, Rieckmann JC, Russo C, Bauer T, Flecken T, Giesen D, Engel D, Jung S, Busch DH, Protzer U, Thimme R, Mann M, Kurts C, Schultze JL *et al* (2015) Functional classification of memory CD8(+) T cells by CX3CR1 expression. *Nat Commun* 6: 8306

Cheung KP, Yang E, Goldrath AW (2009) Memory-like CD8+ T cells generated during homeostatic proliferation defer to antigen-experienced memory cells. *J Immunol* 183: 3364–3372

Chiu BC, Martin BE, Stolberg VR, Chensue SW (2013) Cutting edge: central memory CD8 T cells in aged mice are virtual memory cells. *J Immunol* 191: 5793–5796

Cho JH, Kim HO, Ju YJ, Kye YC, Lee GW, Lee SW, Yun CH, Bottini N, Webster K, Goodnow CC, Surh CD, King C, Sprent J (2016) CD45-mediated control of TCR tuning in naive and memory CD8+ T cells. *Nat Commun* 7: 13373

Chu T, Tyznik AJ, Roepke S, Berkley AM, Woodward-Davis A, Pattacini L, Bevan MJ, Zehn D, Prlic M (2013) Bystander-activated memory CD8 T cells control early pathogen load in an innate-like, NKG2D-dependent manner. *Cell Rep* 3: 701–708

Curtsinger JM, Lins DC, Mescher MF (1998) CD8(+) memory T cells (CD44 (high), Ly-6C(+)) are more sensitive than naive cells (CD44(low), Ly-6C (-)) to TCR/CD8 signaling in response to antigen. *J Immunol* 160: 3236–3243

Daniels MA, Teixeiro E, Gill J, Hausmann B, Roubaty D, Holmberg K, Werlen G, Hollander GA, Gascoigne NRJ, Palmer E (2006) Thymic selection threshold defined by compartmentalization of Ras/MAPK signalling. *Nature* 444: 724–729

Decman V, Laidlaw BJ, Doering TA, Leng J, Ertl HC, Goldstein DR, Wherry EJ (2012) Defective CD8 T cell responses in aged mice are due to quantitative and qualitative changes in virus-specific precursors. *J Immunol* 188: 1933–1941

Dobin A, Davis CA, Schlesinger F, Drenkow J, Zaleski C, Jha S, Batut P, Chaisson M, Gingeras TR (2013) STAR: ultrafast universal RNA-seq aligner. *Bioinformatics* 29: 15–21

Erman B, Alag AS, Dahle O, van Laethem F, Sarafova SD, Guinter TI, Sharrow SO, Grinberg A, Love PE, Singer A (2006) Coreceptor signal strength regulates positive selection but does not determine CD4/CD8 lineage choice in a physiologic *in vivo* model. *J Immunol* 177: 6613–6625

Fink PJ, Swan K, Turk G, Moore MW, Carbone FR (1992) Both intrathymic and peripheral selection modulate the differential expression of V-Beta-5 among Cd4+ and Cd8+ T-Cells. *J Exp Med* 176: 1733–1738

Gaidatzis D, Lerch A, Hahne F, Stadler MB (2015) QuasR: quantification and annotation of short reads in R. *Bioinformatics* 31: 1130–1132

Gattinoni L, Lugli E, Ji Y, Pos Z, Paulos CM, Quigley MF, Almeida JR, Gostick E, Yu ZY, Carpenito C, Wang E, Douek DC, Price DA, June CH, Marincola FM, Roederer M, Restifo NP (2011) A human memory T cell subset with stem cell-like properties. *Nat Med* 17: 1290–1297

Ge Q, Bai A, Jones B, Eisen HN, Chen J (2004) Competition for self-peptide-MHC complexes and cytokines between naive and memory CD8+ T cells expressing the same or different T cell receptors. *Proc Natl Acad Sci USA* 101: 3041–3046

Gerlach C, Moseman EA, Loughhead SM, Alvarez D, Zwijnenburg AJ, Waanders L, Garg R, de la Torre JC, von Andrian UH (2016) The chemokine receptor CX3CR1 defines three antigen-experienced CD8 T cell subsets with distinct roles in immune surveillance and homeostasis. *Immunity* 45: 1270–1284

Graef P, Buchholz VR, Stemberger C, Flossdorf M, Henkel L, Schiemann M, Drexler I, Hofer T, Riddell SR, Busch DH (2014) Serial transfer of single-cell-derived immunocompetence reveals stemness of CD8(+) central memory T cells. *Immunity* 41: 116–126

Haluszczak C, Akue AD, Hamilton SE, Johnson LD, Pujanauski L, Teodorovic L, Jameson SC, Kedl RM (2009) The antigen-specific CD8+ T cell repertoire in unimmunized mice includes memory phenotype cells bearing markers of homeostatic expansion. *J Exp Med* 206: 435–448

Hogan T, Shuvaev A, Commenges D, Yates A, Callard R, Thiebaut R, Seddon B (2013) Clonally diverse T cell homeostasis is maintained by a common program of cell-cycle control. *J Immunol* 190: 3985–3993

Jacomet F, Cayssials E, Basbous S, Levescot A, Piccirilli N, Desmier D, Robin A, Barra A, Giraud C, Guilhot F, Roy L, Herbelin A, Gombert JM (2015) Evidence for eomesodermin-expressing innate-like CD8(+) KIR/NKG2A(+) T cells in human adults and cord blood samples. *Eur J Immunol* 45: 1926–1933

Kaech SM, Hemby S, Kersh E, Ahmed R (2002) Molecular and functional profiling of memory CD8 T cell differentiation. *Cell* 111: 837–851

Kimura MY, Pobezinsky LA, Guinter TI, Thomas J, Adams A, Park JH, Tai XG, Singer A (2013) IL-7 signaling must be intermittent, not continuous, during CD8(+) T cell homeostasis to promote cell survival instead of cell death. *Nat Immunol* 14: 143–151

King CG, Koehli S, Hausmann B, Schmaler M, Zehn D, Palmer E (2012) T cell affinity regulates asymmetric division, effector cell differentiation, and tissue pathology. *Immunity* 37: 709–720

Knudson KM, Goplen NP, Cunningham CA, Daniels MA, Teixeiro E (2013) Low-affinity T cells are programmed to maintain normal primary responses but are impaired in their recall to low-affinity ligands. *Cell Rep* 4: 554–565

Kurts C, Miller JFAP, Subramaniam RM, Carbone FR, Heath WR (1998) Major histocompatibility complex class I-restricted cross-presentation is biased towards high dose antigens and those released during cellular destruction. *J Exp Med* 188: 409–414

Kurzweil V, LaRoche A, Oliver PM (2014) Increased peripheral IL-4 leads to an expanded virtual memory CD8+ population. *J Immunol* 192: 5643–5651

Lee JY, Hamilton SE, Akue AD, Hogquist KA, Jameson SC (2013) Virtual memory CD8 T cells display unique functional properties. *Proc Natl Acad Sci USA* 110: 13498–13503

London CA, Lodge MP, Abbas AK (2000) Functional responses and costimulator dependence of memory CD4(+) T cells. *J Immunol* 164: 265–272

Luckey CJ, Bhattacharya D, Goldrath AW, Weissman IL, Benoist C, Mathis D (2006) Memory T and memory B cells share a transcriptional program of self-renewal with long-term hematopoietic stem cells. *Proc Natl Acad Sci USA* 103: 3304–3309

Mehlhop-Williams ER, Bevan MJ (2014) Memory CD8+ T cells exhibit increased antigen threshold requirements for recall proliferation. *J Exp Med* 211: 345–356

Oberle SG, Hanna-El-Daher L, Chennupati V, Enouz S, Scherer S, Prlic M, Zehn D (2016) A minimum epitope overlap between infections strongly narrows the emerging T cell repertoire. *Cell Rep* 17: 627–635

Palmer E, Drobek A, Stepanek O (2016) Opposing effects of actin signaling and LFA-1 on establishing the affinity threshold for inducing effector T-cell responses in mice. *Eur J Immunol* 46: 1887–1901

Park JH, Adoro S, Lucas PJ, Sarafova SD, Alag AS, Doan LL, Erman B, Liu X, Ellmeier W, Bosselut R, Feigenbaum L, Singer A (2007) 'Coreceptor tuning': cytokine signals transcriptionally tailor CD8 coreceptor expression to the self-specificity of the TCR. *Nat Immunol* 8: 1049–1059

Pihlgren M, Dubois PM, Tomkowiak M, Sjogren T, Marvel J (1996) Resting memory CD8(+) T cells are hyperreactive to antigenic challenge *in vitro*. *J Exp Med* 184: 2141–2151

Renkema KR, Li G, Wu A, Smithey MJ, Nikolich-Zugich J (2014) Two separate defects affecting true naive or virtual memory T cell precursors combine to reduce naive T cell responses with aging. *J Immunol* 192: 151–159

Robinson MD, McCarthy DJ, Smyth GK (2010) edgeR: a Bioconductor package for differential expression analysis of digital gene expression data. *Bioinformatics* 26: 139–140

Ruedl C, Khameneh HJ, Karjalainen K (2008) Manipulation of immune system via immortal bone marrow stem cells. *Int Immunol* 20: 1211–1218

Salmond RJ, Brownlie RJ, Morrison VL, Zamoyska R (2014) The tyrosine phosphatase PTPN22 discriminates weak self peptides from strong agonist TCR signals. *Nat Immunol* 15: 875–883

Santori FR, Kieper WC, Brown SM, Lu Y, Neubert TA, Johnson KL, Naylor S, Vukmanovic S, Hogquist KA, Jameson SC (2002) Rare, structurally homologous self-peptides promote thymocyte positive selection. *Immunity* 17: 131–142

Shotton DM, Attaran A (1998) Variant antigenic peptide promotes cytotoxic T lymphocyte adhesion to target cells without cytotoxicity. *Proc Natl Acad Sci USA* 95: 15571–15576

Sosinowski T, White JT, Cross EW, Haluszczak C, Marrack P, Gapin L, Kedl RM (2013) CD8alpha+ dendritic cell trans presentation of IL-15 to naive CD8+ T cells produces antigen-inexperienced T cells in the periphery with memory phenotype and function. *J Immunol* 190: 1936–1947

Stepanek O, Prabhakar AS, Osswald C, King CG, Bulek A, Naeher D, Beaufils-Hugot M, Abanto ML, Galati V, Hausmann B, Lang R, Cole DK, Huseby ES, Sewell AK, Chakraborty AK, Palmer E (2014) Coreceptor scanning by the T cell receptor provides a mechanism for T cell tolerance. *Cell* 159: 333–345

Su LF, Kidd BA, Han A, Kotzin JJ, Davis MM (2013) Virus-specific CD4(+) memory-phenotype T cells are abundant in unexposed adults. *Immunity* 38: 373–383

Subramanian A, Tamayo P, Mootha VK, Mukherjee S, Ebert BL, Gillette MA, Paulovich A, Pomeroy SL, Golub TR, Lander ES, Mesirov JP (2005) Gene set enrichment analysis: a knowledge-based approach for interpreting genome-wide expression profiles. *Proc Natl Acad Sci USA* 102: 15545–15550

Tripathi P, Morris SC, Perkins C, Sholl A, Finkelman FD, Hildeman DA (2016) IL-4 and IL-15 promotion of virtual memory CD8+ T cells is determined by genetic background. *Eur J Immunol* 46: 2333–2339

Wherry EJ, Ha SJ, Kaech SM, Haining WN, Sarkar S, Kalia V, Subramaniam S, Blattman JN, Barber DL, Ahmed R (2007) Molecular signature of CD8+ T cell exhaustion during chronic viral infection. *Immunity* 27: 670–684

White JT, Cross EW, Burchill MA, Danhorn T, McCarter MD, Rosen HR, O'Connor B, Kedl RM (2016) Virtual memory T cells develop and mediate bystander protective immunity in an IL-15-dependent manner. *Nat Commun* 7: 11291

White JT, Cross EW, Kedl RM (2017) Antigen-inexperienced memory CD8+ T cells: where they come from and why we need them. *Nat Rev Immunol* 17: 391–400

Wu D, Lim E, Vaillant F, Asselin-Labat ML, Visvader JE, Smyth GK (2010) ROAST: rotation gene set tests for complex microarray experiments. *Bioinformatics* 26: 2176–2182

Zehn D, Bevan MJ (2006) T cells with low avidity for a tissue-restricted antigen routinely evade central and peripheral tolerance and cause autoimmunity. *Immunity* 25: 261–270

Zehn D, Lee SY, Bevan MJ (2009) Complete but curtailed T-cell response to very low-affinity antigen. *Nature* 458: 211–214

Zhang Y, Joe G, Hexner E, Zhu J, Emerson SG (2005) Host-reactive CD8(+) memory stem cells in graft-versus-host disease. *Nat Med* 11: 1299–1305

Table EV1

TCR clone	V-gene	J-gene	CDR3-junction	Clone count (naïve/VM)			
				Exp1	Exp2	Exp3	Exp4
TRAV14 Clones				**(19/18)**	**(16/16)**	**(21/17)**	**(17/17)**
V14-c1	TRAV14-1 a) TRAV14D-1 TRAV14D-2	TRAJ6	CAAGGNYKPTF	-/9	-/10	12/12	1/8
V14-c2	TRAV14-1 b) TRAV14D-1	TRAJ6	CASGGNYKPTF	2/6	-/3	4/5	2/1
V14-c3	TRAV14-1	TRAJ6	CASGGNYQPIC	-/1	-	-	-
V14-c4	TRAV14-1	TRAJ6	CASGGNYKPTC	-/1	-	-	-
V14-c5	TRAV14-3	TRAJ5	CAASPQVVGQLTF	-/1	-	-	-
V14-c6	TRAV14-1 c) TRAV14D-3/DV8	TRAJ6	CAAGNYAQGLTF	2/-	7/-	4/-	-
V14-c7	TRAV14-1	TRAJ31	CAAGDNNRIFF	4/-	-	-	3/-
V14-c8	TRAV14-1	TRAJ34	CAAGDTNKVVF	6/-	-	-	-
V14-c9	TRAV14-1	TRAJ47	CAASDPNKMIF	3/-	-	-	-
V14-c10	TRAV14-1	TRAJ33	CAASDNYQFIC	1/-	-	-	-
V14-c11	TRAV14-1	TRAJ31	CAAADNNRIFF	-	-/1	-	-
V14-c12	TRAV14-1 d)	TRAJ6	CAGGGNYKPTF	-	-/2	-	-
V14-c13	TRAV14-1	TRAJ7	CAASDNNRLTL	-	2/-	1/-	-
V14-c14	TRAV14-3	TRAJ43	CAASDNNNNAPRF	-	1/-	-	-
V14-c15	TRAV14-2	TRAJ35	CAARRGFASALTF	-	3/-	-	-
V14-c16	TRAV14-1	TRAJ33	CAAASNYQLIW	-	1/-	-	-
V14-c17	TRAV14-1	TRAJ31	CAASDDNRIFF	-	2/-	-	-
V14-c18	TRAV14D-3/DV8	TRAJ39	CAARDNAGAKLTF	1/-	-	-	-
V14-c19	TRAV14-1	TRAJ45	CAASAAGADRLTF	-	-	-	1/-
V14-c20	TRAV14-1	TRAJ6	CAASETSGGNYKPTF	-	-	-	1/-
V14-c21	TRAV14-2	TRAJ33	CAASGDSNYQLIW	-	-	-	2/-
V14-c22	TRAV14D-1	TRAJ6	CAVGGNYKPTF	-	-	-	1/-
V14-c23	TRAV14-1	TRAJ12	CAASEGGGYKVVF	-	-	-	1/-
V14-c24	TRAV14-1	TRAJ31	CAASDNNRIFF	-	-	-	2/-
V14-c25	TRAV14-1	TRAJ7	CAASDINRLTL	-	-	-	1/-
V14-c26	TRAV14D-1	TRAJ49	CAASSTGYQNFYF	-	-	-	1/-
V14-c27	TRAV14-1	TRAJ7	CAAGDNNRLTL	-	-	-	1/-
V14-c28	TRAV14-1	TRAJ6	CAAGGNYKPIF	-	-	-	-/1
V14-c29	TRAV14D-3/DV8	TRAJ52	CAASADTGANTGKLTF	-	-	-	-/2
V14-c30	TRAV14-2	TRAJ12	CAAWTGGYKVVF	-	-	-	-/1
V14-c31	TRAV14-1	TRAJ27	CAASDNTNTGKLTF	-	-	-	-/1
V14-c32	TRAV14-1	TRAJ6	CAAAGNYKPTF	-	-	-	-/1
V14-c33	TRAV14-1	TRAJ58	CAASAAGTGSKLSF	-	-	-	-/1
TRAV12 Clones				**(17/18)**	**(20/12)**	**(18/16)**	**(20/15)**
V12-c1	TRAV12N-3	TRAJ28	CALSVRLPGTGSNRLTF	-/2	-	-	-
V12-c2	TRAV12D-1	TRAJ23	CALSAEMNYNQGKLIF	-/2	-	-	-
V12-c3	TRAV12D-2	TRAJ27	CALSDRGTNTGKLTF	-/2	-	-	-/1
V12-c4	TRAV12N-3	TRAJ31	CALSGSNNRIFF	-/3	1/-	3/-	-

Table EV1

V12-c5	TRAV12N-3	TRAJ34	CAPTSNTNKVVF	-/1	-	-	-
V12-c6	TRAV12N-3	TRAJ28	CAPSIKMLTF	-/1	-	-	-
V12-c7	TRAV12N-3	TRAJ5	CALGTQVVGQLTF	-/1	-	-	-
V12-c8	TRAV12N-3	TRAJ28	CAPGSNRLTF	-/3	1/-	-	-
V12-c9	TRAV12-3	TRAJ28	CALSETGTGSNRLTF	-/2	8/-	-	-
V12-c10	TRAV12D-2	TRAJ4	CALMLSGSFNKLTF	-/1	1/12	-/8	-
V12-c11	TRAV12D-2	TRAJ34	TNKVVF	3/-	-	7/-	17/1
V12-c12	TRAV12-3	TRAJ27	CALSDQGTNTGKLTF	2/-	-	3/-	-
V12-c13	TRAV12-3	TRAJ32	CALGMNYGSSGNKLIF	2/-	-	-	-
V12-c14	TRAV12-3	TRAJ52	CALSGGCGANTGKLTF	1/-	1/-	-	-
V12-c15	TRAV12N-3	TRAJ38	CALSRVGDYCKLIW	1/-	-	-	-
V12-c16	TRAV12-3	TRAJ31	CAPNSNNRIFF	1/-	-	-	-
V12-c17	TRAV12-3	TRAJ42	CALKGGSNAKLTF	1/-	-	-	-
V12-c18	TRAV12-3	TRAJ45	CAPLHTEGADRLTF	2/-	-	-	-
V12-c19	TRAV12N-3	TRAJ23	CALTGEMNYNQGKLIF	2/-	-	-	-
V12-c20	TRAV12-3	TRAJ50	CALSGPASSFSKLVF	1/-	-	-	-
V12-c21	TRAV12-3	TRAJ49	CALSPNTGYQNFYF	1/-	-	-	-
V12-c22	TRAV12-3	TRAJ27	CALSVPNTNTGKLTF	-	1/-	-	-
V12-c23	TRAV12-3	TRAJ5	CAPGTQVVGQLTF	-	1/-	-	-
V12-c24	TRAV12D-1	TRAJ32	CALSDGSSGNKLIF	-	2/-	-	-
V12-c25	TRAV12-3	TRAJ2	CALSVMNTGGLSGKLTF	-	1/-	1/-	-
V12-c26	TRAV12D-2	TRAJ4	CALSQESGSFNKLTF	-	1/-	-	-
V12-c27	TRAV12D-1	TRAJ42	CGLGGGSNAKLTF	-	1/-	-	-
V12-c28	TRAV12D-2	TRAJ25	CALSGVPGANTGKLTF	-	1/-	-	-
V12-c29	TRAV12D-2	TRAJ37	CALSDRRTGNTGKLIF	-	-	1/-	-
V12-c30	TRAV12N-3	TRAJ38	CALSRVGDNSKLIW	-	-	3/8	-
V12-c31	TRAV12-3	TRAJ27	CALSDIGTNTGKLTF	-	-	-	1/-
V12-c32	TRAV12D-2	TRAJ26	CALSDAAQGLTF	-	-	-	1/-
V12-c33	TRAV12D-25	TRAJ30	CALSADDTNAYKVIF	-	-	-	1/-
V12-c34	TRAV12D-2	TRAJ33	CALSDHNSNYQLIW	-	-	-	-/1
V12-c35	TRAV12D-2	TRAJ30	CALSSDTNAHKVIF	-	-	-	-/1
V12-c36	TRAV12D-2	TRAJ43	CALSGNNAPRF	-	-	-	-/2
V12-c37	TRAV12-3	TRAJ32	CALSDPYGSSGNKLIF	-	-	-	-/1
V12-c38	TRAV12N-3	TRAJ15	CAPYQGGRALIF	-	-	-	-/1
V12-c39	TRAV12N-3 e)	TRAJ23	CALSDRNYNQGKLIF	-	-	-	-/2
V12-c40	TRAV12-3	TRAJ42	CALGSNAKLTF	-	-	-	-/1
V12-c41	TRAV12-3	TRAJ42	CALRTQVVGQLTF	-	-	-	-/1
V12-c42	TRAV12-3	TRAJ27	CALSDRHTNTGKLTF	-	-	-	-/1
V12-c43	TRAV12N-3	TRAJ39	CALSDRYAGVILTF	-	-	-	-/1
V12-c44	TRAV12N-3	TRAJ34	CALSELSSNTNKVVF	-	-	-	-/1

Table EV2

EntrezID	Symbol	GeneName	log2 expression VirtualMemory/Naïve	log2A	P.Value	adj.P.Val
12769	Ccr9	chemokine (C-C motif) receptor 9	-6.350395037	7.176986	1.42E-120	2.18E-117
15980	Ifngr2	interferon gamma receptor 2	-4.298353125	4.816081	7.48E-81	4.36E-78
238377	Gpr68	G protein-coupled receptor 68	-2.859278614	6.450385	3.02E-68	1.34E-65
331524	Xkrx	X-linked Kx blood group related, X-linked	-3.103140805	4.699717	4.45E-58	1.39E-55
53623	Gria3	glutamate receptor, ionotropic, AMPA3 (alpha 3)	-4.421937035	2.552687	2.35E-57	7.23E-55
20776	Tmie	transmembrane inner ear	-3.311999362	4.885848	3.04E-56	8.87E-54
211401	Mtss1	metastasis suppressor 1	-3.071829263	4.715969	3.44E-54	8.95E-52
54524	Syt6	synaptotagmin VI	-3.622021518	2.903752	2.78E-51	6.62E-49
17969	Ncf1	neutrophil cytosolic factor 1	-2.32993895	5.008346	6.46E-51	1.50E-48
16407	Itgae	integrin alpha E, epithelial-associated	-4.498504879	7.116383	1.00E-49	2.20E-47
192734	Lrrc75b	leucine rich repeat containing 75B	-2.915791416	5.08748	8.83E-44	1.80E-41
67220	Plekho1	pleckstrin homology domain containing, family O member 1	-2.107114969	4.811871	2.82E-43	5.55E-41
17364	Trpm1	transient receptor potential cation channel, subfamily M, member 1	-3.3312674	3.087703	3.79E-43	7.36E-41
74338	Slc6a19	solute carrier family 6 (neurotransmitter transporter), member 19	-3.304883073	5.581412	3.86E-42	7.34E-40
74039	Nfam1	Nfat activating molecule with ITAM motif 1	-2.953798386	3.134234	2.22E-40	4.09E-38
16010	Igfbp4	insulin-like growth factor binding protein 4	-4.297724377	6.986738	9.00E-40	1.64E-37
21814	Tgfbr3	transforming growth factor, beta receptor III	-2.851100121	5.369416	3.78E-39	6.66E-37
14608	Gpr83	G protein-coupled receptor 83	-4.108893798	1.223212	1.76E-38	2.98E-36
18213	Ntrk3	neurotrophic tyrosine kinase, receptor, type 3	-3.123310862	4.251681	7.40E-38	1.21E-35
66214	Rgcc	regulator of cell cycle	-3.181994862	4.746344	1.85E-37	2.93E-35
70574	Cpm	carboxypeptidase M	-2.344921265	5.040643	2.79E-37	4.32E-35
18793	Plaur	plasminogen activator, urokinase receptor	-3.519933481	1.981957	7.34E-37	1.12E-34
23890	Gpr34	G protein-coupled receptor 34	-3.859067851	2.837119	3.07E-34	4.19E-32
11472	Actn2	actinin alpha 2	-2.31883903	3.64429	3.60E-34	4.86E-32
227326	Gpr55	G protein-coupled receptor 55	-3.284445381	3.348984	1.43E-33	1.91E-31
11482	Acvrl1	activin A receptor, type II-like 1	-3.284867026	2.517738	1.46E-33	1.94E-31
64297	Gprc5b	G protein-coupled receptor, family C, group 5, member B	-2.751271556	3.079841	7.18E-33	9.20E-31
105827	Amigo2	adhesion molecule with Ig like domain 2	-2.070136967	4.608393	2.47E-32	3.12E-30
98910	Usp6nl	USP6 N-terminal like	-2.424232524	3.801116	1.89E-30	2.26E-28
23887	Ggt5	gamma-glutamyltransferase 5	-2.156405139	4.008439	3.41E-28	3.67E-26
16490	Kcna2	potassium voltage-gated channel, shaker-related subfamily, member 2	-2.484160088	6.205932	8.90E-28	9.23E-26
16001	Igf1r	insulin-like growth factor I receptor	-2.26049971	4.158118	1.68E-27	1.73E-25
56089	Ramp3	receptor (calcitonin) activity modifying protein 3	-3.168930728	0.897521	2.67E-27	2.65E-25
19411	Rarg	retinoic acid receptor, gamma	-2.002138763	5.790988	6.59E-27	6.37E-25
27410	Abca3	ATP-binding cassette, sub-family A (ABC1), member 3	-2.394379113	6.272915	1.85E-26	1.76E-24
77318	Ankrd55	ankyrin repeat domain 55	-2.896159193	1.344472	1.37E-25	1.26E-23
74498	Gorasp1	golgi reassembly stacking protein 1	-3.083895558	1.471453	2.08E-25	1.88E-23
18548	Pcsk1	proprotein convertase subtilisin/kexin type 1	-4.568417689	2.068979	2.99E-25	2.69E-23
20449	St8sia1	ST8 alpha-N-acetyl-neuraminide alpha-2,8-sialyltransferase 1	-2.003935877	6.793321	1.57E-24	1.34E-22
54195	Gucy1b3	guanylate cyclase 1, soluble, beta 3	-3.507106103	0.579637	7.00E-24	5.80E-22
71994	Cnn3	calponin 3, acidic	-2.512228075	4.070063	2.02E-22	1.61E-20
74134	Cyp2s1	cytochrome P450, family 2, subfamily s, polypeptide 1	-2.678149671	2.77669	2.79E-22	2.20E-20
20775	Sqle	squalene epoxidase	-2.178173264	2.471383	3.08E-20	2.15E-18
99543	Olfml3	olfactomedin-like 3	-2.790896586	2.024588	4.50E-20	3.10E-18
60440	Iigp1	interferon inducible GTPase 1	-2.433454467	4.754881	8.87E-20	6.02E-18
21673	Dntt	deoxynucleotidyltransferase, terminal	-3.276563243	2.613742	1.06E-19	7.12E-18
60596	Gucy1a3	guanylate cyclase 1, soluble, alpha 3	-3.586261669	1.385817	1.05E-18	6.76E-17
93840	Vangl2	vang-like 2 (van gogh, Drosophila)	-2.793263674	-0.32426	2.25E-18	1.42E-16
51801	Ramp1	receptor (calcitonin) activity modifying protein 1	-2.535295653	4.77629	3.45E-18	2.15E-16
240752	Pik3c2b	phosphoinositide-3-kinase, class 2, beta polypeptide	-2.044885263	2.090452	3.52E-18	2.18E-16
16835	Ldlr	low density lipoprotein receptor	-2.439577937	2.529963	8.36E-18	5.08E-16
213980	Fbxw10	F-box and WD-40 domain protein 10	-2.442373773	1.067478	2.06E-17	1.21E-15
16553	Kif13a	kinesin family member 13A	-3.151429523	1.497715	2.94E-17	1.71E-15
72190	2510009E07Rik	RIKEN cDNA 2510009E07 gene	-2.110569076	1.711601	4.93E-17	2.83E-15
108072	Grm6	glutamate receptor, metabotropic 6	-3.511921259	1.866868	8.07E-17	4.52E-15
215789	Phactr2	phosphatase and actin regulator 2	-2.16036281	1.892707	3.72E-15	1.88E-13
20678	Sox5	SRY (sex determining region Y)-box 5	-2.336619286	-0.26655	3.95E-15	1.97E-13
106042	Prickle1	prickle planar cell polarity protein 1	-2.232142551	1.480702	3.95E-15	1.97E-13
72805	Zfp839	zinc finger protein 839	-2.110215852	2.993953	6.64E-15	3.26E-13
27413	Abcb11	ATP-binding cassette, sub-family B (MDR/TAP), member 11	-2.226958184	-0.84945	1.41E-14	6.74E-13
228071	Sestd1	SEC14 and spectrin domains 1	-2.114029297	1.172825	1.49E-14	7.84E-13
59010	Sqrdl	sulfide quinone reductase-like (yeast)	-2.396865315	1.862234	1.85E-13	8.16E-12
81840	Sorcs2	sortilin-related VPS10 domain containing receptor 2	-2.346767129	3.181874	3.21E-13	1.39E-11
21416	Tcf7l2	transcription factor 7 like 2, T cell specific, HMG box	-2.375967121	-0.11201	8.97E-13	3.78E-11
68939	Rasl11b	RAS-like, family 11, member B	-2.396106758	1.980582	1.20E-12	5.01E-11
72693	Zcchc12	zinc finger, CCHC domain containing 12	-2.429530152	-0.21085	5.32E-12	2.08E-10
319757	Smo	smoothened, frizzled class receptor	-2.053884708	-0.50532	5.63E-12	2.18E-10
20741	Sptb	spectrin beta, erythrocytic	-2.015166518	0.139188	1.38E-11	5.09E-10
245469	Pdzd4	PDZ domain containing 4	-2.0482655	1.001796	2.67E-11	9.69E-10
20341	Selenbp1	selenium binding protein 1	-2.064057875	-0.46892	2.68E-11	9.69E-10
99031	Osbpl6	oxysterol binding protein-like 6	-2.375109307	0.530373	4.77E-10	1.53E-08
13655	Egr3	early growth response 3	-2.076543649	2.740951	1.42E-09	4.25E-08
30794	Pdlim4	PDZ and LIM domain 4	-2.363264063	-0.16161	3.14E-07	7.05E-06

Table EV3

EntrezID	Symbol	GeneName	log2 expression TrueMemory/ VirtualMemory	log2A	P.Value	adj.P.Val
13034	Ctse	cathepsin E	4.341197999	7.021500902	2.15E-200	3.64E-196
13051	Cx3cr1	chemokine (C-X3-C motif) receptor 1	7.283469818	4.637218433	3.01E-158	2.54E-154
94226	S1pr5	sphingosine-1-phosphate receptor 5	6.088892822	4.900951022	9.01E-144	5.08E-140
24136	Zeb2	zinc finger E-box binding homeobox 2	6.727614209	4.855712624	1.73E-136	7.29E-133
14939	Gzmb	granzyme B	6.137367136	4.946781585	7.53E-136	2.55E-132
27007	Klrk1	killer cell lectin-like receptor subfamily K, member 1	4.529819199	6.859450186	3.14E-125	8.84E-122
50928	Klrg1	killer cell lectin-like receptor subfamily G, member 1	6.872469144	3.268289042	1.10E-123	2.67E-120
110454	Ly6a	lymphocyte antigen 6 complex, locus A	4.691447042	6.646424644	6.88E-109	1.45E-105
16952	Anxa1	annexin A1	5.609303288	3.032648752	4.36E-88	7.38E-85
12362	Casp1	caspase 1	4.363072509	3.773901698	3.40E-79	4.78E-76
100042480	Nhsl2	NHS-like 2	6.224557643	3.098458843	2.68E-69	3.24E-66
16411	Itgax	integrin alpha X	4.174517492	6.35914259	2.95E-68	3.33E-65
14945	Gzmk	granzyme K	5.708143871	3.046635306	4.44E-67	4.69E-64
11567	Avil	advillin	4.651463949	2.566488378	2.56E-60	2.55E-57
19271	Ptprj	protein tyrosine phosphatase, receptor type, J	4.312755685	3.509984899	7.53E-58	7.07E-55
20200	S100a6	S100 calcium binding protein A6 (calcyclin)	3.228453034	5.662745936	8.69E-57	7.73E-54
72747	Ttc39c	tetratricopeptide repeat domain 39C	4.410832054	2.697234973	1.06E-56	8.97E-54
216438	March9	membrane-associated ring finger (C3HC4) 9	3.033084492	4.153825352	1.14E-56	9.16E-54
16184	Il2ra	interleukin 2 receptor, alpha chain	3.741674529	3.108901004	1.67E-56	1.28E-53
12363	Casp4	caspase 4, apoptosis-related cysteine peptidase	4.507497571	2.541041298	7.08E-56	5.20E-53
17969	Ncf1	neutrophil cytosolic factor 1	2.52747911	5.00834567	4.05E-55	2.85E-52
16069	Jchain	immunoglobulin joining chain	7.795705628	5.077480972	7.99E-54	5.40E-51
109700	Itga1	integrin alpha 1	4.431859516	2.376420169	9.73E-54	6.32E-51
16854	Lgals3	lectin, galactose binding, soluble 3	4.675106511	2.225439476	3.78E-52	2.37E-49
16543	Mdfic	MyoD family inhibitor domain containing	3.26977802	3.410362658	8.91E-51	5.38E-48
20198	S100a4	S100 calcium binding protein A4	4.091750536	3.859410132	4.46E-50	2.60E-47
12769	Ccr9	chemokine (C-C motif) receptor 9	3.626619556	7.176985659	1.51E-48	8.52E-46
14190	Fgl2	fibrinogen-like protein 2	3.176347158	4.187152526	1.83E-48	1.00E-45
12567	Cdk4	cyclin-dependent kinase 4	2.011406647	8.146975816	8.17E-45	4.32E-42
238377	Gpr68	G protein-coupled receptor 68	2.32867584	6.450384535	4.91E-44	2.44E-41
14747	Cmklr1	chemokine-like receptor 1	4.862748299	1.554313461	1.16E-42	5.45E-40
56013	Srcin1	SRC kinase signaling inhibitor 1	4.510061355	1.061014046	2.48E-41	1.13E-38
16898	Rps2	ribosomal protein S2	2.310339554	6.708935648	2.99E-41	1.33E-38
15368	Hmox1	heme oxygenase 1	5.562539142	4.720075989	3.49E-41	1.51E-38
16409	Itgam	integrin alpha M	3.864188873	3.301165172	2.00E-40	8.46E-38
18186	Nrp1	neuropilin 1	3.798327409	3.38171724	7.97E-39	3.28E-36
666926	Gm8369	predicted gene 8369	3.386055297	4.325303558	2.20E-38	8.66E-36
15902	Id2	inhibitor of DNA binding 2	2.401953294	7.240500275	5.56E-38	2.14E-35
227326	Gpr55	G protein-coupled receptor 55	3.634221714	3.348984251	9.11E-38	3.42E-35
20308	Ccl9	chemokine (C-C motif) ligand 9	4.182031358	0.891449091	9.81E-38	3.61E-35
24110	Usp18	ubiquitin specific peptidase 18	2.122906954	6.15670161	1.05E-35	3.79E-33
16523	Kcnj8	potassium inwardly-rectifying channel, subfamily J, member 8	2.269277175	4.522805178	3.36E-35	1.18E-32
12346	Car1	carbonic anhydrase 1	4.053915059	0.627660293	4.02E-35	1.39E-32
16768	Lag3	lymphocyte-activation gene 3	4.464152849	2.70058959	5.68E-35	1.92E-32
17364	Trpm1	transient receptor potential cation channel, subfamily M, member 1	3.008847384	3.087703136	2.11E-34	6.99E-32
21942	Tnfrsf9	tumor necrosis factor receptor superfamily, member 9	2.499048611	4.122593859	2.82E-34	9.16E-32
74732	Stx11	syntaxin 11	2.756948651	2.653152835	2.33E-33	7.28E-31
21928	Tnfaip2	tumor necrosis factor, alpha-induced protein 2	3.929390043	0.579745809	2.39E-33	7.36E-31
11801	Cd5l	CD5 antigen-like	5.0219911	2.894525895	1.41E-32	4.25E-30
15199	Hebp1	heme binding protein 1	3.994350592	0.898516868	2.16E-32	6.41E-30
60440	Iigp1	interferon inducible GTPase 1	3.389978409	4.75488106	2.40E-32	7.01E-30
20568	Slpi	secretory leukocyte peptidase inhibitor	4.313830104	2.641507491	4.41E-32	1.26E-29
69816	Mzb1	marginal zone B and B1 cell-specific protein 1	3.744818666	0.310685231	9.14E-32	2.54E-29
20970	Sdc3	syndecan 3	2.655216715	4.465479713	9.16E-32	2.54E-29
99899	Ifi44	interferon-induced protein 44	3.603121289	2.898854788	2.80E-31	7.65E-29
327766	Tmem26	transmembrane protein 26	3.849127803	0.721249088	3.84E-31	1.03E-28
16641	Klrc1	killer cell lectin-like receptor subfamily C, member 1	3.022425361	4.89698058	3.90E-31	1.03E-28
63913	Fam129a	family with sequence similarity 129, member A	2.168087188	4.31286203	7.33E-31	1.88E-28
394432	Ugt1a7c	UDP glucuronosyltransferase 1 family, polypeptide A7C	3.808015111	0.497135412	7.67E-31	1.93E-28
56791	Ube2l6	ubiquitin-conjugating enzyme E2L 6	3.891038557	1.465088008	1.16E-30	2.89E-28
56078	Car5b	carbonic anhydrase 5b, mitochondrial	3.837248368	0.952772412	1.95E-30	4.77E-28
20304	Ccl5	chemokine (C-C motif) ligand 5	2.115718196	9.5112044	2.02E-30	4.84E-28
56644	Clec7a	C-type lectin domain family 7, member a	4.054785889	0.68995907	2.03E-30	4.84E-28
20305	Ccl6	chemokine (C-C motif) ligand 6	3.840582918	1.067710364	2.14E-30	5.03E-28
12180	Smyd1	SET and MYND domain containing 1	3.362283147	1.788224354	2.56E-30	5.77E-28
12495	Entpd1	ectonucleoside triphosphate diphosphohydrolase 1	2.749552714	3.590144277	5.72E-30	1.27E-27
13058	Cybb	cytochrome b-245, beta polypeptide	5.061212805	2.418208185	7.36E-30	1.61E-27
69169	Fcmr	Fc fragment of IgM receptor	4.010644426	0.608790274	1.09E-29	2.33E-27
17228	Cma1	chymase 1, mast cell	4.11331059	0.804931666	1.83E-29	3.86E-27
17079	Cd180	CD180 antigen	4.223524706	0.853295897	4.12E-29	8.60E-27
66412	Arrdc4	arrestin domain containing 4	2.980436636	2.534445629	4.80E-29	9.89E-27
100034251	Wfdc17	WAP four-disulfide core domain 17	2.785147639	-0.584236171	1.17E-28	2.39E-26
108086	Rnf216	ring finger protein 216	2.67528237	3.102679694	1.38E-28	2.78E-26
16590	Kit	kit oncogene	3.75700724	1.217917436	2.43E-28	4.84E-26
12983	Csf2rb	colony stimulating factor 2 receptor, beta, low-affinity (granulocyte-macrophage)	3.869057592	0.720907729	4.76E-28	9.36E-26
58860	Adamdec1	ADAM-like, decysin 1	3.991068683	1.171909993	1.87E-27	3.64E-25
57740	Stk32c	serine/threonine kinase 32C	3.560386412	0.261761562	2.93E-27	5.63E-25
16835	Ldlr	low density lipoprotein receptor	3.208263311	2.529962935	1.22E-26	2.32E-24
212937	Tifab	TRAF-interacting protein with forkhead-associated domain, family member B	3.430240759	0.224049275	3.67E-26	6.82E-24
229731	Slc25a24	solute carrier family 25 (mitochondrial carrier, phosphate carrier), member 24	2.213178665	4.202310445	4.03E-26	7.40E-24
16173	Il18	interleukin 18	3.715786365	0.580930831	4.27E-26	7.76E-24
66259	Camk2n1	calcium/calmodulin-dependent protein kinase II inhibitor 1	2.4742192	2.588576384	4.73E-26	8.51E-24
18619	Penk	preproenkephalin	3.42907664	0.064924408	1.09E-25	1.94E-23
76933	Ifi27l2a	interferon, alpha-inducible protein 27 like 2A	2.026222433	6.457989662	1.14E-25	2.01E-23
72043	Sulf2	sulfatase 2	4.254112556	1.529348427	1.32E-25	2.30E-23
223920	Soat2	sterol O-acyltransferase 2	3.418323094	2.761001221	1.74E-25	3.00E-23
21391	Tbxas1	thromboxane A synthase 1, platelet	3.523159761	0.294920434	3.63E-25	6.19E-23
26904	Sh2d1b1	SH2 domain containing 1B1	3.53479179	0.179942001	4.60E-25	7.77E-23
20775	Sqle	squalene epoxidase	2.524125985	2.471382521	6.79E-25	1.12E-22
14938	Gzma	granzyme A	4.745964691	5.731727912	7.32E-25	1.20E-22
56620	Clec4n	C-type lectin domain family 4, member n	4.995191634	1.926039642	7.66E-25	1.25E-22
14425	Galnt3	UDP-N-acetyl-alpha-D-galactosamine:polypeptide N-acetylgalactosaminyltransferase 3	3.771046594	0.972123998	7.79E-25	1.25E-22
233274	Siglech	sialic acid binding Ig-like lectin H	3.32849484	-0.152010931	1.00E-24	1.59E-22
20375	Spi1	spleen focus forming virus (SFFV) proviral integration oncogene	3.326250315	0.237489731	1.13E-24	1.77E-22
12262	C1qc	complement component 1, q subcomponent, C chain	4.955532687	2.914726502	1.51E-24	2.33E-22
17060	Blnk	B cell linker	3.699344959	0.422331693	1.61E-24	2.48E-22
246256	Fcgr4	Fc receptor, IgG, low affinity IV	4.117969185	1.015397566	2.61E-24	3.94E-22
13733	Adgre1	adhesion G protein-coupled receptor E1	5.152906665	3.023203912	2.69E-24	4.02E-22
20893	Bhlhe40	basic helix-loop-helix family, member e40	3.297244336	4.7833539	2.94E-24	4.43E-22
433424	Zeb2os	zinc finger E-box binding homeobox 2, opposite strand	3.27254059	-0.059181558	4.15E-24	6.10E-22
15130	Hbb-b2	hemoglobin, beta adult minor chain	3.265869405	0.079842844	4.83E-24	7.03E-22
101488143	Hbb-bt	hemoglobin, beta adult t chain	3.265862302	0.079842844	4.90E-24	7.07E-22
18566	Pdcd1	programmed cell death 1	3.337055421	1.577426794	8.83E-24	1.27E-21
100340	Smpdl3b	sphingomyelin phosphodiesterase, acid-like 3B	3.191676654	3.217067312	9.30E-24	1.32E-21
11658	Alcam	activated leukocyte cell adhesion molecule	3.134366343	1.932232762	1.95E-23	2.73E-21
23890	Gpr34	G protein-coupled receptor 34	3.130870357	2.837119237	2.00E-23	2.77E-21

227737	Fam129b	family with sequence similarity 129, member B	2.979772694	0.584081093	2.16E-23	2.97E-21
331474	Rgag4	retrotransposon gag domain containing 4	3.254529425	0.566300832	2.33E-23	3.18E-21
50918	Myadm	myeloid-associated differentiation marker	3.186690039	1.796552456	2.76E-23	3.73E-21
140497	AF251705	cDNA sequence AF251705	3.521939288	0.430979525	5.19E-23	6.91E-21
192734	Lrrc75b	leucine rich repeat containing 75B	2.09821966	5.087479583	6.67E-23	8.73E-21
72446	Prr5l	proline rich 5 like	3.233309977	0.466883107	6.80E-23	8.84E-21
74039	Nfam1	Nfat activating molecule with ITAM motif 1	2.204892702	3.134233688	1.08E-22	1.37E-20
21817	Tgm2	transglutaminase 2, C polypeptide	4.533106766	1.841207676	1.31E-22	1.65E-20
98256	Kmo	kynurenine 3-monooxygenase (kynurenine 3-hydroxylase)	3.293655289	0.066286044	1.52E-22	1.73E-20
94284	Ugt1a6a	UDP glucuronosyltransferase 1 family, polypeptide A6A	3.144226158	-0.184995646	1.53E-22	1.89E-20
394434	Ugt1a9	UDP glucuronosyltransferase 1 family, polypeptide A9	3.144224807	-0.184995646	1.53E-22	1.89E-20
98752	Fcrla	Fc receptor-like A	3.557469503	0.263954508	1.55E-22	1.90E-20
394435	Ugt1a6b	UDP glucuronosyltransferase 1 family, polypeptide A6B	3.140879646	-0.188160068	1.73E-22	2.11E-20
17289	Mertk	c-mer proto-oncogene tyrosine kinase	4.114080185	1.328567664	1.98E-22	2.39E-20
394436	Ugt1a1	UDP glucuronosyltransferase 1 family, polypeptide A1	3.134184338	-0.194514244	2.02E-22	2.41E-20
394430	Ugt1a10	UDP glycosyltransferase 1 family, polypeptide A10	3.13418276	-0.194514244	2.04E-22	2.41E-20
394433	Ugt1a5	UDP glucuronosyltransferase 1 family, polypeptide A5	3.134182398	-0.194514244	2.04E-22	2.41E-20
16541	Napsa	napsin A aspartic peptidase	3.984416847	0.729704464	2.05E-22	2.41E-20
22236	Ugt1a2	UDP glucuronosyltransferase 1 family, polypeptide A2	3.134178256	-0.194514244	2.08E-22	2.43E-20
14025	Bcl11a	B cell CLL/lymphoma 11A (zinc finger protein)	2.827457718	-0.399152425	2.57E-22	2.98E-20
74760	Rab3il1	RAB3A interacting protein (rabin3)-like 1	3.388460222	0.266827275	4.39E-22	5.05E-20
214968	Sema6d	sema domain, transmembrane domain (TM), and cytoplasmic domain, (semaphorin) 6D	3.312999279	0.638974293	4.98E-22	5.69E-20
240168	Rasgrp3	RAS, guanyl releasing protein 3	3.013836522	-0.149794923	5.13E-22	5.82E-20
18782	Pla2g2d	phospholipase A2, group IID	3.66830479	0.470111304	5.65E-22	6.33E-20
215789	Phactr2	phosphatase and actin regulator 2	2.748918835	1.89270672	1.28E-21	1.42E-19
14999	H2-DMb1	histocompatibility 2, class II, locus Mb1	3.482315511	0.653412404	1.45E-21	1.59E-19
19249	Ptpn13	protein tyrosine phosphatase, non-receptor type 13	3.092644536	2.532067936	1.51E-21	1.64E-19
16956	Lpl	lipoprotein lipase	3.619470539	0.488585092	1.97E-21	2.12E-19
74191	P2ry13	purinergic receptor P2Y, G-protein coupled 13	3.673598364	1.028622544	2.30E-21	2.45E-19
14255	Flt3	FMS-like tyrosine kinase 3	3.201415101	0.109694877	3.06E-21	3.21E-19
17260	Mef2c	myocyte enhancer factor 2C	4.051999192	0.78504479	3.19E-21	3.32E-19
234779	Plcg2	phospholipase C, gamma 2	2.309553342	3.18175569	3.64E-21	3.75E-19
76650	Srxn1	sulfiredoxin 1 homolog (S. cerevisiae)	2.895203434	-0.512857648	3.95E-21	4.02E-19
226519	Lamc1	laminin, gamma 1	3.081401662	0.865098024	3.97E-21	4.02E-19
12984	Csf2rb2	colony stimulating factor 2 receptor, beta 2, low-affinity (granulocyte-macrophage)	3.150808629	-0.094138838	6.07E-21	6.11E-19
212073	Syne3	spectrin repeat containing, nuclear envelope family member 3	2.141327709	3.634153637	7.32E-21	7.33E-19
100504703	A730063M14Rik	RIKEN cDNA A730063M14 gene	2.830956657	1.587844266	9.37E-21	9.27E-19
14766	Adgrg1	adhesion G protein-coupled receptor G1	2.843478999	-0.10436943	9.81E-21	9.64E-19
21944	Tnfsf12	tumor necrosis factor (ligand) superfamily, member 12	3.007096309	-0.207762641	1.06E-20	1.04E-18
12260	C1qb	complement component 1, q subcomponent, beta polypeptide	4.919490459	3.305240127	1.18E-20	1.15E-18
619441	Tnfsfm13	tumor necrosis factor (ligand) superfamily, membrane-bound member 13	3.198000167	0.074762084	1.29E-20	1.24E-18
15007	H2-Q10	histocompatibility 2, Q region locus 10	2.483190708	4.039986313	1.80E-20	1.71E-18
74568	Mlkl	mixed lineage kinase domain-like	2.817786871	1.678465062	2.10E-20	1.99E-18
14961	H2-Ab1	histocompatibility 2, class II antigen A, beta 1	5.858694702	3.754539931	2.97E-20	2.79E-18
210029	Metrnl	meteorin, glial cell differentiation regulator-like	2.869776073	0.387006217	5.02E-20	4.66E-18
246730	Oas1a	2'-5' oligoadenylate synthetase 1A	2.215051069	3.926648744	6.04E-20	5.58E-18
12143	Blk	B lymphoid kinase	3.414986735	0.17148756	6.18E-20	5.68E-18
20430	Cyfip1	cytoplasmic FMR1 interacting protein 1	2.025872854	2.912120476	7.68E-20	7.02E-18
12491	Cd36	CD36 antigen	2.90184861	-0.250250349	1.07E-19	9.75E-18
80885	Hcar2	hydroxycarboxylic acid receptor 2	3.595566085	0.397327316	1.15E-19	1.04E-17
236285	Lancl3	LanC lantibiotic synthetase component C-like 3 (bacterial)	2.663761663	2.016521264	1.20E-19	1.08E-17
230787	Themis2	thymocyte selection associated family member 2	3.039558501	1.951679219	1.60E-19	1.42E-17
20715	Serpina3g	serine (or cysteine) peptidase inhibitor, clade A, member 3G	2.263300346	4.85667031	1.68E-19	1.49E-17
14128	Fcer2a	Fc receptor, IgE, low affinity II, alpha polypeptide	3.533997989	0.294132925	1.69E-19	1.49E-17
20728	Spic	Spi-C transcription factor (Spi-1/PU.1 related)	4.484899183	1.79362394	1.76E-19	1.54E-17
16149	Cd74	CD74 antigen (invariant polypeptide of major histocompatibility complex, class II antigen-associated)	5.73340598	5.747066096	1.90E-19	1.65E-17
15162	Hck	hemopoietic cell kinase	4.193445051	1.285315308	1.91E-19	1.66E-17
12520	Cd81	CD81 antigen	3.826535158	2.254825036	2.11E-19	1.82E-17
52614	Adgre4	adhesion G protein-coupled receptor E4	4.673068187	2.190785099	2.20E-19	1.88E-17
16513	Kcnj10	potassium inwardly-rectifying channel, subfamily J, member 10	4.08568809	1.75094162	2.52E-19	2.14E-17
20148	Dhrs3	dehydrogenase/reductase (SDR family) member 3	3.058444869	0.606656674	2.56E-19	2.16E-17
109225	Ms4a7	membrane-spanning 4-domains, subfamily A, member 7	2.947515277	-0.229675328	2.89E-19	2.41E-17
53374	Chst3	carbohydrate (chondroitin 6/keratan) sulfotransferase 3	3.030931688	0.577255097	3.30E-19	2.74E-17
18733	Pirb	paired Ig-like receptor B	3.540429984	0.840481171	3.63E-19	2.99E-17
104099	Itga9	integrin alpha 9	3.586736162	1.438316633	4.14E-19	3.40E-17
64095	Gpr35	G protein-coupled receptor 35	3.071628406	-0.226586402	4.95E-19	4.05E-17
12478	Cd19	CD19 antigen	3.402868792	0.758045167	4.99E-19	4.06E-17
101488	Slco2b1	solute carrier organic anion transporter family, member 2b1	3.456217962	0.782297417	6.35E-19	5.14E-17
231805	Pilra	paired immunoglobin-like type 2 receptor alpha	3.711821676	1.165690494	6.89E-19	5.54E-17
13508	Dscam	Down syndrome cell adhesion molecule	2.756207879	-0.467054861	1.07E-18	8.52E-17
69202	Ptms	parathymosin	2.512531623	3.321684384	1.58E-18	1.26E-16
17084	Ly86	lymphocyte antigen 86	3.614498163	1.219498546	1.70E-18	1.35E-16
14389	Gab2	growth factor receptor bound protein 2-associated protein 2	3.5292714	0.818744219	1.74E-18	1.37E-16
20302	Ccl3	chemokine (C-C motif) ligand 3	2.511924004	3.174186042	1.76E-18	1.38E-16
66141	Ifitm3	interferon induced transmembrane protein 3	3.429024942	1.202333897	1.84E-18	1.43E-16
27053	Asns	asparagine synthetase	3.024627565	0.9863462	1.88E-18	1.45E-16
12266	C3	complement component 3	3.438153002	0.862540792	1.91E-18	1.46E-16
14293	Fpr1	formyl peptide receptor 1	2.924681143	-0.374087817	2.19E-18	1.65E-16
12265	Ciita	class II transactivator	3.580688928	0.654520234	2.22E-18	1.66E-16
12902	Cr2	complement receptor 2	3.94255885	0.855226452	2.37E-18	1.77E-16
228765	Sdcbp2	syndecan binding protein (syntenin) 2	2.048394312	2.781370396	2.40E-18	1.79E-16
67092	Gatm	glycine amidinotransferase (L-arginine:glycine amidinotransferase)	3.265369671	0.159787009	2.63E-18	1.94E-16
22164	Tnfsf4	tumor necrosis factor (ligand) superfamily, member 4	2.942393468	0.16785909	3.31E-18	2.44E-16
16529	Kcnk5	potassium channel, subfamily K, member 5	2.530462494	3.422786372	3.45E-18	2.52E-16
19261	Sirpa	signal-regulatory protein alpha	5.423362762	3.324828876	3.55E-18	2.58E-16
12818	Col14a1	collagen, type XIV, alpha 1	2.854364451	0.032170175	3.70E-18	2.69E-16
68337	Crip2	cysteine rich protein 2	2.474827321	0.830780944	4.41E-18	3.16E-16
12263	C2	complement component 2 (within H-2S)	2.672723657	0.047899455	4.77E-18	3.40E-16
108956	Apol7c	apolipoprotein L 7c	3.792727431	0.730438468	5.29E-18	3.74E-16
56615	Mgst1	microsomal glutathione S-transferase 1	2.69249269	-0.610345682	5.50E-18	3.87E-16
66857	Plbd1	phospholipase B domain containing 1	4.982229854	2.338405568	6.05E-18	4.24E-16
12771	Ccr3	chemokine (C-C motif) receptor 3	4.304022689	1.943428689	7.33E-18	5.08E-16
19016	Pparg	peroxisome proliferator activated receptor gamma	2.98905432	-0.30489845	7.99E-18	5.50E-16
240327	Gm4951	predicted gene 4951	2.711614719	-0.448529052	8.10E-18	5.54E-16
20512	Slc1a3	solute carrier family 1 (glial high affinity glutamate transporter), member 3	2.758264459	-0.417994964	8.40E-18	5.73E-16
14103	Fasl	Fas ligand (TNF superfamily, member 6)	2.70191922	4.282283393	1.06E-17	7.20E-16
13587	Ear2	eosinophil-associated, ribonuclease A family, member 2	2.893710786	-0.245043994	1.13E-17	7.60E-16
72925	March1	membrane-associated ring finger (C3HC4) 1	3.500062773	0.749130525	1.16E-17	7.78E-16
13830	Stom	stomatin	3.438517346	0.697876663	1.26E-17	8.43E-16
16909	Lmo2	LIM domain only 2	3.16633974	0.391576255	1.38E-17	9.13E-16
217303	Cd300a	CD300A antigen	4.528077597	1.543953879	1.67E-17	1.10E-15
17523	Mpo	myeloperoxidase	2.586290619	-0.799026454	1.86E-17	1.22E-15
12522	Cd83	CD83 antigen	3.006260375	2.600523885	1.97E-17	1.29E-15
66775	Hacd4	3-hydroxyacyl-CoA dehydratase 4	2.582800607	-0.760630341	2.23E-17	1.45E-15
69574	Cmbl	carboxymethylenebutenolidase-like (Pseudomonas)	2.600895223	-0.715994964	2.33E-17	1.51E-15
237711	Eml6	echinoderm microtubule associated protein like 6	2.463659181	0.396300548	2.60E-17	1.68E-15
28240	Trpm2	transient receptor potential cation channel, subfamily M, member 2	3.684105288	1.082456548	3.01E-17	1.93E-15
225594	Gm4841	predicted gene 4841	2.716548194	-0.528401547	3.12E-17	1.99E-15
80876	Ifitm2	interferon induced transmembrane protein 2	2.725651858	-0.500791891	3.12E-17	1.99E-15
19713	Ret	ret proto-oncogene	2.483160732	-0.410635312	3.44E-17	2.19E-15
320706	Soga1	suppressor of glucose, autophagy associated 1	2.628857033	-0.575700253	3.39E-17	2.38E-15
56760	Clec1b	C-type lectin domain family 1, member b	3.133780236	-0.10504714	3.98E-17	2.50E-15
246707	Emilin2	elastin microfibril interfacer 2	3.37641826	0.359476717	4.32E-17	2.71E-15

22038	Plscr1	phospholipid scramblase 1	2.526882544	1.447757417	4.54E-17	2.83E-15
243958	Siglecg	sialic acid binding Ig-like lectin G	2.651238539	-0.662948218	4.62E-17	2.87E-15
217306	Cd300e	CD300e antigen	3.565292533	0.33925608	5.25E-17	3.24E-15
17068	Ly6d	lymphocyte antigen 6 complex, locus D	3.772152942	0.502917582	5.89E-17	3.62E-15
16971	Lrp1	low density lipoprotein receptor-related protein 1	4.259800734	2.594536629	5.92E-17	3.62E-15
74189	Phactr3	phosphatase and actin regulator 3	2.541665296	-0.789210809	6.41E-17	3.91E-15
65256	Asb2	ankyrin repeat and SOCS box-containing 2	3.686631426	1.472777264	7.10E-17	4.32E-15
17329	Cxcl9	chemokine (C-X-C motif) ligand 9	2.873494906	-0.24983129	7.30E-17	4.42E-15
69583	Tnfsf13	tumor necrosis factor (ligand) superfamily, member 13	2.837365741	-0.254800973	7.40E-17	4.47E-15
226101	Myof	myoferlin	3.315464982	0.15115122	7.55E-17	4.54E-15
11421	Ace	angiotensin I converting enzyme (peptidyl-dipeptidase A) 1	2.703114114	-0.575760071	7.96E-17	4.77E-15
320407	Klri2	killer cell lectin-like receptor family I member 2	3.091863726	2.96190623	8.02E-17	4.79E-15
20963	Syk	spleen tyrosine kinase	4.247991607	2.798430036	8.15E-17	4.85E-15
53857	Tuba8	tubulin, alpha 8	2.954411991	0.539124996	9.48E-17	5.62E-15
71690	Esm1	endothelial cell-specific molecule 1	2.728443128	-0.595852176	1.04E-16	6.14E-15
140795	P2ry14	purinergic receptor P2Y, G-protein coupled, 14	2.378446539	0.705706494	1.08E-16	6.39E-15
66222	Serpinb1a	serine (or cysteine) peptidase inhibitor, clade B, member 1a	3.05389929	0.841713406	1.20E-16	7.04E-15
432572	Specc1	sperm antigen with calponin homology and coiled-coil domains 1	2.617286365	0.023769737	1.33E-16	7.77E-15
12475	Cd14	CD14 antigen	2.740498107	-0.251683681	1.43E-16	8.28E-15
235380	Dmxl2	Dmx-like 2	2.635697123	-0.631958362	1.48E-16	8.54E-15
15000	H2-DMb2	histocompatibility 2, class II, locus Mb2	2.363041003	-0.717890787	1.52E-16	8.71E-15
224840	Treml4	triggering receptor expressed on myeloid cells-like 4	4.658079568	1.855461654	1.58E-16	9.01E-15
75552	Paqr9	progestin and adipoQ receptor family member IX	2.784517386	-0.365997317	1.60E-16	9.12E-15
16000	Igf1	insulin-like growth factor 1	3.984937938	1.346170665	1.61E-16	9.14E-15
17533	Mrc1	mannose receptor, C type 1	4.597226309	3.530373847	1.64E-16	9.27E-15
320129	Adrbk2	adrenergic receptor kinase, beta 2	3.522063742	0.739789025	1.69E-16	9.55E-15
17118	Marcks	myristoylated alanine rich protein kinase C substrate	3.63306921	2.555179588	1.76E-16	9.87E-15
76408	Abcc3	ATP-binding cassette, sub-family C (CFTR/MRP), member 3	4.148767031	1.808966768	1.80E-16	1.01E-14
15216	Hfe	hemochromatosis	3.290337954	1.053958748	1.85E-16	1.03E-14
21810	Tgfbi	transforming growth factor, beta induced	3.971760392	1.174905385	1.95E-16	1.08E-14
242248	Bank1	B cell scaffold protein with ankyrin repeats 1	2.507259215	2.487038394	2.12E-16	1.17E-14
14962	Cfb	complement factor B	2.837983748	-0.062784425	2.25E-16	1.24E-14
17105	Lyz2	lysozyme 2	5.488949106	3.15361806	2.50E-16	1.36E-14
67824	Nmral1	NmrA-like family domain containing 1	2.122238825	1.191435703	3.04E-16	1.64E-14
545030	Wdfy4	WD repeat and FYVE domain containing 4	4.769268688	2.395123447	3.15E-16	1.69E-14
17086	Ncr1	natural cytotoxicity triggering receptor 1	5.732166517	3.113852773	3.18E-16	1.70E-14
19141	Lgmn	legumain	3.828503625	2.893243287	3.21E-16	1.71E-14
11629	Aif1	allograft inflammatory factor 1	4.250361405	1.608124481	3.32E-16	1.76E-14
12484	Cd24a	CD24a antigen	4.248183149	1.847400339	3.71E-16	1.96E-14
66066	Gng11	guanine nucleotide binding protein (G protein), gamma 11	2.605253662	-0.7040502	3.87E-16	2.04E-14
18131	Notch3	notch 3	2.987062641	-0.220369531	3.99E-16	2.09E-14
16517	Kcnj16	potassium inwardly-rectifying channel, subfamily J, member 16	2.731178868	0.947580431	4.03E-16	2.11E-14
353346	Gpr141	G protein-coupled receptor 141	2.869973187	-0.397692502	4.12E-16	2.15E-14
12274	C6	complement component 6	4.09162367	1.242447155	5.81E-16	2.99E-14
66859	Slc16a9	solute carrier family 16 (monocarboxylic acid transporters), member 9	3.205197521	0.11974927	5.85E-16	2.99E-14
14461	Gata2	GATA binding protein 2	2.518943052	-0.834988105	8.67E-16	4.39E-14
29815	Bcar3	breast cancer anti-estrogen resistance 3	2.257695683	-1.183699344	1.13E-15	5.72E-14
17132	Maf	avian musculoaponeurotic fibrosarcoma oncogene homolog	2.360571646	1.194321555	1.25E-15	6.15E-14
65221	Slc15a3	solute carrier family 15, member 3	3.039681855	0.416017883	1.26E-15	6.30E-14
626578	Gbp10	guanylate-binding protein 10	2.067175005	3.467079587	1.27E-15	6.32E-14
67880	Dcxr	dicarbonyl L-xylulose reductase	2.621170953	0.546686325	1.51E-15	7.50E-14
110095	Pygl	liver glycogen phosphorylase	2.352824263	1.493015478	1.56E-15	7.69E-14
320736	Vstm4	V-set and transmembrane domain containing 4	2.670690717	-0.523811929	1.74E-15	8.48E-14
11826	Aqp1	aquaporin 1	2.490640765	-0.760988707	1.75E-15	8.50E-14
217304	Cd300lb	CD300 antigen like family member B	2.527813043	-0.652450267	1.99E-15	9.63E-14
226421	Rab7b	RAB7B, member RAS oncogene family	2.829453248	-0.287841895	2.09E-15	1.01E-13
13036	Ctsh	cathepsin H	4.319326969	1.841608021	2.15E-15	1.03E-13
19224	Ptgs1	prostaglandin-endoperoxide synthase 1	3.972437362	1.240757705	2.26E-15	1.08E-13
211550	Tifa	TRAF-interacting protein with forkhead-associated domain	2.531750532	-0.49873188	2.75E-15	1.31E-13
232413	Clec12a	C-type lectin domain family 12, member a	3.907355832	1.309653438	2.87E-15	1.36E-13
11816	Apoe	apolipoprotein E	2.880364918	3.870502284	2.97E-15	1.40E-13
66895	Pxdc1	PX domain containing 1	2.308379199	-0.979309097	3.01E-15	1.42E-13
545812	Pilrb2	paired immunoglobin-like type 2 receptor beta 2	2.910344364	0.019388654	3.51E-15	1.64E-13
14268	Fn1	fibronectin 1	3.680796146	0.412040827	3.81E-15	1.78E-13
17476	Mpeg1	macrophage expressed gene 1	5.670805762	4.499348904	3.95E-15	1.84E-13
241041	Gm4956	predicted gene 4956	2.911332132	0.961542713	4.09E-15	1.90E-13
80719	Igsf6	immunoglobulin superfamily, member 6	3.615900406	0.958806411	5.20E-15	2.41E-13
72054	Cyp4f18	cytochrome P450, family 4, subfamily f, polypeptide 18	2.5070889	-0.79149377	6.63E-15	3.05E-13
14133	Fcna	ficolin A	5.296339228	3.143328038	6.86E-15	3.14E-13
109901	Cela1	chymotrypsin-like elastase family, member 1	2.879879679	0.432204468	7.91E-15	3.61E-13
12519	Cd80	CD80 antigen	2.654074037	-0.318540772	1.09E-14	4.96E-13
14159	Fes	feline sarcoma oncogene	2.675722161	0.878886852	1.22E-14	5.57E-13
21349	Tal1	T cell acute lymphocytic leukemia 1	2.244674563	-0.9827465	1.25E-14	5.67E-13
381308	Mnda	myeloid cell nuclear differentiation antigen	2.609873834	-0.555447285	1.31E-14	5.89E-13
16162	Il12rb2	interleukin 12 receptor, beta 2	2.154027432	3.679195291	1.42E-14	6.36E-13
12259	C1qa	complement component 1, q subcomponent, alpha polypeptide	4.963703582	3.112267373	1.54E-14	6.90E-13
53945	Slc40a1	solute carrier family 40 (iron-regulated transporter), member 1	5.356174157	4.559621049	1.61E-14	7.17E-13
73914	Irak3	interleukin-1 receptor-associated kinase 3	2.663319141	-0.064223018	1.61E-14	7.17E-13
11669	Aldh2	aldehyde dehydrogenase 2, mitochondrial	3.544290741	1.948006427	1.77E-14	7.84E-13
18022	Nfe2	nuclear factor, erythroid derived 2	2.405163901	-0.385466756	1.78E-14	7.87E-13
22177	Tyrobp	TYRO protein tyrosine kinase binding protein	4.606977071	3.695004208	1.91E-14	7.97E-13
14538	Gcnt2	glucosaminyl (N-acetyl) transferase 2, I-branching enzyme	2.427606068	-0.666125099	1.91E-14	8.36E-13
140570	Plxnb2	plexin B2	3.882275826	1.505703878	1.91E-14	8.37E-13
12977	Csf1	colony stimulating factor 1 (macrophage)	2.761295899	0.375925649	1.93E-14	8.45E-13
18173	Slc11a1	solute carrier family 11 (proton-coupled divalent metal ion transporters), member 1	3.930677166	1.24224994	2.06E-14	8.97E-13
54381	Cpq	carboxypeptidase Q	2.683272217	2.312874056	2.17E-14	9.43E-13
71653	Shtn1	shootin 1	3.266724952	0.050823385	2.29E-14	9.91E-13
545486	Tubb1	tubulin, beta 1 class VI	2.512866758	-0.59263867	2.83E-14	1.22E-12
14129	Fcgr1	Fc receptor, IgG, high affinity I	3.225392524	0.126079679	3.09E-14	1.33E-12
171285	Havcr2	hepatitis A virus cellular receptor 2	3.411268175	0.391495295	3.31E-14	1.41E-12
70839	P2ry12	purinergic receptor P2Y, G-protein coupled 12	2.440416571	0.008837518	3.38E-14	1.44E-12
11746	Anxa4	annexin A4	2.290862738	1.289422796	3.40E-14	1.44E-12
11975	Atp6v0a1	ATPase, H+ transporting, lysosomal V0 subunit A1	2.176514076	1.021816304	3.52E-14	1.49E-12
234797	6430548M08Rik	RIKEN cDNA 6430548M08 gene	2.455569171	0.828177978	5.07E-14	2.12E-12
217305	Cd300ld	CD300 molecule-like family member d	2.660333188	-0.546138086	5.23E-14	2.18E-12
15446	Hpgd	hydroxyprostaglandin dehydrogenase 15 (NAD)	4.193526342	1.775330205	5.23E-14	2.18E-12
108800	Ston2	stonin 2	2.217665097	-0.285882079	5.26E-14	2.18E-12
54725	Cadm1	cell adhesion molecule 1	3.88239063	1.255102462	5.46E-14	2.26E-12
17470	Cd200	CD200 antigen	2.437254194	2.388585836	5.64E-14	2.33E-12
66102	Cxcl16	chemokine (C-X-C motif) ligand 16	2.84929216	-0.124162372	5.66E-14	2.33E-12
14586	Gfra2	glial cell line derived neurotrophic factor family receptor alpha 2	3.559420057	0.662800862	6.89E-14	2.81E-12
71409	Fmnl2	formin-like 2	3.154247438	0.559637048	7.38E-14	3.00E-12
74145	F13a1	coagulation factor XIII, A1 subunit	3.113744392	0.185817455	7.92E-14	3.21E-12
73340	Nptxr	neuronal pentraxin receptor	2.244262389	-0.448942792	8.73E-14	3.53E-12
68166	Spire1	spire homolog 1 (Drosophila)	2.487606828	0.076803451	9.18E-14	3.70E-12
69660	Tmbim1	transmembrane BAX inhibitor motif containing 1	2.157943154	1.785323539	9.19E-14	3.70E-12
16553	Kif13a	kinesin family member 13A	2.757402099	1.497715091	1.18E-13	4.67E-12
21898	Tlr4	toll-like receptor 4	3.039945625	0.128200461	1.33E-13	5.25E-12
53876	Ear3	eosinophil-associated, ribonuclease A family, member 3	2.568260509	-0.589737436	1.59E-13	6.23E-12
503845	Ear12	eosinophil-associated, ribonuclease A family, member 12	2.568256865	-0.589737436	1.60E-13	6.27E-12
67916	Plpp3	phospholipid phosphatase 3	2.384145906	-0.737742684	1.93E-13	7.50E-12
233806	Tmem159	transmembrane protein 159	2.100779292	1.130313345	2.75E-13	1.06E-11
12229	Btk	Bruton agammaglobulinemia tyrosine kinase	3.363130668	0.472177598	2.88E-13	1.10E-11

320560	Dennd5b	DENN/MADD domain containing 5B	2.325462674	-0.926638936	3.20E-13	1.22E-11
16010	Igfbp4	insulin-like growth factor binding protein 4	2.261946117	6.986737905	3.26E-13	1.24E-11
11656	Alas2	aminolevulinic acid synthase 2, erythroid	2.373380625	-0.848044279	3.38E-13	1.28E-11
15978	Ifng	interferon gamma	2.801104341	4.792950269	3.42E-13	1.29E-11
20661	Sort1	sortilin 1	3.530618012	1.367140991	3.57E-13	1.35E-11
195646	Hs3st2	heparan sulfate (glucosamine) 3-O-sulfotransferase 2	2.162789507	-1.156755218	3.65E-13	1.38E-11
14728	Lilrb4a	leukocyte immunoglobulin-like receptor, subfamily B, member 4A	2.499236211	2.640725106	3.86E-13	1.45E-11
246746	Cd300lf	CD300 antigen like family member F	2.665336994	-0.228433992	4.28E-13	1.60E-11
22041	Trf	transferrin	4.847633944	3.979193786	4.57E-13	1.70E-11
69288	Rhobtb1	Rho-related BTB domain containing 1	2.229504805	-1.097613952	4.57E-13	1.70E-11
16168	Il15	interleukin 15	2.166317505	0.211976762	4.63E-13	1.72E-11
12035	Bcat1	branched chain aminotransferase 1, cytosolic	2.661340608	0.698864976	5.10E-13	1.89E-11
16658	Mafb	v-maf musculoaponeurotic fibrosarcoma oncogene family, protein B (avian)	2.995800004	1.054340943	5.28E-13	1.95E-11
14619	Gjb2	gap junction protein, beta 2	2.126633335	-1.276189946	5.83E-13	2.14E-11
65963	Tmem176b	transmembrane protein 176B	2.475696784	1.950505269	6.36E-13	2.33E-11
12978	Csf1r	colony stimulating factor 1 receptor	4.582441023	4.161173399	6.47E-13	2.36E-11
19883	Rora	RAR-related orphan receptor alpha	2.429240516	1.757165128	6.48E-13	2.36E-11
102278	Cpne7	copine VII	2.220448119	-0.085733346	6.78E-13	2.47E-11
338365	Slc41a2	solute carrier family 41, member 2	2.381653779	-0.480674401	8.53E-13	3.06E-11
20541	Slc8a1	solute carrier family 8 (sodium/calcium exchanger), member 1	3.030313136	0.518499381	9.54E-13	3.42E-11
12518	Cd79a	CD79A antigen (immunoglobulin-associated alpha)	3.902402841	1.043600963	9.61E-13	3.44E-11
26888	Clec4a2	C-type lectin domain family 4, member a2	2.804982458	-0.325328756	1.05E-12	3.76E-11
14126	Ms4a2	membrane-spanning 4-domains, subfamily A, member 2	2.068256334	-1.318859461	1.16E-12	4.13E-11
14537	Gcnt1	glucosaminyl (N-acetyl) transferase 1, core 2	3.019068519	0.578503278	1.20E-12	4.27E-11
13421	Dnase1l3	deoxyribonuclease 1-like 3	4.350049265	1.557756453	1.21E-12	4.29E-11
64011	Nrgn	neurogranin	2.452312779	-0.020159865	1.21E-12	4.29E-11
192188	Stab2	stabilin 2	3.493111077	0.822432615	1.26E-12	4.42E-11
11745	Anxa3	annexin A3	2.683395402	-0.429630687	1.27E-12	4.46E-11
23859	Dlg2	discs, large homolog 2 (Drosophila)	2.152001225	-1.107741271	1.29E-12	4.54E-11
17970	Ncf2	neutrophil cytosolic factor 2	2.483987153	0.365721471	1.34E-12	4.70E-11
15114	Hap1	huntingtin-associated protein 1	2.42105312	-0.547941407	1.35E-12	4.71E-11
74030	Rin2	Ras and Rab interactor 2	2.25659566	-0.921374161	1.40E-12	4.88E-11
193740	Hspa1a	heat shock protein 1A	3.558277881	3.748856461	1.46E-12	5.07E-11
65970	Lima1	LIM domain and actin binding 1	3.009540833	0.73777835	1.50E-12	5.20E-11
19731	Rgl1	ral guanine nucleotide dissociation stimulator,-like 1	3.267295274	1.330842291	1.53E-12	5.30E-11
27056	Irf5	interferon regulatory factor 5	3.153377012	1.503327322	1.55E-12	5.35E-11
15951	Ifi204	interferon activated gene 204	2.301804654	1.336765673	1.75E-12	6.01E-11
67299	Dock7	dedicator of cytokinesis 7	2.190393697	-0.663891968	2.27E-12	7.74E-11
65973	Asph	aspartate-beta-hydroxylase	2.001756821	0.976900856	2.28E-12	7.76E-11
66058	Tmem176a	transmembrane protein 176A	2.334428463	1.178073359	2.31E-12	7.83E-11
14960	H2-Aa	histocompatibility 2, class II antigen A, alpha	5.881394424	4.503203036	2.46E-12	8.33E-11
23972	Papss2	3'-phosphoadenosine 5'-phosphosulfate synthase 2	2.430743771	-0.597975715	2.56E-12	8.64E-11
232414	Clec9a	C-type lectin domain family 9, member a	2.563290863	-0.554470389	3.10E-12	1.05E-10
170741	Pilrb1	paired immunoglobin-like type 2 receptor beta 1	2.985014838	-0.023255544	3.32E-12	1.12E-10
80281	Cttnbp2nl	CTTNBP2 N-terminal like	2.321230236	-0.64645448	3.34E-12	1.12E-10
70423	Tspan15	tetraspanin 15	2.460495254	-0.726190185	3.59E-12	1.20E-10
224014	Fgd4	FYVE, RhoGEF and PH domain containing 4	2.04119486	-1.368502562	3.60E-12	1.20E-10
109270	Prr5	proline rich 5 (renal)	2.404374029	-0.718898412	4.10E-12	1.37E-10
20971	Sdc4	syndecan 4	2.651413984	0.132677955	4.22E-12	1.40E-10
14969	H2-Eb1	histocompatibility 2, class II antigen E beta	5.723721469	3.830409339	4.34E-12	1.43E-10
16456	F11r	F11 receptor	2.175253714	-0.81686312	5.70E-12	1.87E-10
13823	Epb41l3	erythrocyte membrane protein band 4.1 like 3	3.429722041	0.867821483	5.98E-12	1.95E-10
72948	Tppp	tubulin polymerization promoting protein	2.153502473	1.045783363	6.29E-12	2.05E-10
18951	Sept5	septin 5	2.139389186	-0.964200672	6.43E-12	2.09E-10
70789	Kynu	kynureninase (L-kynurenine hydrolase)	2.138191526	-1.177991613	6.47E-12	2.10E-10
13400	Dmpk	dystrophia myotonica-protein kinase	2.295969451	-0.897653848	6.71E-12	2.17E-10
226691	AI607873	expressed sequence AI607873	3.231675403	0.485369225	7.09E-12	2.28E-10
19274	Ptprm	protein tyrosine phosphatase, receptor type, M	3.246838229	0.225228327	7.10E-12	2.28E-10
19074	Prg2	proteoglycan 2, bone marrow	2.109571898	-1.242702327	7.26E-12	2.33E-10
26362	Axl	AXL receptor tyrosine kinase	2.651841654	4.460136675	7.98E-12	2.55E-10
27226	Pla2g7	phospholipase A2, group VII (platelet-activating factor acetylhydrolase, plasma)	3.71825315	1.481152622	8.90E-12	2.83E-10
70546	Zdhhc2	zinc finger, DHHC domain containing 2	2.168660095	1.923345517	9.41E-12	2.88E-10
211228	Lrrc25	leucine rich repeat containing 25	2.625768034	-0.559701106	9.41E-12	2.98E-10
19201	Pstpip2	proline-serine-threonine phosphatase-interacting protein 2	2.120383016	-1.002126435	1.08E-11	3.40E-10
12290	Cacna1e	calcium channel, voltage-dependent, R type, alpha 1E subunit	2.086476764	-1.240573866	1.12E-11	3.54E-10
17059	Klrb1c	killer cell lectin-like receptor subfamily B member 1C	2.909422211	4.838119384	1.16E-11	3.63E-10
14727	Lilr4b	leukocyte immunoglobulin-like receptor, subfamily B, member 4B	2.520295499	2.397935488	1.21E-11	3.78E-10
21934	Tnfrsf11a	tumor necrosis factor receptor superfamily, member 11a, NFKB activator	2.119665191	-1.179173307	1.25E-11	3.90E-10
16905	Lmna	lamin A	2.356631541	0.825940336	1.35E-11	4.21E-10
71310	Tbc1d9	TBC1 domain family, member 9	3.416258582	0.68007742	1.38E-11	4.28E-10
56743	Lat2	linker for activation of T cells family, member 2	2.566188575	1.883065201	1.47E-11	4.54E-10
23832	Xcr1	chemokine (C motif) receptor 1	2.272911384	-0.952134994	1.79E-11	5.47E-10
319939	Tns3	tensin 3	3.47678491	0.943176459	1.79E-11	5.48E-10
81897	Tlr9	toll-like receptor 9	2.249701759	-0.131144724	2.08E-11	6.31E-10
15129	Hbb-b1	hemoglobin, beta adult major chain	4.667086449	1.639493071	2.16E-11	6.54E-10
24108	Ubd	ubiquitin D	2.059909997	-1.101880241	2.17E-11	6.56E-10
100503605	Hbb-bs	hemoglobin, beta adult s chain	4.66708602	1.639493071	2.18E-11	6.57E-10
18805	Pld1	phospholipase D1	2.164104632	-0.946832647	2.24E-11	6.74E-10
17748	Mt1	metallothionein 1	2.203216732	-0.869683022	2.32E-11	6.97E-10
18106	Cd244	CD244 natural killer cell receptor 2B4	3.761990248	1.989413332	2.35E-11	7.05E-10
100628611	Mir5107	microRNA 5107	2.040887141	-1.200013059	2.63E-11	7.84E-10
279572	Tlr13	toll-like receptor 13	2.596348727	0.067712631	2.89E-11	8.55E-10
347722	Agap1	ArfGAP with GTPase domain, ankyrin repeat and PH domain 1	2.77020095	0.050623144	2.96E-11	8.73E-10
381269	Mreg	melanoregulin	2.270258174	-0.999504823	3.42E-11	1.00E-09
68481	Mpzl1	myelin protein zero-like 1	2.655383572	0.028547577	3.42E-11	1.00E-09
15511	Hspa1b	heat shock protein 1B	2.748730651	4.774156042	4.32E-11	1.26E-09
20259	Scin	scinderin	2.084071405	-0.951540233	4.38E-11	1.27E-09
19223	Ptgis	prostaglandin I2 (prostacyclin) synthase	2.177814429	-0.810056254	4.80E-11	1.39E-09
58996	Arhgap23	Rho GTPase activating protein 23	2.613657217	-0.119368808	4.82E-11	1.39E-09
16790	Anpep	alanyl (membrane) aminopeptidase	2.68787969	-0.300443079	5.66E-11	1.62E-09
55963	Slc1a4	solute carrier family 1 (glutamate/neutral amino acid transporter), member 4	2.09469168	0.205443714	6.09E-11	1.73E-09
21816	Tgm1	transglutaminase 1, K polypeptide	2.93866053	0.08685856	6.30E-11	1.79E-09
104086	Cyp27a1	cytochrome P450, family 27, subfamily a, polypeptide 1	2.206687906	-0.859816717	6.50E-11	1.84E-09
14544	Gda	guanine deaminase	2.328904352	-0.810665347	7.50E-11	2.12E-09
66205	Cd302	CD302 antigen	3.206837746	0.136996413	7.78E-11	2.18E-09
20725	Serpinb8	serine (or cysteine) peptidase inhibitor, clade B, member 8	2.078500505	-1.08420947	8.38E-11	2.34E-09
22371	Vwf	Von Willebrand factor homolog	2.176289666	-0.747677514	8.72E-11	2.44E-09
319387	Adgrl3	adhesion G protein-coupled receptor L3	2.049242162	-1.186728182	9.87E-11	2.74E-09
22329	Vcam1	vascular cell adhesion molecule 1	4.581048167	4.827832207	9.97E-11	2.76E-09
272382	Spib	Spi-B transcription factor (Spi-1/PU.1 related)	3.716295801	0.594524143	9.98E-11	2.76E-09
212980	Slc45a3	solute carrier family 45, member 3	2.602411725	0.274566876	1.01E-10	2.79E-09
104445	Cdc42ep1	CDC42 effector protein (Rho GTPase binding) 1	2.061987092	-1.14232463	1.05E-10	2.89E-09
23792	Adam23	a disintegrin and metallopeptidase domain 23	2.760163867	-0.264510467	1.39E-10	3.78E-09
59010	Sqrdl	sulfide quinone reductase-like (yeast)	2.124449429	1.862233589	1.53E-10	4.14E-09
19122	Prnp	prion protein	2.110079694	0.841330845	1.72E-10	4.61E-09
15248	Hic1	hypermethylated in cancer 1	2.59409494	0.792594066	1.76E-10	4.71E-09
12606	Cebpa	CCAAT/enhancer binding protein (C/EBP), alpha	2.15105964	-0.7862855	2.37E-10	6.23E-09
74365	Lonrf3	LON peptidase N-terminal domain and ring finger 3	2.224446001	-0.50476994	2.98E-10	7.78E-09
21416	Tcf7l2	transcription factor 7 like 2, T cell specific, HMG box	2.016681687	-0.112007405	2.99E-10	7.81E-09
17000	Ltbr	lymphotoxin B receptor	2.100328646	-1.041149838	3.04E-10	7.92E-09
70097	Sash1	SAM and SH3 domain containing 1	3.36702003	0.795721127	3.18E-10	8.24E-09
21825	Thbs1	thrombospondin 1	2.271568397	-0.592397875	3.31E-10	8.55E-09
83553	Tktl1	transketolase-like 1	2.187331871	-1.119894637	3.35E-10	8.64E-09

29813	Zfp385a	zinc finger protein 385A	2.13633302	-0.309959757	4.03E-10	1.03E-08
433638	I830077J02Rik	RIKEN cDNA I830077J02 gene	2.073107041	-0.954617874	4.04E-10	1.03E-08
56461	Kcnip3	Kv channel interacting protein 3, calsenilin	2.152713279	1.942515036	4.46E-10	1.13E-08
15122	Hba-a1	hemoglobin alpha, adult chain 1	3.134819751	0.28574767	4.63E-10	1.17E-08
110257	Hba-a2	hemoglobin alpha, adult chain 2	3.134819682	0.28574767	4.63E-10	1.17E-08
67689	Aldh3b1	aldehyde dehydrogenase 3 family, member B1	2.639216924	-0.154152638	4.72E-10	1.20E-08
26382	Fgd2	FYVE, RhoGEF and PH domain containing 2	2.194958213	-0.038683324	5.12E-10	1.29E-08
20612	Siglec1	sialic acid binding Ig-like lectin 1, sialoadhesin	2.319049164	-0.386509986	5.15E-10	1.30E-08
16164	Il13ra1	interleukin 13 receptor, alpha 1	2.592478442	-0.263536723	5.85E-10	1.47E-08
368204	Khdc1a	KH domain containing 1A	2.04776524	-1.202214621	5.94E-10	1.49E-08
269823	Pon3	paraoxonase 3	2.235650415	0.236061782	6.08E-10	1.52E-08
108686	Ccdc88a	coiled coil domain containing 88A	2.116556201	0.28565911	6.27E-10	1.56E-08
60596	Gucy1a3	guanylate cyclase 1, soluble, alpha 3	2.32353454	1.385816915	6.43E-10	1.60E-08
17095	Lyl1	lymphoblastomic leukemia 1	2.073460019	-1.069148652	6.50E-10	1.61E-08
20193	S100a1	S100 calcium binding protein A1	2.000923737	0.524710721	9.56E-10	2.34E-08
67305	Gpx7	glutathione peroxidase 7	2.013270191	-0.494447664	1.13E-09	2.75E-08
381091	H2-Eb2	histocompatibility 2, class II antigen E beta2	2.802327114	0.42382454	1.35E-09	3.27E-08
70747	Tspan2	tetraspanin 2	2.492032536	0.269268021	1.38E-09	3.34E-08
76477	Pcolce2	procollagen C-endopeptidase enhancer 2	2.10898697	-1.051402631	1.48E-09	3.56E-08
12986	Csf3r	colony stimulating factor 3 receptor (granulocyte)	2.161449431	-0.911666	1.53E-09	3.65E-08
12388	Ctnnd1	catenin (cadherin associated protein), delta 1	2.593023249	0.637729089	1.84E-09	4.35E-08
330166	Miat	myocardial infarction associated transcript (non-protein coding)	2.820927588	-0.199762402	1.96E-09	4.63E-08
545622	Ptpn3	protein tyrosine phosphatase, non-receptor type 3	2.420135796	0.345974571	2.16E-09	5.05E-08
19024	Ppfibp2	PTPRF interacting protein, binding protein 2 (liprin beta 2)	2.406756382	-0.339656991	2.21E-09	5.16E-08
17532	Mras	muscle and microspikes RAS	2.001063598	-0.989187105	2.32E-09	5.40E-08
17167	Marco	macrophage receptor with collagenous structure	2.613765666	-0.349132752	2.75E-09	6.31E-08
16176	Il1b	interleukin 1 beta	2.131376278	-0.983481549	2.91E-09	6.66E-08
12482	Ms4a1	membrane-spanning 4-domains, subfamily A, member 1	4.298683073	1.069496915	3.24E-09	7.38E-08
16988	Lst1	leukocyte specific transcript 1	2.108783602	1.525883969	3.57E-09	8.05E-08
276891	Timd4	T cell immunoglobulin and mucin domain containing 4	2.733708368	-0.333429972	4.76E-09	1.06E-07
98496	Pid1	phosphotyrosine interaction domain containing 1	2.549569953	-0.167172221	5.18E-09	1.15E-07
54610	Tbc1d8	TBC1 domain family, member 8	2.604572879	0.510281721	5.40E-09	1.19E-07
16419	Itgb5	integrin beta 5	3.349402297	1.054739355	6.56E-09	1.43E-07
20249	Scd1	stearoyl-Coenzyme A desaturase 1	3.98182552	1.02918653	6.65E-09	1.45E-07
59126	Nek6	NIMA (never in mitosis gene a)-related expressed kinase 6	2.17618074	0.218516453	6.77E-09	1.47E-07
74748	Slamf8	SLAM family member 8	2.18762109	-0.913269307	8.22E-09	1.76E-07
83382	Siglece	sialic acid binding Ig-like lectin E	2.522031161	1.164680548	8.24E-09	1.76E-07
19734	Rgs16	regulator of G-protein signaling 16	3.139461426	1.362234119	9.17E-09	1.94E-07
12297	Cacnb3	calcium channel, voltage-dependent, beta 3 subunit	2.220815333	-0.176060195	9.34E-09	1.97E-07
15945	Cxcl10	chemokine (C-X-C motif) ligand 10	2.036191209	1.457069202	1.04E-08	2.18E-07
50722	Dkkl1	dickkopf-like 1	2.264759214	1.206799775	1.08E-08	2.27E-07
20706	Serpinb9b	serine (or cysteine) peptidase inhibitor, clade B, member 9b	2.195776646	-0.452770499	1.17E-08	2.44E-07
170744	Tlr8	toll-like receptor 8	2.566814982	-0.301182164	1.21E-08	2.53E-07
54371	Chst2	carbohydrate sulfotransferase 2	2.338869352	0.326108395	1.26E-08	2.63E-07
381924	Itgad	integrin, alpha D	2.546686478	3.232130601	1.53E-08	3.14E-07
16633	Klra2	killer cell lectin-like receptor, subfamily A, member 2	2.137051736	-0.473376918	1.57E-08	3.23E-07
18647	Cdk14	cyclin-dependent kinase 14	3.025771424	0.031059454	1.80E-08	3.66E-07
11496	Adam22	a disintegrin and metallopeptidase domain 22	2.100901184	-1.084788303	1.80E-08	3.66E-07
73102	Slc22a23	solute carrier family 22, member 23	2.172597332	-0.697149976	1.83E-08	3.72E-07
14086	Fscn1	fascin actin-bundling protein 1	3.782158618	1.111671201	1.92E-08	3.88E-07
12759	Clu	clusterin	2.571331736	-0.491567802	1.94E-08	3.92E-07
52793	Fam3b	family with sequence similarity 3, member B	2.132195857	-0.556740754	2.12E-08	4.25E-07
93671	Cd163	CD163 antigen	2.815508912	1.1530117	2.46E-08	4.89E-07
20299	Ccl22	chemokine (C-C motif) ligand 22	3.137069952	0.264376172	2.58E-08	5.12E-07
73149	Clec4a3	C-type lectin domain family 4, member a3	3.341997353	0.510349325	3.14E-08	6.15E-07
218215	Rnf144b	ring finger protein 144B	2.690795958	0.298970514	3.44E-08	6.70E-07
11997	Akr1b7	aldo-keto reductase family 1, member B7	2.055140351	-0.309362341	4.46E-08	8.56E-07
56807	Scamp5	secretory carrier membrane protein 5	2.17064801	-0.697685732	4.84E-08	9.22E-07
226695	Ifi205	interferon activated gene 205	2.11149537	-1.024169958	6.05E-08	1.13E-06
72145	Wdfy3	WD repeat and FYVE domain containing 3	3.364541815	0.85580503	8.11E-08	1.48E-06
18783	Pla2g4a	phospholipase A2, group IVA (cytosolic, calcium-dependent)	2.292058527	-0.00199066	9.07E-08	1.64E-06
57349	Ppbp	pro-platelet basic protein	2.731084475	-0.221751517	9.67E-08	1.74E-06
26464	Vnn3	vanin 3	2.041774001	-0.97171781	1.02E-07	1.83E-06
66725	Lrrk2	leucine-rich repeat kinase 2	3.333115204	0.181182145	1.17E-07	2.09E-06
170736	Parvb	parvin, beta	2.523528075	-0.482521658	1.33E-07	2.35E-06
14127	Fcer1g	Fc receptor, IgE, high affinity I, gamma polypeptide	3.004224882	3.389069101	1.44E-07	2.52E-06
11600	Angpt1	angiopoietin 1	2.046010057	-0.705161493	2.12E-07	3.64E-06
52163	Camk1	calcium/calmodulin-dependent protein kinase I	2.142852756	-0.443016174	2.21E-07	3.80E-06
50934	Slc7a8	solute carrier family 7 (cationic amino acid transporter, y+ system), member 8	2.566433992	0.324845608	2.83E-07	4.76E-06
56177	Olfm1	olfactomedin 1	2.218654706	0.342150212	3.63E-07	6.03E-06
12443	Ccnd1	cyclin D1	2.525262313	-0.172923541	6.26E-07	9.93E-06
269799	Clec4a1	C-type lectin domain family 4, member a1	2.335387626	0.684208043	6.33E-07	1.00E-05
79221	Hdac9	histone deacetylase 9	2.004649374	0.854875692	7.80E-07	1.21E-05
69601	Dab2ip	disabled 2 interacting protein	2.533631248	-0.142196444	1.29E-06	1.93E-05
320832	Sirpb1a	signal-regulatory protein beta 1A	2.291417412	-0.834899227	1.92E-06	2.78E-05
666661	Gm8221	apolipoprotein L 7c pseudogene	3.042548058	0.282253236	1.94E-06	2.80E-05
27052	Aoah	acyloxyacyl hydrolase	2.926885436	0.334784825	2.49E-06	3.54E-05
217262	Abca9	ATP-binding cassette, sub-family A (ABC1), member 9	2.213164563	-0.661202186	3.79E-06	5.18E-05
14131	Fcgr3	Fc receptor, IgG, low affinity III	2.064509267	2.102695244	3.97E-06	5.40E-05
235527	Plscr4	phospholipid scramblase 4	2.120767604	-0.717106873	4.86E-06	6.48E-05
213391	Rassf4	Ras association (RalGDS/AF-6) domain family member 4	2.67442585	1.808952023	6.62E-06	8.61E-05
19018	Scand1	SCAN domain-containing 1	2.929120364	1.964770643	9.91E-06	0.000124063
80782	Klrb1b	killer cell lectin-like receptor subfamily B member 1B	2.786197034	0.996414361	7.29E-05	0.00073262
17096	Lyn	LYN proto-oncogene, Src family tyrosine kinase	2.010404332	2.792000449	7.88E-05	0.00078345

Table EV4

| EntrezID	Symbol	GeneName	log2 expression VirtualMemory/Naïve	log2A	P.Value	adj.P.Val
20304	Ccl5	chemokine (C-C motif) ligand 5	6.2702771	9.5112044	1.29E-185	2.18E-181
12774	Ccr5	chemokine (C-C motif) receptor 5	5.731194909	6.50627808	1.77E-159	1.50E-155
233328	Lrrk1	leucine-rich repeat kinase 1	5.871790262	5.707943508	3.24E-158	1.82E-154
14457	Gas7	growth arrest specific 7	8.051480393	5.598532245	2.41E-154	1.02E-150
268288	Samd3	sterile alpha motif domain containing 3	5.452584325	7.126713504	5.30E-146	1.79E-142
71887	Ppm1j	protein phosphatase 1J	3.985563599	5.85891834	8.40E-138	2.37E-134
16174	Il18rap	interleukin 18 receptor accessory protein	3.866277337	7.10103822	1.77E-129	4.28E-126
12772	Ccr2	chemokine (C-C motif) receptor 2	6.742343103	6.26391726	3.59E-129	7.58E-126
12766	Cxcr3	chemokine (C-X-C motif) receptor 3	3.756682352	7.531337014	1.12E-123	2.10E-120
242523	Dmrta1	doublesex and mab-3 related transcription factor like family A1	6.652331125	5.260993798	2.33E-122	3.94E-119
27007	Klrk1	killer cell lectin-like receptor subfamily K, member 1	5.104981976	6.859450186	2.20E-118	3.09E-115
20303	Ccl4	chemokine (C-C motif) ligand 4	5.058251081	4.061556522	1.14E-115	1.48E-112
56193	Plek	pleckstrin	7.130546885	7.994643009	4.09E-104	4.94E-101
83490	Pik3ap1	phosphoinositide-3-kinase adaptor protein 1	4.43498767	4.501415035	2.27E-103	2.56E-100
75345	Slamf7	SLAM family member 7	4.036893897	6.297026984	1.74E-100	1.84E-97
16523	Kcnj8	potassium inwardly-rectifying channel, subfamily J, member 8	4.714136216	4.522805178	2.30E-98	2.28E-95
12483	Cd22	CD22 antigen	6.408212333	4.656174903	8.39E-98	7.88E-95
629303	Heatr9	HEAT repeat containing 9	4.969583963	4.434818742	3.23E-97	2.87E-94
57765	Tbx21	T-box 21	3.646699637	6.787595677	3.82E-93	3.23E-90
20200	S100a6	S100 calcium binding protein A6 (calcyclin)	4.735554162	5.662745936	2.83E-92	2.28E-89
16904	Gzmm	granzyme M (lymphocyte met-ase 1)	5.267468002	5.749593413	3.37E-91	2.59E-88
69399	1700025G04Rik	RIKEN cDNA 1700025G04 gene	3.279423901	6.705282471	4.56E-91	3.35E-88
71398	5430427O19Rik	RIKEN cDNA 5430427O19 gene	3.766122075	4.327534783	2.17E-88	1.53E-85
12505	Cd44	CD44 antigen	3.487346075	7.866702609	2.25E-86	1.52E-83
71592	Pogk	pogo transposable element with KRAB domain	2.733754273	7.05015404	8.32E-86	5.41E-83
71720	Osbpl3	oxysterol binding protein-like 3	5.117128646	5.000880151	1.43E-85	8.96E-83
13025	Ctla2b	cytotoxic T lymphocyte-associated protein 2 beta	4.781745738	5.313344731	1.49E-82	8.98E-80
12393	Runx2	runt related transcription factor 2	3.631970578	6.096387757	1.74E-80	9.80E-78
58250	Chst11	carbohydrate sulfotransferase 11	3.361900004	5.736801125	2.16E-77	1.18E-74
64008	Aqp9	aquaporin 9	3.177271005	5.123843577	2.04E-75	1.08E-72
19009	Pou6f1	POU domain, class 6, transcription factor 1	2.436114064	7.400548065	5.53E-75	2.83E-72
16628	Klra10	killer cell lectin-like receptor subfamily A, member 10	6.922372096	4.040297181	7.25E-75	3.60E-72
227717	Qrfp	pyroglutamylated RFamide peptide	4.097974747	3.696981275	1.44E-72	6.96E-70
16185	Il2rb	interleukin 2 receptor, beta chain	2.904050991	10.09027365	9.73E-71	4.57E-68
72160	Tmem163	transmembrane protein 163	5.280940742	2.739656781	1.34E-70	6.10E-68
16641	Klrc1	killer cell lectin-like receptor subfamily C, member 1	4.977327463	4.89698058	1.58E-67	6.83E-65
244234	5830411N06Rik	RIKEN cDNA 5830411N06 gene	5.77601543	6.782278293	1.77E-67	7.46E-65
12145	Cxcr5	chemokine (C-X-C motif) receptor 5	4.231243334	5.386936538	4.27E-67	1.76E-64
13024	Ctla2a	cytotoxic T lymphocyte-associated protein 2 alpha	5.230962676	7.952548035	7.76E-67	3.12E-64
269941	Chsy1	chondroitin sulfate synthase 1	2.332295735	7.802422163	4.52E-66	1.78E-63
74318	Hopx	HOP homeobox	2.470414776	6.52217438	1.07E-64	4.13E-62
14130	Fcgr2b	Fc receptor, IgG, low affinity IIb	5.234257236	3.923189806	4.52E-64	1.70E-61
13143	Dapk2	death-associated protein kinase 2	4.556890939	3.119482004	3.48E-63	1.28E-60
63872	Zfp296	zinc finger protein 296	3.354409551	4.246613069	8.11E-62	2.92E-59
243655	Klre1	killer cell lectin-like receptor family E member 1	7.571091741	5.515222652	4.24E-61	1.49E-58
17064	Cd93	CD93 antigen	4.6904351	3.11096614	2.49E-60	8.59E-58
11881	Arsb	arylsulfatase B	2.756000111	7.454694487	4.47E-60	1.51E-57
214230	Pak6	p21 protein (Cdc42/Rac)-activated kinase 6	4.708670522	2.700712328	1.61E-59	5.33E-57
14579	Gem	GTP binding protein (gene overexpressed in skeletal muscle)	4.116463295	4.130734684	1.75E-59	5.70E-57
329731	Fam19a3	family with sequence similarity 19, member A3	4.283056521	2.832900631	2.03E-59	6.46E-57
22724	Zbtb7b	zinc finger and BTB domain containing 7B	3.88173606	3.33752907	8.00E-57	2.42E-54
381738	Drc1	dynein regulatory complex subunit 1	3.585138623	3.854919271	1.85E-56	5.48E-54
16630	Klra12	killer cell lectin-like receptor subfamily A, member 12	8.305771088	8.028550184	4.57E-56	1.31E-53
71228	Dlg5	discs, large homolog 5 (Drosophila)	5.339695001	3.327851655	5.30E-56	1.49E-53
50930	Tnfsf14	tumor necrosis factor (ligand) superfamily, member 14	3.408938523	4.910785996	5.90E-56	1.63E-53
171211	Edaradd	EDAR (ectodysplasin-A receptor)-associated death domain	4.194120138	3.564741085	1.24E-55	3.38E-53
244233	Cd163l1	CD163 molecule-like 1	6.751318456	6.451426196	1.37E-54	3.66E-52
17916	Myo1f	myosin IF	2.279904574	7.958424024	1.98E-54	5.22E-52
100043314	Tigit	T cell immunoreceptor with Ig and ITIM domains	4.990317733	4.143358101	9.86E-54	2.53E-51
100041546	Ly6c2	lymphocyte antigen 6 complex, locus C2	2.606053404	9.608756771	2.70E-53	6.82E-51
77579	Myh10	myosin, heavy polypeptide 10, non-muscle	4.434609251	3.461683454	4.90E-53	1.22E-50
16411	Itgax	integrin alpha X	3.66723972	6.35914259	7.47E-53	1.83E-50
53321	Cntnap1	contactin associated protein-like 1	4.291193517	1.758975489	1.18E-51	2.84E-49
12298	Cacnb4	calcium channel, voltage-dependent, beta 4 subunit	3.917531256	2.229082568	5.55E-51	1.30E-48
16642	Klrc2	killer cell lectin-like receptor subfamily C, member 2	4.228090399	2.334209545	3.08E-50	7.04E-48
24064	Spry2	sprouty homolog 2 (Drosophila)	5.214288394	3.663337166	6.04E-50	1.36E-47
16963	Xcl1	chemokine (C motif) ligand 1	4.42233294	5.282744666	9.50E-50	2.11E-47
20715	Serpina3g	serine (or cysteine) peptidase inhibitor, clade A, member 3G	3.91447928	4.85667031	4.07E-49	8.82E-47
67122	Nrarp	Notch-regulated ankyrin repeat protein	2.63886564	4.051553466	2.91E-47	6.24E-45
79410	Klra23	killer cell lectin-like receptor subfamily A, member 23	8.474374106	8.311758065	4.53E-47	9.58E-45
319876	Cobll1	Cobl-like 1	2.80527109	5.076866974	1.36E-45	2.85E-43
14190	Fgl2	fibrinogen-like protein 2	3.312381935	4.187152526	4.32E-45	8.90E-43
16631	Klra13-ps	killer cell lectin-like receptor subfamily A, member 13, pseudogene	8.45648677	8.262554047	1.01E-43	2.03E-41
73174	Tbkbp1	TBK1 binding protein 1	3.110214398	3.127039654	2.74E-43	5.44E-41
211914	Asap2	ArfGAP with SH3 domain, ankyrin repeat and PH domain 2	2.679640441	3.584149981	4.09E-43	7.85E-41
11630	Aim1	absent in melanoma 1	2.054087846	8.221949896	1.60E-41	3.01E-39
14103	Fasl	Fas ligand (TNF superfamily, member 6)	4.34762142	4.282283393	3.02E-41	5.61E-39
80981	Arl4d	ADP-ribosylation factor-like 4D	4.73155242	4.992743495	2.26E-39	4.07E-37
20502	Slc16a2	solute carrier family 16 (monocarboxylic acid transporters), member 2	4.068492227	3.011365498	2.34E-39	4.17E-37
71862	Gpr160	G protein-coupled receptor 160	3.061241922	3.428619027	1.11E-38	1.91E-36
73598	1700001O22Rik	RIKEN cDNA 1700001O22 gene	3.828191356	1.868060344	1.74E-38	2.96E-36
13813	Eomes	eomesodermin	2.416311451	7.945748855	2.19E-38	3.67E-36
14841	Gsg2	germ cell-specific gene 2	2.763499404	4.114459936	7.71E-38	1.25E-35
16431	Itm2a	integral membrane protein 2A	3.195599115	7.670105337	8.64E-38	1.39E-35
17948	Naip2	NLR family, apoptosis inhibitory protein 2	2.215004695	4.099373564	1.83E-37	2.91E-35
102502	Pls1	plastin 1 (I-isoform)	5.969015226	3.319311027	2.57E-37	4.02E-35
170706	Tmem37	transmembrane protein 37	3.252058423	2.604926676	2.64E-36	3.98E-34
71223	Gpr15	G protein-coupled receptor 15	3.058380034	3.258529946	3.03E-36	4.53E-34
16529	Kcnk5	potassium channel, subfamily K, member 5	3.697887879	3.422786372	6.08E-36	8.93E-34
16634	Klra3	killer cell lectin-like receptor, subfamily A, member 3	5.260167716	4.6193793	6.20E-36	9.04E-34
93971	Klra19	killer cell lectin-like receptor, subfamily A, member 19	7.113278285	5.705663613	1.07E-35	1.54E-33
104215	Rhoq	ras homolog family member Q	2.52593434	4.724010254	1.16E-35	1.65E-33
22612	Yes1	YES proto-oncogene 1, Src family tyrosine kinase	3.041917335	3.092246197	1.91E-35	2.67E-33
16637	Klra6	killer cell lectin-like receptor, subfamily A, member 6	7.102016055	5.727889103	3.81E-35	5.28E-33
20302	Ccl3	chemokine (C-C motif) ligand 3	3.574817777	3.174186642	5.62E-35	7.72E-33
11540	Adora2a	adenosine A2a receptor	2.092394129	5.65982001	1.97E-33	2.58E-31

213402	Armc2	armadillo repeat containing 2	4.233187689	1.696886094	5.49E-33	7.13E-31
231510	Agpat9	1-acylglycerol-3-phosphate O-acyltransferase 9	5.609964718	4.184592174	5.76E-33	7.43E-31
18591	Pdgfb	platelet derived growth factor, B polypeptide	3.745477246	3.829362587	1.39E-32	1.77E-30
215114	Hip1	huntingtin interacting protein 1	2.767519721	3.306510286	4.26E-32	5.33E-30
26386	Hsf4	heat shock transcription factor 4	3.302939721	2.220704693	7.17E-32	8.91E-30
16639	Klra8	killer cell lectin-like receptor, subfamily A, member 8	6.401494139	4.21776864	2.33E-31	2.86E-29
93968	Klra21	killer cell lectin-like receptor subfamily A, member 21	5.812129469	3.472140588	2.93E-31	3.57E-29
70025	Acot7	acyl-CoA thioesterase 7	2.150740554	4.777421818	4.36E-30	5.19E-28
243931	Tshz3	teashirt zinc finger family member 3	3.568802276	1.975455558	8.70E-30	1.03E-27
13074	Cyp17a1	cytochrome P450, family 17, subfamily a, polypeptide 1	3.306940956	1.258236444	9.91E-30	1.16E-27
654449	Klra14-ps	killer cell lectin-like receptor subfamily A, member 14, pseudogene	4.164228632	1.896887242	1.93E-29	2.25E-27
17951	Naip5	NLR family, apoptosis inhibitory protein 5	3.101516979	2.498246414	2.39E-29	2.77E-27
94226	S1pr5	sphingosine-1-phosphate receptor 5	2.556985048	4.900951022	3.04E-29	3.47E-27
263406	Plekhg3	pleckstrin homology domain containing, family G (with RhoGef domain) member 3	2.182258662	4.402930766	3.30E-29	3.74E-27
17920	Myo6	myosin VI	2.585649113	4.002081005	1.10E-28	1.22E-26
77383	C030029H02Rik	RIKEN cDNA C030029H02 gene	4.802807491	1.423349114	1.81E-28	2.00E-26
52589	Ncald	neurocalcin delta	2.452918759	3.586234315	2.56E-28	2.81E-26
16640	Klra9	killer cell lectin-like receptor subfamily A, member 9	5.467986714	3.557304717	3.05E-28	3.30E-26
22658	Pcgf2	polycomb group ring finger 2	2.909660591	2.43567753	5.41E-28	5.75E-26
11554	Adrb1	adrenergic receptor, beta 1	3.100854574	0.098913941	7.80E-28	8.14E-26
58179	Klrc3	killer cell lectin-like receptor subfamily C, member 3	3.352269688	0.883661467	1.13E-27	1.17E-25
66995	Zcchc18	zinc finger, CCHC domain containing 18	2.192709519	5.037257601	2.22E-27	2.23E-25
77300	Raph1	Ras association (RalGDS/AF-6) and pleckstrin homology domains 1	2.365064699	2.910975191	2.77E-27	2.74E-25
381693	Wdr95	WD40 repeat domain 95	2.259220883	4.245549497	3.81E-27	3.75E-25
16638	Klra7	killer cell lectin-like receptor, subfamily A, member 7	6.914252056	5.528691757	2.04E-26	1.94E-24
20187	Ryk	receptor-like tyrosine kinase	3.194619661	1.603903358	2.06E-26	1.95E-24
216551	Lgalsl	lectin, galactoside binding-like	2.118633133	3.211162247	3.64E-26	3.42E-24
217866	Cdc42bpb	CDC42 binding protein kinase beta	2.859568851	0.323233587	5.73E-26	5.35E-24
320802	Ifitm10	interferon induced transmembrane protein 10	2.627941244	4.055508664	8.26E-26	7.67E-24
15978	Ifng	interferon gamma	3.987690662	4.792950269	8.50E-26	7.85E-24
70784	Rasl12	RAS-like, family 12	3.190854576	1.424799764	3.31E-25	2.96E-23
100502942	Gm4814	predicted gene 4814	3.235422076	3.177425083	4.78E-25	4.23E-23
11853	Rhoc	ras homolog family member C	3.250503383	1.76861909	4.81E-25	4.23E-23
11811	Apobec2	apolipoprotein B mRNA editing enzyme, catalytic polypeptide 2	3.182555265	2.268221669	4.91E-25	4.30E-23
381290	Atp2b4	ATPase, Ca++ transporting, plasma membrane 4	2.187721242	6.067461153	5.97E-25	5.20E-23
243659	Styk1	serine/threonine/tyrosine kinase 1	5.395618493	2.783839088	8.54E-25	7.40E-23
56018	Stard10	START domain containing 10	2.312929619	3.428899069	8.70E-25	7.50E-23
98970	Fibcd1	fibrinogen C domain containing 1	3.773137577	1.96069003	1.11E-24	9.56E-23
329650	Med12l	mediator complex subunit 12-like	2.489439659	3.014531175	1.93E-24	1.63E-22
380686	Cnrip1	cannabinoid receptor interacting protein 1	2.727642262	2.682843835	2.40E-24	2.02E-22
18830	Pltp	phospholipid transfer protein	2.206059232	3.625930739	4.35E-24	3.64E-22
15007	H2-Q10	histocompatibility 2, Q region locus 10	2.606777357	4.039986313	7.28E-23	5.92E-21
106369	Ypel1	yippee-like 1 (Drosophila)	2.830689395	1.594277427	1.24E-22	1.00E-20
236285	Lancl3	LanC lantibiotic synthetase component C-like 3 (bacterial)	2.619836838	2.016521264	1.39E-22	1.12E-20
27355	Pald1	phosphatase domain containing, paladin 1	2.44193114	2.300668667	4.09E-22	3.19E-20
104759	Pld4	phospholipase D family, member 4	3.543349945	2.635011833	5.26E-22	4.08E-20
16636	Klra5	killer cell lectin-like receptor, subfamily A, member 5	4.765995554	2.122732795	6.31E-22	4.87E-20
20708	Serpinb6b	serine (or cysteine) peptidase inhibitor, clade B, member 6b	2.007989698	6.107810329	7.48E-22	5.72E-20
20198	S100a4	S100 calcium binding protein A4	2.520577978	3.859410132	8.48E-22	6.45E-20
13861	Epx	eosinophil peroxidase	2.988741145	-0.444580052	8.80E-22	6.67E-20
14561	Gdf11	growth differentiation factor 11	2.159907582	3.468191388	2.91E-21	2.16E-19
17952	Naip6	NLR family, apoptosis inhibitory protein 6	2.713075451	0.664413073	5.86E-21	4.33E-19
320407	Klri2	killer cell lectin-like receptor family I member 2	3.017848187	2.96190623	6.99E-21	5.11E-19
16332	Inppl1	inositol polyphosphate phosphatase-like 1	2.240836198	2.845080124	1.11E-20	8.14E-19
233038	Nccrp1	non-specific cytotoxic cell receptor protein 1 homolog (zebrafish)	2.59912876	0.379235717	1.13E-20	8.14E-19
12306	Anxa2	annexin A2	2.685979881	6.266729925	2.78E-20	1.96E-18
76574	Mfsd2a	major facilitator superfamily domain containing 2A	2.715881825	1.039758301	3.32E-20	2.31E-18
320398	Lrig3	leucine-rich repeats and immunoglobulin-like domains 3	2.953243247	1.111658677	5.32E-20	3.64E-18
76469	Cmya5	cardiomyopathy associated 5	2.210516025	2.517105751	6.00E-20	4.09E-18
214359	Tmem51	transmembrane protein 51	2.836514234	1.29844724	1.07E-19	7.16E-18
192120	Bspry	B-box and SPRY domain containing	2.735824138	1.479992492	1.94E-19	1.28E-17
14064	F2rl2	coagulation factor II (thrombin) receptor-like 2	2.225180109	3.255401395	2.12E-19	1.40E-17
27423	Klra15	killer cell lectin-like receptor, subfamily A, member 15	6.609548416	5.200565433	5.51E-19	3.60E-17
14314	Fstl1	follistatin-like 1	2.89599064	0.050864644	8.13E-19	5.27E-17
13052	Cxadr	coxsackie virus and adenovirus receptor	2.926447729	1.054552638	1.05E-18	6.76E-17
74050	4921525O09Rik	RIKEN cDNA 4921525O09 gene	2.120100569	4.174770303	1.32E-18	8.42E-17
53880	Naip7	NLR family, apoptosis inhibitory protein 7	2.522691444	0.192270595	1.64E-18	1.04E-16
93969	Klra22	killer cell lectin-like receptor subfamily A, member 22	6.104829292	4.720394538	4.36E-18	2.68E-16
12981	Csf2	colony stimulating factor 2 (granulocyte-macrophage)	2.761769138	0.906850821	4.81E-18	2.94E-16
227327	B3gnt7	UDP-GlcNAc:betaGal beta-1,3-N-acetylglucosaminyltransferase 7	2.694384971	0.651183157	9.03E-18	5.41E-16
20856	Stc2	stanniocalcin 2	3.235290818	0.917458024	5.47E-17	3.11E-15
18799	Plcd1	phospholipase C, delta 1	2.289219248	0.159255599	6.24E-17	3.54E-15
209378	Itih5	inter-alpha (globulin) inhibitor H5	2.545348053	4.03522086	7.67E-17	4.31E-15
14727	Lilr4b	leukocyte immunoglobulin-like receptor, subfamily B, member 4B	2.721100668	2.397935488	9.70E-17	5.39E-15
52150	Kcnk6	potassium inwardly-rectifying channel, subfamily K, member 6	2.353613367	2.525340431	1.46E-16	8.07E-15
100340	Smpdl3b	sphingomyelin phosphodiesterase, acid-like 3B	2.425825679	3.217067312	1.62E-16	8.97E-15
231821	Adap1	ArfGAP with dual PH domains 1	2.526940631	2.57013392	1.63E-16	8.99E-15
93970	Klra18	killer cell lectin-like receptor, subfamily A, member 18	7.004320724	6.163992459	1.85E-16	1.01E-14
14465	Gata6	GATA binding protein 6	2.718613567	-0.38680703	2.77E-16	1.50E-14
16635	Klra4	killer cell lectin-like receptor, subfamily A, member 4	6.861580643	5.901332438	2.90E-16	1.57E-14
15900	Irf8	interferon regulatory factor 8	2.074202735	4.3000673	4.41E-16	2.34E-14
654450	NA	NA	6.790541978	5.800631874	6.10E-16	3.22E-14
238393	Serpina3f	serine (or cysteine) peptidase inhibitor, clade A, member 3F	2.497073239	1.162302947	6.73E-16	3.53E-14
223254	Farp1	FERM, RhoGEF (Arhgef) and pleckstrin domain protein 1 (chondrocyte-derived)	2.031201823	2.336044996	1.24E-15	6.43E-14
29857	Mapk12	mitogen-activated protein kinase 12	2.249177635	0.606279591	1.34E-15	6.89E-14
12398	Cbfa2t3	core-binding factor, runt domain, alpha subunit 2, translocated to, 3 (human)	2.690623758	0.454695647	1.97E-15	1.01E-13
56857	Slc37a2	solute carrier family 37 (glycerol-3-phosphate transporter), member 2	2.179628764	3.957221866	3.38E-15	1.71E-13
102871	D330045A20Rik	RIKEN cDNA D330045A20 gene	2.369914843	-0.635199716	4.49E-15	2.22E-13
16627	Klra1	killer cell lectin-like receptor, subfamily A, member 1	5.836380243	5.647000642	1.31E-14	6.32E-13
21873	Tjp2	tight junction protein 2	2.566122078	2.630123942	1.39E-14	6.67E-13
59056	Evc	Ellis van Creveld syndrome	2.523974485	-0.329640917	1.86E-14	8.87E-13
68428	Steap3	STEAP family member 3	2.356239585	2.840328373	2.77E-14	1.29E-12
64540	Tspan4	tetraspanin 4	2.32050499	2.76311836	2.97E-14	1.38E-12
20893	Bhlhe40	basic helix-loop-helix family, member e40	2.286373832	4.7833539	3.24E-14	1.50E-12
72097	2010300C02Rik	RIKEN cDNA 2010300C02 gene	2.020150851	2.662223951	7.64E-14	3.45E-12
17059	Klrb1c	killer cell lectin-like receptor subfamily B member 1C	3.014921933	4.838119384	9.54E-14	4.30E-12
244694	Kdm4d	lysine (K)-specific demethylase 4D	2.148139481	0.770171213	1.05E-13	4.71E-12
68070	Pdzd2	PDZ domain containing 2	2.471796201	-0.119874746	1.52E-13	6.79E-12
12777	Ccr10	chemokine (C-C motif) receptor 10	2.084843738	-1.155622404	3.13E-13	1.36E-11
12162	Bmp7	bone morphogenetic protein 7	2.515280874	0.614602441	3.26E-13	1.41E-11
14728	Lilrb4a	leukocyte immunoglobulin-like receptor, subfamily B, member 4A	2.281180883	2.640725106	5.64E-13	2.39E-11
75906	Fam184a	family with sequence similarity 184, member A	3.318802121	0.45261117	1.97E-12	8.06E-11
19663	Rbpms	RNA binding protein gene with multiple splicing	3.15024523	0.979131611	2.49E-12	1.01E-10

56461	Kcnip3	Kv channel interacting protein 3, calsenilin	2.176159988	1.942515036	3.15E-12	1.26E-10
12348	Car11	carbonic anhydrase 11	2.166656546	1.374134222	4.96E-12	1.95E-10
16398	Itga2	integrin alpha 2	2.338179091	2.594421998	7.51E-12	2.86E-10
330958	A730043L09Rik	RIKEN cDNA A730043L09 gene	2.315168559	-0.184893678	8.28E-12	3.12E-10
18719	Pip5k1b	phosphatidylinositol-4-phosphate 5-kinase, type 1 beta	2.269441538	1.9158842	1.72E-11	6.28E-10
13511	Dsg2	desmoglein 2	2.521783292	-0.26534081	3.53E-11	1.26E-09
14938	Gzma	granzyme A	2.515222602	5.731727912	1.37E-10	4.70E-09
70788	Klhl30	kelch-like 30	2.465629397	0.016859754	1.47E-10	5.03E-09
107889	Gcm2	glial cells missing homolog 2 (Drosophila)	2.033806282	-0.966307196	2.64E-10	8.75E-09
66184	Rps4l	ribosomal protein S4-like	2.07505066	-0.245694637	2.72E-10	9.00E-09
52480	Snhg14	small nucleolar RNA host gene 14	2.072697875	0.851443902	2.51E-09	7.27E-08
71602	Myo1e	myosin IE	2.061657057	1.772877515	2.84E-09	8.16E-08
18768	Pkib	protein kinase inhibitor beta, cAMP dependent, testis specific	2.652985859	0.642307276	6.63E-09	1.83E-07
14127	Fcer1g	Fc receptor, IgE, high affinity I, gamma polypeptide	2.74986366	3.389069101	1.28E-08	3.43E-07
17756	Map2	microtubule-associated protein 2	2.069310644	2.015695423	3.14E-08	8.05E-07
327957	Scimp	SLP adaptor and CSK interacting membrane protein	2.333132289	0.5496167	4.26E-08	1.07E-06
240672	Dusp5	dual specificity phosphatase 5	2.295709109	3.905207413	8.02E-08	1.94E-06
17096	Lyn	LYN proto-oncogene, Src family tyrosine kinase	2.429641272	2.792000449	1.14E-07	2.69E-06
12919	Crhbp	corticotropin releasing hormone binding protein	2.656732191	0.429781237	1.69E-06	3.45E-05

Table EV5

EntrezID	Symbol	GeneName	log2 expression TrueMemory/ VirtualMemory	log2A	P.Value	adj.P.Val
75617	Rps25	ribosomal protein S25	-3.83826292	6.047787	1.57E-92	2.95E-89
22186	Uba52	ubiquitin A-52 residue ribosomal protein fusion product 1	-4.269284505	4.096962	3.52E-84	5.40E-81
19921	Rpl19	ribosomal protein L19	-3.510922923	5.483165	3.59E-71	4.66E-68
69539	Trnp1	TMF1-regulated nuclear protein 1	-3.755603264	4.455358	2.01E-44	1.03E-41
74055	Plce1	phospholipase C, epsilon 1	-3.833164129	2.497437	1.82E-43	8.81E-41
77579	Myh10	myosin, heavy polypeptide 10, non-muscle	-4.051095919	3.461683	1.58E-38	6.36E-36
53321	Cntnap1	contactin associated protein-like 1	-3.503825331	1.758975	5.85E-34	1.87E-31
11931	Atp1b1	ATPase, Na+/K+ transporting, beta 1 polypeptide	-2.626360015	7.54306	4.44E-31	1.15E-28
381738	Drc1	dynein regulatory complex subunit 1	-2.718619792	3.854919	2.48E-30	5.67E-28
272322	Arntl2	aryl hydrocarbon receptor nuclear translocator-like 2	-3.209411511	0.755977	8.51E-30	1.84E-27
244234	5830411N06Rik	RIKEN cDNA 5830411N06 gene	-3.60040232	6.782278	1.40E-26	2.63E-24
74050	4921525O09Rik	RIKEN cDNA 4921525O09 gene	-2.836531327	4.17477	4.95E-25	8.28E-23
231510	Agpat9	1-acylglycerol-3-phosphate O-acyltransferase 9	-5.18463465	4.184592	1.83E-23	2.57E-21
16431	Itm2a	integral membrane protein 2A	-2.511187682	7.670105	1.27E-20	1.23E-18
244233	Cd163l1	CD163 molecule-like 1	-3.85659019	6.451426	2.17E-19	1.86E-17
170770	Bbc3	BCL2 binding component 3	-2.424385351	5.370029	9.95E-19	7.97E-17
83993	Tbx19	T-box 19	-2.32018112	-0.38254	3.88E-17	2.45E-15
54403	Slc4a4	solute carrier family 4 (anion exchanger), member 4	-3.124675546	1.025047	2.45E-16	1.34E-14
98970	Fibcd1	fibrinogen C domain containing 1	-3.216211263	1.96069	4.26E-16	2.22E-14
12945	Dmbt1	deleted in malignant brain tumors 1	-2.651652109	1.74311	1.15E-15	5.80E-14
102502	Pls1	plastin 1 (I-isoform)	-3.941453245	3.319311	1.70E-15	8.35E-14
238405	Adam6b	a disintegrin and metallopeptidase domain 6B	-2.452324235	2.922671	1.93E-15	9.38E-14
56874	Rnf32	ring finger protein 32	-2.050738351	2.305162	2.51E-15	1.19E-13
100043314	Tigit	T cell immunoreceptor with Ig and ITIM domains	-2.521583287	4.143358	3.22E-15	1.51E-13
213402	Armc2	armadillo repeat containing 2	-2.802088747	1.696886	3.21E-14	1.37E-12
77057	Ston1	stonin 1	-2.138268753	0.569512	6.55E-14	2.68E-12
17996	Neb	nebulin	-2.227739172	3.86386	2.10E-13	8.17E-12
67198	Spats2l	spermatogenesis associated, serine-rich 2-like	-2.035954084	0.744552	4.02E-13	1.51E-11
71228	Dlg5	discs, large homolog 5 (Drosophila)	-2.355360327	3.327852	6.19E-13	2.27E-11
16628	Klra10	killer cell lectin-like receptor subfamily A, member 10	-2.395448771	4.040297	6.82E-12	2.20E-10
13861	Epx	eosinophil peroxidase	-2.304552382	-0.44458	1.49E-11	4.61E-10
16785	Rpsa	ribosomal protein SA	-2.209236976	6.116528	1.54E-11	4.74E-10
68428	Steap3	STEAP family member 3	-2.183442207	2.840328	9.63E-11	2.68E-09
70809	Clec2g	C-type lectin domain family 2, member g	-2.567802325	0.539402	1.17E-10	3.18E-09
320974	Lrrn4	leucine rich repeat neuronal 4	-2.227722805	0.74763	1.26E-10	3.44E-09
751556	Mir682	microRNA 682	-3.087834706	3.946063	7.77E-10	1.92E-08
330958	A730043L09Rik	RIKEN cDNA A730043L09 gene	-2.126027312	-0.18489	1.74E-09	4.13E-08
77383	C030029H02Rik	RIKEN cDNA C030029H02 gene	-3.038362091	1.423349	4.12E-09	9.23E-08
12919	Crhbp	corticotropin releasing hormone binding protein	-3.340837161	0.429781	7.03E-09	1.52E-07
17756	Map2	microtubule-associated protein 2	-2.212085297	2.015695	6.99E-08	1.29E-06
16630	Klra12	killer cell lectin-like receptor subfamily A, member 12	-2.292623408	8.02855	3.51E-07	5.83E-06
79410	Klra23	killer cell lectin-like receptor subfamily A, member 23	-2.171070475	8.311758	1.25E-05	0.000153
14924	Magi1	membrane associated guanylate kinase, WW and PDZ domain containing 1	-2.354933409	0.247941	1.78E-05	0.000209
16627	Klra1	killer cell lectin-like receptor, subfamily A, member 1	-3.265781887	5.647001	1.87E-05	0.000219
16631	Klra13-ps	killer cell lectin-like receptor subfamily A, member 13, pseudogene	-2.171203734	8.262554	2.58E-05	0.000292
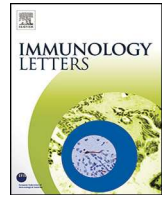
Invited Review

Opinion: Virtual memory CD8 T cells and lymphopenia-induced memory CD8 T cells represent a single subset: Homeostatic memory T cells

Michaela Pribikova, Alena Moudra, Ondrej Stepanek*

Laboratory of Adaptive Immunity, Institute of Molecular Genetics of the Czech Academy of Sciences, Prague, Czech Republic

ABSTRACT

It is well established that lymphopenia induces the formation of the memory-phenotype T cells without the exposure to foreign antigens. More recently, the memory-phenotype antigen-inexperienced memory T cells were described in lymphoreplete mice and called virtual memory T cells. In this review, we compare multiple aspects of the biology of lymphopenia-induced memory T cells and virtual memory T cells, including cytokine requirements, the role of T-cell receptor specificity in the differentiation process, gene expression signature, and the immune response. Based on this comparison, we conclude that lymphopenia-induced memory T cells and virtual memory T cells most likely represent a single T-cell subset, for which we propose a term 'homeostatic memory T cells'.

1. Introduction

T cells play a major role in adaptive immune responses. Conventional αβT cells use their T-cell antigen receptor (TCR) to recognize antigens, i.e., peptides derived from proteins of invading pathogens that are presented by antigen presenting cells. The hallmark of the immune protection by T cells is the clonal heterogeneity. Each T-cell clone expresses a unique TCR and recognizes a different set of antigens. Activation of the TCR induces rapid proliferation and differentiation into short-lived effector T cells and memory T cells which facilitate long-term protection against the identical pathogen. Memory T cells can be distinguished from naïve T cells using specific surface markers such as CD44, which is expressed in memory, but not in naïve mouse T cells.

However, the T-cell compartment contains memory-phenotype T cells that have not encountered their foreign cognate antigen previously (reviewed in [1]). Although these antigen-inexperienced memory T cells (AIMT) were reported in both CD8+ and CD4+ compartments [2,3], we are focusing exclusively on the CD8+ subset in this review. The classification of CD8+ AIMT cells has not been unified, yet. However, we divide them into three major subsets for the purpose of this review article. These are lymphopenia-induced memory (LIM) T cells [4,5], peripherally induced virtual memory (VM) T cells [6], and innate memory T cells that are generated in the thymus [7,8] (Fig. 1). The aim of this review is to compare LIM T cells with VM T cells and to conclude

whether or not these two populations represent a single T-cell subset.

2. Nomenclature of antigen-inexperienced memory-like T cells

The nomenclature of antigen-inexperienced memory-like T cells is not fully established yet and the understanding of some terms slightly varies among different studies. Some nomenclature issues arose even during the peer-review of this article. For that reason, we are including a chapter that aims to clarify the usage of terms 'innate memory', 'virtual memory', and 'HP memory'.

In line with some previous studies [1,9,10], we use the term 'innate memory T cells' for the memory-phenotype T cells that are formed in the thymus. These T cells were described in Balb/c mice and in some genetically modified C57Bl/6 mouse strains [11–13]. In the early studies, these cells were called 'innate CD8+ T cells' [11,14]. Later, these two terms were used interchangeably [15]. Some authors use the term 'innate memory T cells' in a broader sense that covers all AIMT cells [16–18].

Some authors [1,6,19] and we use the term 'virtual memory T cells' for the memory-phenotype T cells formed at the periphery without encountering a foreign antigen. However, some authors use this term for antigen-inexperienced memory T cells which are specific for a given model antigen, irrespective of their thymic or peripheral origin [19,20].

'HP memory' T cells stand for 'homeostatic proliferation memory' T cells. This term was used to describe memory-like T cells induced by

* Corresponding author at: Laboratory of Adaptive Immunity, Institute of Molecular Genetics of the Czech Academy of Sciences, Videnska 1083, 14220, Prague, Czech Republic.
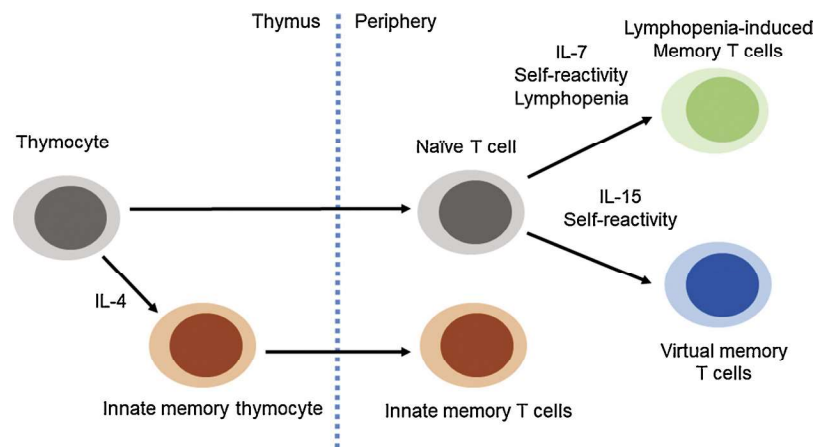 *E-mail address:* ondrej.stepanek@img.cas.cz (O. Stepanek).

Fig. 1. Origin of antigen-inexperienced memory T cells.
Formation of innate memory, virtual memory, and lymphopenia-induced memory CD8$^+$ T cells.

lymphopenia [21–24]. Thus, we understand the term 'HP memory T cells' as a synonym for LIM T cells.

3. AIMT cells and innate-like lymphocytes

Thymic derived AIMT cell are called 'innate memory T cells' [1] and some authors even use the term 'innate memory T cells' for all AIMT cells [17,18] to emphasize that the formation of AIMT cells is not an adaptive response to a foreign antigen. However, the AIMT cells are predominantly formed from conventional αβTCR T cells, which distinguishes them from the TCR-deficient innate lymphoid cells and γδT cells. Unlike, invariant or semi-invariant T cells like MAIT cells or iNKT cells, CD8$^+$ LIM and VM T cells are restricted to canonical MHCI molecules [19,25–27]. The antigenic specificity of thymic innate memory T cells is less understood, but a recent study identified AIMT cells specific for an LCMV antigen presented by a conventional MHCI molecule in Balb/c mice. Because the AIMT population in Balb/c mice is formed predominantly by innate memory T cells, it seems that innate memory T cells are, or at least overlap with, conventional αβT cells.

4. Definition of LIM and VM T cells

Experimentally-induced lymphopenia drives homeostatic proliferation of CD8$^+$ T cells and their conversion into memory-phenotype T cells in mice [4,5,28]. LIM T cells resemble true antigen-experienced memory (TM) T cells by the expression of the typical memory markers [4,5], by rapid production of IFNγ upon antigenic stimulation [5], and by a similar gene expression profile [27]. Interestingly, the homeostatic proliferation and memory phenotype seem to be tightly linked as only T cells that underwent a few division cycles acquire the memory phenotype [28]. Although this phenomenon has been studied for almost two decades, the physiological importance of LIM T cells is unclear, because the experimental setup for their generation usually involves an adoptive transfer of T cells into irradiated hosts or hosts with genetically compromised T-cell development (e.g. Rag-deficient strains).

VM T cells are memory-like T cells that occur in healthy non-manipulated lymphoreplete mice [6]. VM T cells might be specific to foreign antigens, although they have not been exposed to these antigens previously [6,25]. Although the term "virtual memory" was originally developed to define only cells with known antigenic specificity [6,25,29], we prefer extending this term to cover a subset of phenotypically and functionally identical T cells induced by strong homeostatic signals from self-antigens, irrespective of their known or unknown TCR specificity to foreign antigens [19] (Table 1).

It has been suggested that VM T cells are generated during natural neonatal period of lymphopenia [30,31]. However, VM T cells can be generated from naïve T cells even in adult lymphoreplete mice [32]. Similarities between VM T cells and LIM T cells were noticed already in the seminal study describing VM T cells for the first time [6]. Because a substantial amount of data concerning AIMTs has accumulated in recent years, we aim to analyze the current evidence to elucidate whether LIM and VM T cells represent the identical subset. In the following chapters, we are going to review multiple aspects of LIM and VM T cells in a comparative manner.

5. Role of cytokines and dendritic cells in the formation of LIM and VM T cells

Both LIM and VM T cells are generated from naïve T cells at the immunological peripheral organs. One of the main factors for their generation and/or maintenance are specific cytokines. The presence of AIMT cells depends largely on IL-15 and partially on IL-4 in lymphoreplete C57Bl/6 mice [9,31]. In Balb/c mice, IL-4 is more important than IL-15 [33,34]. This discrepancy most likely reflects the fact that the AIMT population consists mostly of peripherally-induced VM T cells in C57Bl/6 mice, whereas Balb/c mice predominantly contain a thymic-derived innate memory subset [35]. Thus, it seems that IL-15 is the major cytokine involved in the formation and/or survival of peripherally-induced VM T cells, while IL-4 supports the formation and/or survival of innate memory T cells.

It has been shown that IL-7, but not IL-15 or IL-4, is essential for the homeostatic proliferation of naïve CD8$^+$ T cells in lymphopenic mice [36,37]. Accordingly, IL-7, but not IL-15, is required for the generation of the memory-phenotype T cells from naïve CD8$^+$ T cells adoptively transferred into a newborn (naturally lymphopenic) host [30].

Homeostatic proliferation of naïve and TM CD8$^+$ T cells is partially impaired in lymphopenic hosts depleted for CD11c^{high} dendritic cells [38]. Albeit not addressed by the authors [38], the tight connection between homeostatic proliferation and LIM formation [28] suggests that CD11c^{high} dendritic cells might be essential for the formation of LIM T cells. CD8$^+$ VM T-cell population is significantly reduced in Batf3$^{-/-}$ mice that lack CD8α$^+$ DCs, which might be the main cell type that presents IL-15 [9].

Although LIM T cells depend mostly on IL-7, whereas VM T cells require IL-15, this apparent discrepancy does not necessarily mean that these two cell types represent distinct T-cell subsets. It is possible that the distinct requirements for particular cytokines reflect the different environments in which these memory-phenotype cells arise. While IL-7 might be crucial for the homeostatic expansion required for LIM T cell generation, IL-15 might be more important for the expansion and/or maintenance of VM T cells generated in lymphoreplete mice, where the IL-7 availability is limited.

Table 1

Summary of LIM, VM, and TM T cells. Characteristics of mouse LIM T cells, VM T cells, and antigen-experienced central memory T cells based on references [9,18,19,32,36,64].

	LIM T cells	VM T cells	Ag-experienced CM T cells
Gene expression profile	CD44$^+$, CD122^{++}, CD49d^{low}, Drc1/Ccdc164$^+$, NKG2D/Klrk1$^-$	CD44$^+$, CD122^{++}, CD49d^{low}, Drc1/Ccdc164$^+$, NKG2D/Klrk1$^-$	CD44$^+$, CD122$^+$, CD49d$^+$, T-bet$^+$, Eomes$^+$, Drc1/Ccdc164$^-$, NKG2D/Klrk1$^+$
Key cytokines for formation	IL-7	IL-15	IL-7, IL-15 and others
Role of TCR	Formed from highly self-reactive clones	Formed from highly self-reactive clones	Induced by cognate foreign antigens
Immune response	Rapid IFNγ production, robust protection against infection (Listeria)	Rapid IFNγ production, robust protection against infection (Listeria)	Rapid IFNγ production, robust protection against infection (Listeria, virus)
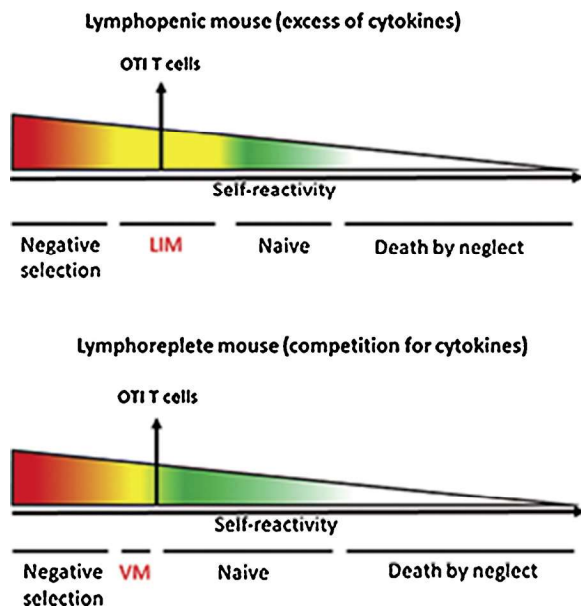
Fig. 2. TCR repertoires in LIM and VM T cells.
Schematic representation of different T-cell fates based on their self-reactivity in lymphopenic and lymphoreplete conditions. In lymphoreplete mice, only peripheral CD8$^+$ T cells with relatively high self-reactivity (but below the threshold for negative selection) can differentiate into virtual memory T cells. Availability of cytokines (e.g., IL-7, IL-15) under lymphopenia enables generation of LIM T cell from CD8$^+$ T-cell clones with moderate self-reactivity.

Receptors for IL-7 and for IL-15 both use the common γ-chain to trigger similar intracellular signaling pathways [39–42]. Although some differences between the signaling pathways triggered by IL-7 and IL-15 do exist [39–42], both cytokines might provide a similar differentiation signals to T cells. Likewise, although some gain-of-function studies (addition of the cytokine) or loss-of-function studies (deficiency of the receptor or cytokine) showed differential effects of IL-7 and IL-15 signals [41–43], these differences could be explained by differential levels of expression of these two receptors and/or differences in the availability of the cytokines, not necessarily by qualitative differences between IL-7 and IL-15-mediated signals [42]. Thus, it is unclear whether or not the induction of LIM T cells by IL-7 and the induction/ maintenance of VM T cells by IL-15 might trigger unique differentiation programs in these subsets.

6. Role of TCR

Homeostatic signals from self-antigens (self-pMHCI) to T-cell receptors are required for the homeostatic proliferation of naïve CD8$^+$ T cells and subsequent generation of CD8$^+$ LIM T cells [44,45]. Particular T-cell clones in a polyclonal population differ in their level of self-reactivity. Although the self-reactivity (i.e., response to self-antigens) of a single T cell cannot be measured directly, levels of CD5 serve as a

commonly used proxy for T-cell self-reactivity [46]. Based on the CD5 levels, it has been shown that T-cell clones with a relatively high level of self-reactivity undergo a significantly more robust homeostatic expansion and LIM formation than T-cell clones with a lower self-reactivity [47,48].

Pilot studies suggested that the TCR specificity plays a role in the formation of VM T cells. In a TCR transgenic OT-I Rag$^+$ population, VM T cells were more efficiently formed from clones using endogenous TCRα than from those using only the transgenic OT-I receptor during aging [49]. One possible explanation of this observation is that the dominant OT-I T cells compete with each other for the homeostatic signals from a limited set of self-antigens, whereas the relatively rare clones with endogenous TCRα have unlimited access to self-antigens they recognize. Recently, it has been shown that CD5^{high} naïve T cells more frequently differentiate into VM T cells upon an adoptive transfer to lymphoreplete hosts than CD5^{low} T cells (ca. 30% vs. 5–10%) [32], suggesting a link between the strength of the homeostatic TCR signals from self-antigens and the VM formation. We have recently elucidated this question on a level of particular T-cell clones. Only highly self-reactive T-cell clones can differentiate into VM T cells, whereas less self-reactive T cells preserve their naïve phenotype [19].

Overall, the intensity of homeostatic TCR signals triggered by self-antigens is the key factor in the induction of the LIM and VM T cells. However, stronger homeostatic TCR signals are required for the generation of VM than for the generation of LIM memory T cells. Some T cell clones, including widely used OT-I T cells are very potent in the formation of LIM T cells [5,28], but they differentiate into VM memory T cells with a relatively low frequency [19]. Most likely, the availability of IL-7 and other cytokines during lymphopenia lowers the TCR signaling threshold for the acquisition of the memory phenotype. Indeed, it has been shown that excess IL-15 delivered via IL-15 complexes generates VM memory from clones with lower CD5 levels in the lymphoreplete mice [32]. Overall, these data imply the importance of homeostatic TCR interactions with self-antigens in the formation of LIM and VM T cells. However, the TCR repertoires of polyclonal LIM and VM T cells might differ because of different cytokine availability and requirements for homeostatic TCR signals (Fig. 2).

7. Gene expression profile

Both LIM and VM T cells express markers typical for TM T cells, including CD44, Ly6c, CD122, and CD62 L [5,6,26]. Unfortunately, a direct comparison of gene expression profiles of VM T cells and LIM T cells has not been performed, yet.

The global transcriptome profile of LIM T cells is very similar to the profile of TM T cells and the analysis did not identify any specific set of genes expressed or downregulated in LIM memory T cells in comparison to other T-cell subsets [27]. They found only a single gene specifically upregulated in LIM T cells in comparison to naïve, memory, and effector T cells, Drc1 (alias Ccdc164) [27]. Interestingly, our gene expression data revealed that VM T cells upregulate Drc1/Ccdc164 when compared to naïve and TM T cells, making this gene the only known candidate marker of LIM and VM T cells (Fig. 3) [19]. However, the
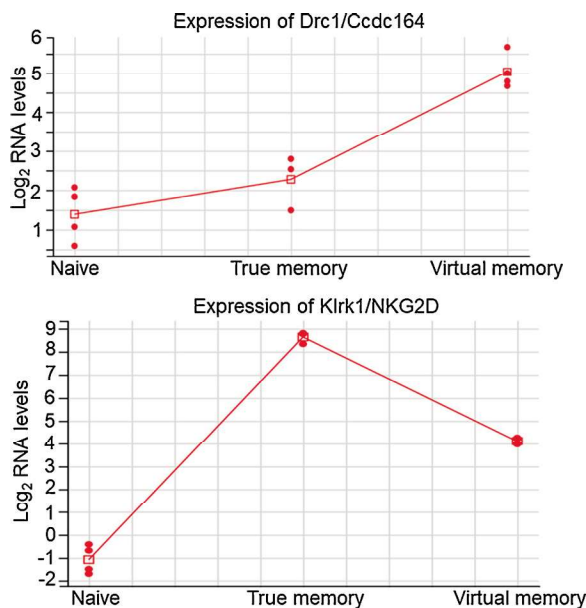
Fig. 3. Novel markers for antigen-inexperienced memory T cells.
Expression levels of Drc1/Ccdc164 and NKG2D/Klrk1 in naïve, TM, and VM T cells analyzed by deep RNA sequencing [19].

evidence on the protein level is required to establish Drc1/Ccdc164 as a marker expressed uniquely in LIM and VM T cells.

Although LIM T cells do not seem to have a large set of specifically downregulated and upregulated genes, they still show differences when compared to naïve or TM T cells separately. The most prominent example is low expression of CD49d (integrin α4, part of VLA4) in LIM T cells [26]. VM T cells also exhibit low levels of surface CD49d [6,9]. A recent publication showed that NKG2D (alias Killer cell lectin-like receptor; Klrk1) discriminated VM T cells (NKG2D⁻) from TM T cells (NKG2D⁺) [18]. Our data also revealed a significantly lower expression of NKG2D/Klrk1 in VM T cells than in TM T cells (Fig. 3) [19]. Accordingly, the earlier study focusing on LIM T cells did not identify an upregulation of NKG2D upon the transition from naïve to LIM T cells [27].

Overall, LIM and VM T cells exhibit similar expression pattern of three genes (Drc1, CD49d, and NKG2D/Klrk1), which can be used to distinguish LIM/VM T cells from TM T cells.

LIM T cells and TM T cells show differential expression of some chemokines and chemokine receptors during infection [26]. Whereas activated LIM T cells expressed relatively high levels of Ccr7, Cxcr4, Cxcr7, Cxcr3, and Cxcr5, activated TM T cells expressed higher levels of Ccr9, Ltb4r2, Cxc3cr1, Ccr1, and Ccr8. Accordingly, our transcriptomic analysis of resting T cells showed that VM T cells express higher levels of Cxcr4 and Cxcr5, but lower levels of Ccr9, Cx3cr1, and Ccr1 than TM T cells [19]. Although it is difficult to compare gene expression data from activated [26] and resting T cells [19], these data indicate that LIM and VM memory T cells might have similar profiles of chemokine receptors.

Although a direct comparison of the gene expression profiles of LIM and VM T cells has not been carried out, the available data suggest that the gene expression signatures of LIM and VM T cells are similar, if not identical.

8. Immune response

Both LIM and VM CD8⁺ T cells rapidly produce IFNγ after TCR stimulation in vitro [5,19,25,45]. VM T cells produce IFNγ after stimulation with IL-12/IL-18 cytokines in vitro [6], but this feature has not been addressed in LIM T cells. In vivo, LIM and VM T cells are more efficient than naïve T cells with the same specificity in protecting against pathogenic bacteria *Listeria monocytogenes* [23,25,26]. In addition, LIM T cells induce an efficient immune response to implanted tumors in an antigen-dependent manner [4], which has not been addressed in VM T cells yet.

Both LIM and VM T cells exhibit the features of memory T cells including rapid IFNγ production and protection from *Listeria* infection.

9. The function of LIM and VM T cells

The physiological function of LIM and VM T cells is largely unclear. VM T cells show efficient clearance of *Listeria* infection on a per cell basis [25] and were proposed to be involved in the bystander immune protection [32]. Thus, the role of VM T cells might contribute to the competence of the immune system to clear pathogens. It is unclear, if the LIM formation is beneficial for the lymphopenic host. As lymphopenia in the adulthood is not a physiological condition, it is possible that LIM formation is not an evolutionary adaption, but only a coincidental consequence of the altered environment.

10. LIM and VM T cells in humans

Human naïve CD8⁺ T cells expand and acquire memory phenotype in lymphopenic humanized mice [50], suggesting that AIMT cells exist in humans.

Recently, a population of human T cells that exhibited features similar to murine VM CD8⁺ T cells has been described [32,51]. This population expresses NK-receptors KIRs and/or NKG2A, high levels of Eomes, T-bet, and CD122 and rapidly produce of IFNγ after stimulation with IL-12/IL-18 or PMA/ionomycine [32,51]. These cells are present in human cord blood, albeit at a relatively low frequency [32,51]. Based on these features, White et al. proposed that these cells might be human virtual memory T cells [32]. The putative human VM cells accumulate during aging, which is similar to murine VM cells [32,52]. However, unlike murine VM T cells, these putative human VM cells express low levels of CD5. More importantly, these cells are negative for CD27 and CCR7 and positive for CD57 and CD45RA [32,51], suggesting that these cells are terminally differentiated cells rather than central memory-phenotype T cells [53,54]. Although these discrepancies indicate that these human and mouse T-cell populations might not correspond to each other, it is still possible that there are interspecies differences in the expression of particular surface markers.

It has not been addressed whether these putative human VM T cells overlap with nonconventional innate-like lymphocyte subsets. Because the majority of CD8⁺ human blood T cell producing IFNγ upon stimulation with IL-12/IL-18 are mucosal-associated invariant T (MAIT) cells, it is a question whether the putative human VM T cells are related to MAIT cells [55]. Although both the putative human VM T cells and CD8⁺ MAIT cells showed the homing preference to the liver [56], MAIT cells differ from the putative human VM T cells by being CD27⁺CD45RO⁺ [57]. Moreover, MAIT cells decrease with age [58,59] whereas the putative VM T cells were reported to increase with age [1]. CD161 is a marker of MAIT cells, but is also expressed on some polyclonal CD8⁺ T cells (i.e., negative for the semi-invariant Vα7.2 TCR) that produce IFNγ upon stimulation with IL-12/IL18 [60]. It would be interesting to address whether these CD161⁺ CD8⁺ Vα7.2⁻ T cells are related to the putative VM T cells.

Moreover, it is very difficult to address experimentally whether any human population of memory- or effector-phenotype cells was induced by foreign antigens. Thus, we cannot exclude that some putative human VM T cells in adult humans were derived from naïve T cells specific for pathogens or vaccines. For instance, chronic CMV infection induces a population of CD45RA⁺CD27⁻CD8⁺ T cells expressing some NK receptors [61,62]. Thus, these cells resemble the putative VM T cells in some aspects. A possible experimental approach for the identification of human VM T cells should include a single-cell transcriptomic profiling coupled with the analysis of the TCR usage and analysis of the antigenic

specificity.

11. Conclusion

Based on our current knowledge of these two populations, we can conclude that peripherally induced VM T cells and LIM T cells most likely represent the identical cell type. They exhibit similar gene expression patterns and responses to antigens. Moreover, they are both induced by homeostatic TCR signals triggered by self-antigens and by common γ-chain cytokines. It seems that VM T cells are formed from relatively highly self-reactive T cells in lymphoreplete mice, whereas LIM T-cell generation is a more robust process induced by IL-7 mediated expansion and LIM conversion during lymphopenia. Overall, LIM T cells could be generated from relatively less self-reactive T cells than VM T cells. This probably leads to distinct TCR repertoires of VM T cells in lymphoreplete mice and LIM T cells in animals with experimentally induced lymphopenia. We cannot exclude the possibility that the dependence on different γ-chain cytokines primes substantial differences between LIM and VM T cells, but we could not find any direct evidence for this possibility in the literature. In accordance with the old scientific principle of Occam's razor, we have a preference to adopt the less complex model out of 2 or more possible scenarios, until it is disproved by possible new evidence. The simplest scenario here is to consider LIM and VM T cells as a single subset.

We believe that this study will contribute to the streamlining of the nomenclature of T-cell subsets which is required for the general understanding of the T-cell diversity. We propose that LIM and VM T cells should adopt a common name that will cover this cell type independently of their route of origin (lymphopenia vs. lymphoreplete homeostasis) and will distinguish them from other cell types (e.g., innate memory, antigen-experienced memory). Because the term 'HP memory' has often been used interchangeably with LIM (see above), we propose that the umbrella term for LIM and VM cells can be 'homeostatic memory T cells'. The term 'homeostatic memory T cells' has been used previously to describe LIM T cells [63], but has not been defined in the connection with lymphopenia as tightly as 'HP memory T cells'.

Conflict of interest statement

All the authors have no conflict of interest.

Acknowledgements

References

[1] J.T. White, et al., Nat. Rev. Immunol. 17 (2017) 391–400.
[2] A.I. Marusina, et al., J. Autoimmun. 77 (2017) 76–88.
[3] T. Kawabe, et al., Sci. Immunol. (2017) 2.
[4] B.K. Cho, et al., J. Exp. Med. 192 (2000) 549–556.
[5] A.W. Goldrath, et al., J. Exp. Med. 192 (2000) 557–564.
[6] C. Haluszczak, et al., J. Exp. Med. 206 (2009) 435–448.
[7] L.O. Atherly, et al., Immunity 25 (2006) 79–91.
[8] C. Broussard, et al., Immunity 25 (2006) 93–104.
[9] T. Sosinowski, et al., J. Immunol. 190 (2013) 1936–1947.
[10] V. Martinet, et al., Nat. Commun. (2015) 6.
[11] M.A. Weinreich, et al., Nat. Immunol. 11 (2010) 709–U75.
[12] L. O Atherly, et al., Immunity 25 (2006) 79–91.
[13] C. Broussard, et al., Immunity 25 (2006) 849.
[14] L.J. Berg, Nat. Rev. Immunol. 7 (2007) 479–485.
[15] Y.J. Lee, et al., Trends Immunol. 32 (2011) 50–56.
[16] L. Van Kaer, Eur. J. Immunol. 45 (2015) 1916–1920.
[17] S.C. Jameson, et al., Adv. Immunol. 126 (126) (2015) 173–213.
[18] M. Grau, et al., J. Immunol. (2018).
[19] A. Drobek, et al., EMBO J. (2018) e98518.
[20] P. Tripathi, et al., Eur. J. Immunol. (2016).
[21] S.E. Hamilton, S.C. Jameson, Proc. Natl. Acad. Sci. U. S. A. 105 (2008) 18484–18489.
[22] K.P. Cheung, et al., J. Immunol. (2009) 182.
[23] S.E. Hamilton, et al., Nat. Immunol. 7 (2006) 475–481.
[24] K.M. Knudson, et al., J. Immunol. 191 (2013) 5797–5801.
[25] J.Y. Lee, et al., Proc. Natl. Acad. Sci. U. S. A. 110 (2013) 13498–13503.
[26] K.P. Cheung, et al., J. Immunol. 183 (2009) 3364–3372.
[27] A.W. Goldrath, et al., Proc. Natl. Acad. Sci. U. S. A. 101 (2004) 16885–16890.
[28] T. Hogan, et al., J. Immunol. 190 (2013) 3985–3993.
[29] A.D. Akue, et al., J. Immunol. 188 (2012) 2516–2523.
[30] T. Schuler, et al., J. Immunol. 172 (2004) 15–19.
[31] A.D. Akue, et al., J. Immunol. 188 (2012) 2516–2523.
[32] J.T. White, et al., Nat. Commun. 7 (2016) 11291.
[33] K.R. Renkema, et al., J. Exp. Med. 213 (2016) 1319–1329.
[34] P. Tripathi, et al., Eur. J. Immunol. 46 (2016) 2333–2339.
[35] Y.J. Lee, et al., Nat. Immunol. 14 (2013) 1146–1154.
[36] J.T. Tan, et al., Proc. Natl. Acad. Sci. U. S. A. 98 (2001) 8732–8737.
[37] C.E. Martin, et al., Immunity 47 (2017) 171–182 e4.
[38] T. Zaft, et al., J. Immunol. 175 (2005) 6428–6435.
[39] M.J. Palmer, et al., Cell. Mol. Immunol. 5 (2008) 79–89.
[40] S. Gonzalez-Garcia, et al., Notch Regul. Immune Syst. 360 (2012) 47–73.
[41] O. Alpdogan, M.R.M. van den Brink, Trends Immunol. 26 (2005) 56–64.
[42] K.S. Schluns, L. Lefrancois, Nat. Rev. Immunol. 3 (2003) 269–279.
[43] M.P. Rubinstein, et al., Blood 112 (2008) 3704–3712.
[44] A.W. Goldrath, M.J. Bevan, Immunity 11 (1999) 183–190.
[45] K. Murali-Krishna, R. Ahmed, J. Immunol. 165 (2000) 1733–1737.
[46] H.S. Azzam, et al., J. Exp. Med. 188 (1998) 2301–2311.
[47] W.C. Kieper, et al., J. Immunol. 172 (2004) 40–44.
[48] Q. Ge, et al., Proc. Natl. Acad. Sci. U. S. A. 101 (2004) 3041–3046.
[49] K.R. Renkema, et al., J. Immunol. 192 (2014) 151–159.
[50] T. Onoe, et al., J. Immunol. 184 (2010) 6756–6765.
[51] F. Jacomet, et al., Eur. J. Immunol. 45 (2015) 1926–1933.
[52] B.C. Chiu, et al., J. Immunol. 191 (2013) 5793–5796.
[53] Y.D. Mahnke, et al., Eur. J. Immunol. 43 (2013) 2797–2809.
[54] V. Appay, et al., Cytom. Part A 73a (2008) 975–983.
[55] J.R. Fergusson, et al., Cell Rep. 9 (2014) 1075–1088.
[56] A. Kurioka, et al., Clin. Transl. Immunology (2016) 5.
[57] X.X. Xiao, J.P. Cai, Front. Immunol. (2017) 8.
[58] J. Novak, et al., Scand. J. Immunol. 80 (2014) 271–275.
[59] L.J. Walker, et al., Scand. J. Immunol. 80 (2014) 462–463.
[60] J.E. Ussher, et al., Eur. J. Immunol. 44 (2014) 195–203.
[61] A. van Stijn, et al., J. Immunol. 180 (2008) 4550–4560.
[62] T.W. Kuijpers, et al., J. Immunol. 170 (2003) 4342–4348.
[63] Q. Ge, et al., Proc. Natl. Acad. Sci. U. S. A. 99 (2002) 2989–2994.
[64] E.J. Wherry, et al., Nat. Immunol. 4 (2003) 225–234.